Why Study Granular Materials?

Obvious practical importance

collapsed grain elevator

Prototypical system with "jamming"

How do things get stuck?

System far from thermal equilibrium

How do systems behave when "frozen" in metastable states far from equilibrium?

System with friction

Distinctive Features of Granular Material

MACROSCOPIC Material: metaphor for microscopic phenomena

(SOC, flux motion in superconductors, slow relaxation ...)

---

1) Angle of Repose - internal friction (Coulomb 1773).

2) Inelastic collisions

3) Interstitial fluid - even air has viscosity.

4) Density variation - is there an equilibrium?

5) T = 0

6) Dilatancy

7) Arching - inhomogeneous forces.

Rheology of a confined granular material

Guillaume Ovarlez, Evelyne Kolb, and Eric Clément

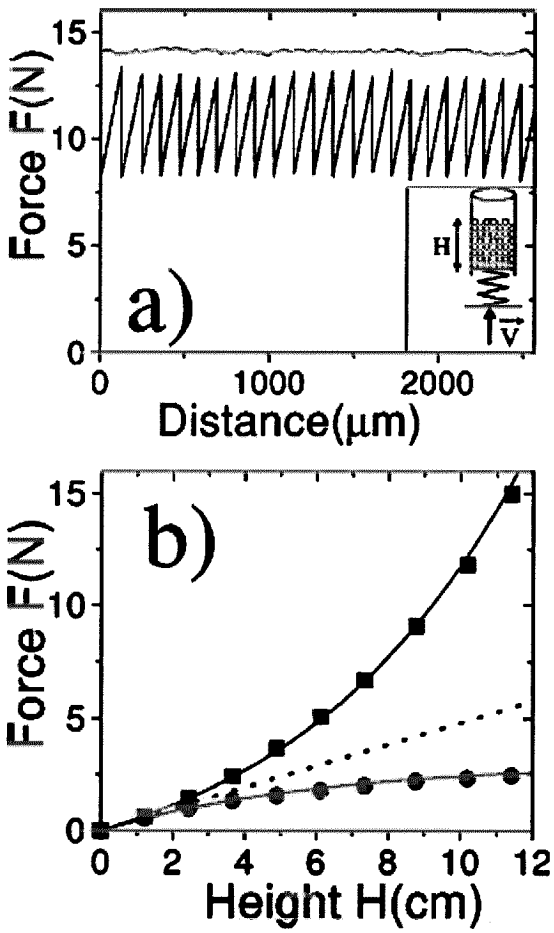

FIG. 1. (a) Resistance force vs the displacement of the stepping motor for $H=4.3R$ steel beads in a duralumin cylinder, for relative humidity $\chi=45\%$ and for $V=30$ nm s^{-1} (stick-slip regime), and $V=100$ μm s^{-1} (steady-sliding regime) shifted by +5 N; the inset is a sketch of the experimental display. (b) Mean force in the steady-sliding regime for $V_{up}=16$ μm s^{-1} (squares) and for $V_{down}=16$ μm s^{-1} (triangles) as a function of the height of the packing; the lines are the fits according to Eq. (1); the dotted line is the hydrostatic curve.

Flow

Gravity compacts particles

$\Rightarrow$ makes a solid

Loosen pack -- vibrations
shear force

Flow occurs in Shear Bands

Shear zones are different from other liquids

Sensitive to: Microstructure
Boundary conditions

What is the feedback between shear and density?

Dilatancy

Sheared sand expands

(Reynolds 1885)

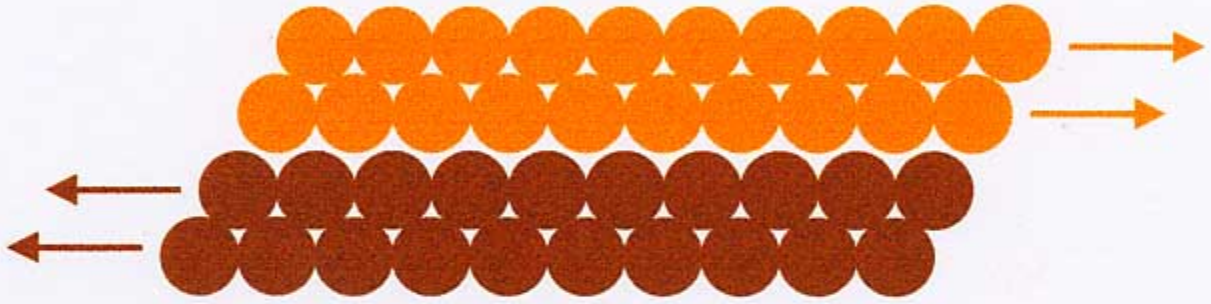

Fluidization from:

Vibrations

$k_B T \ll mgd \Rightarrow$ **vibrations important**

Interstitial gas flow

Density decrease:

Shear

3-D Imaging:
High Spatial and Temporal Resolution

Magnetic Resonance Imaging (MRI)

Requires liquid-containing particles (e.g., seeds, pills)

Spatial resolution >100μm

Applications: velocity profiles, diffusion coefficients

X-ray Tomography

Sensitive to x-ray absorption (works with most types of granular matter)

Spatial resolution >1μm

Applications: local particle configurations, density profiles.

MRI Measurements of Velocity Profile

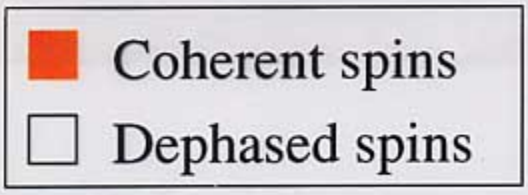

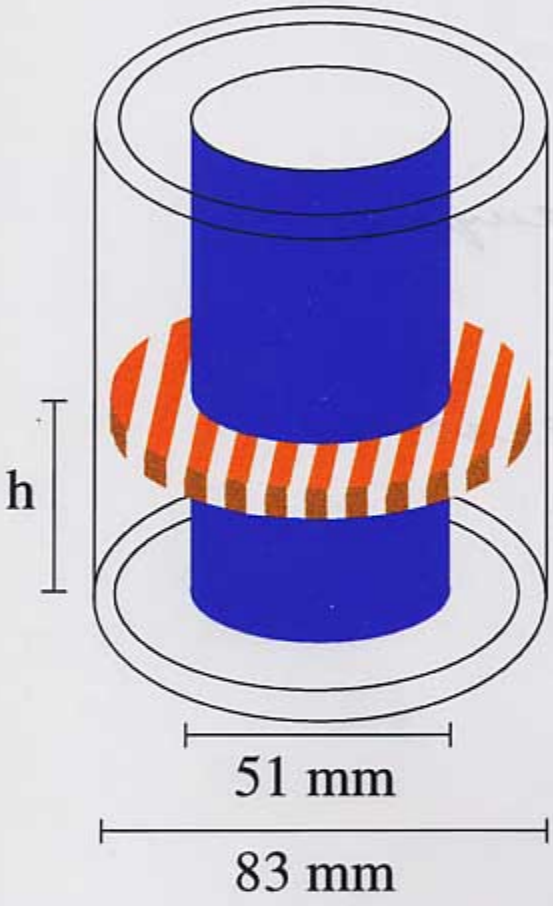

MRI first used on granular avalanches by Nakagawa et al. Expts. In Fluids, 16, 54 (1993).

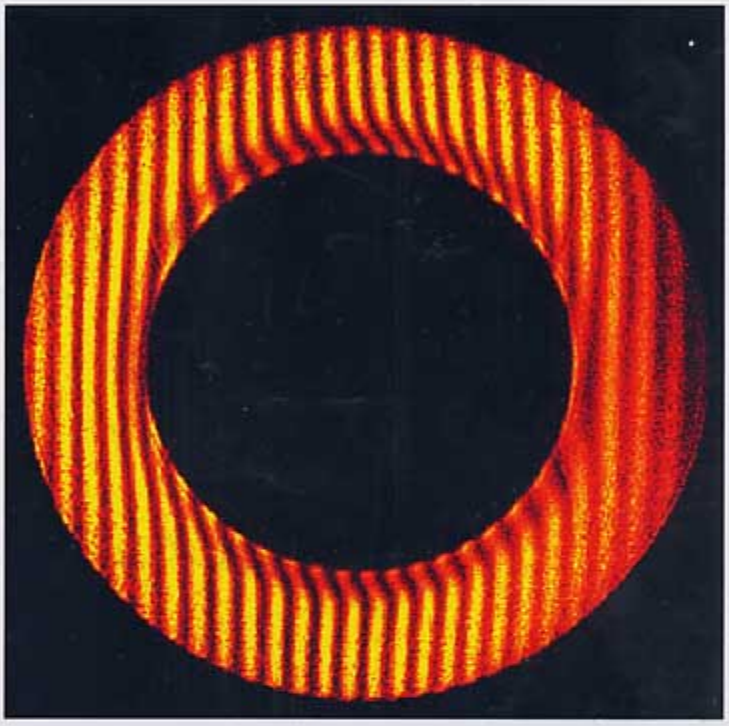

Image After 100 ms of shear

Spin Tagging Experiments

- t=0 Slice is spin tagged
- t=100 ms Image is acquired
- Velocity is determined from stripe deformation
- High precision in velocity and position

Mustard Seed Velocity Profile

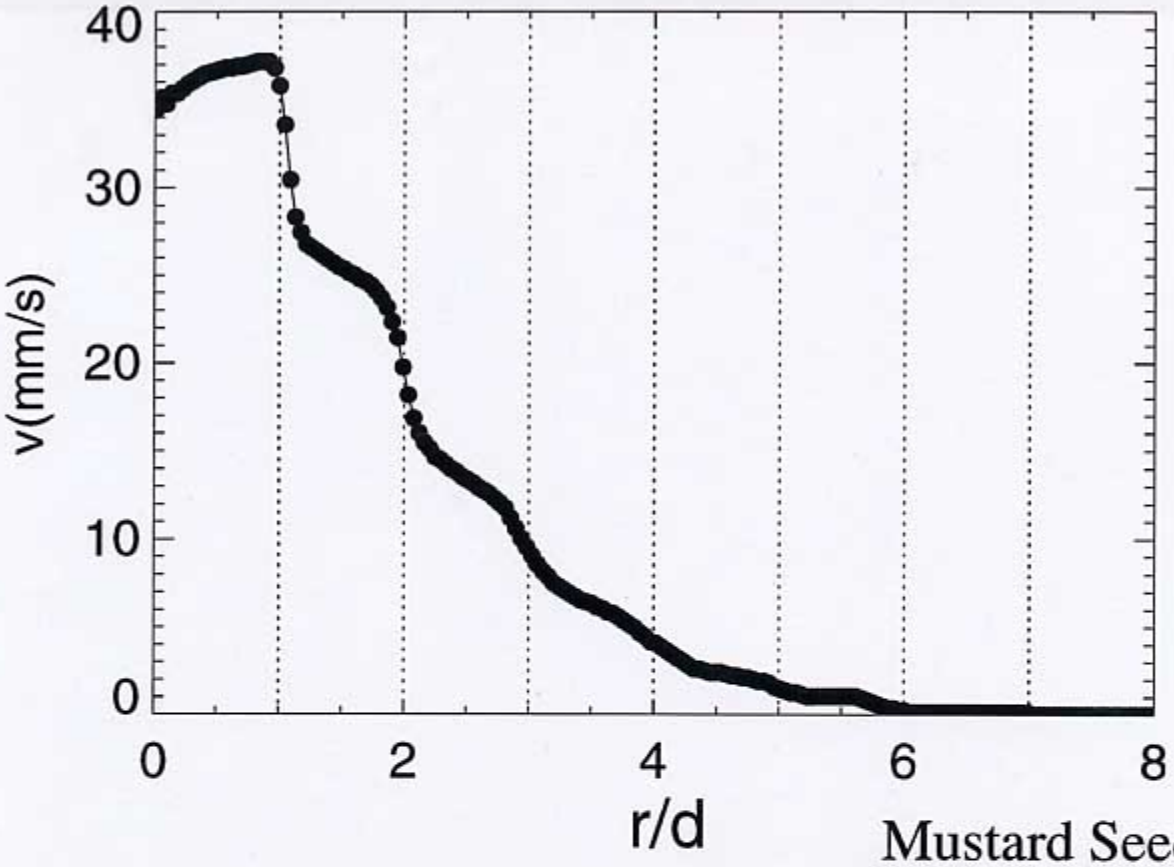

Mustard Seeds

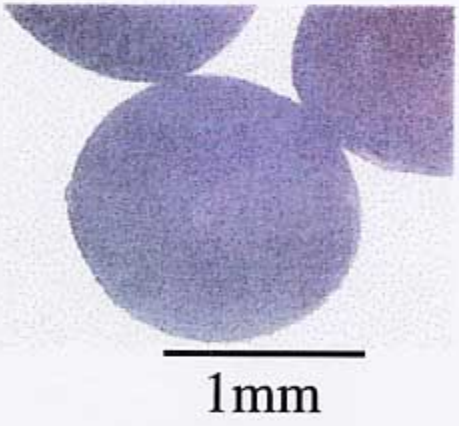

Main Features

Slip occurs between seed layers

Velocity Profile:

$$v(r) = V_0 \exp[-\mathrm{B}(r/d) - \mathrm{C}(r/d)^2]$$

$$\mathrm{B} = 0.5 \pm 0.15$$

$$\mathrm{C} = 0.05 \pm 0.02$$

Poppy Seed Velocity Profile

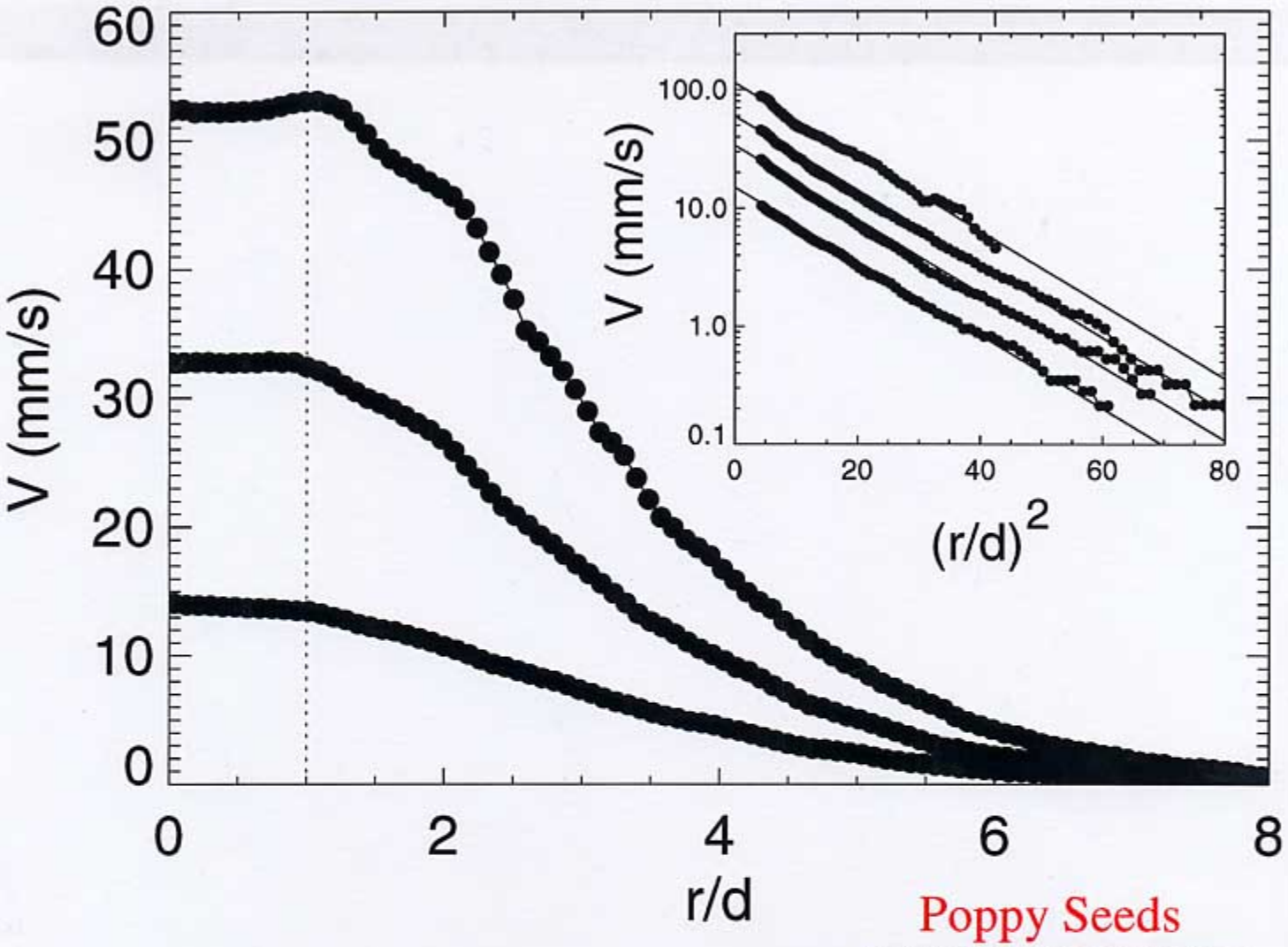

Poppy Seeds

1 mm

Main Features

Rate invariant

Gaussian velocity profile:

$$v(r) = V_0 \exp[-(r/d\lambda)^2] \quad \lambda = 3.1 \pm 0.5$$

Height independent to within 5 mm of surfaces

X-ray Tomography Measurements

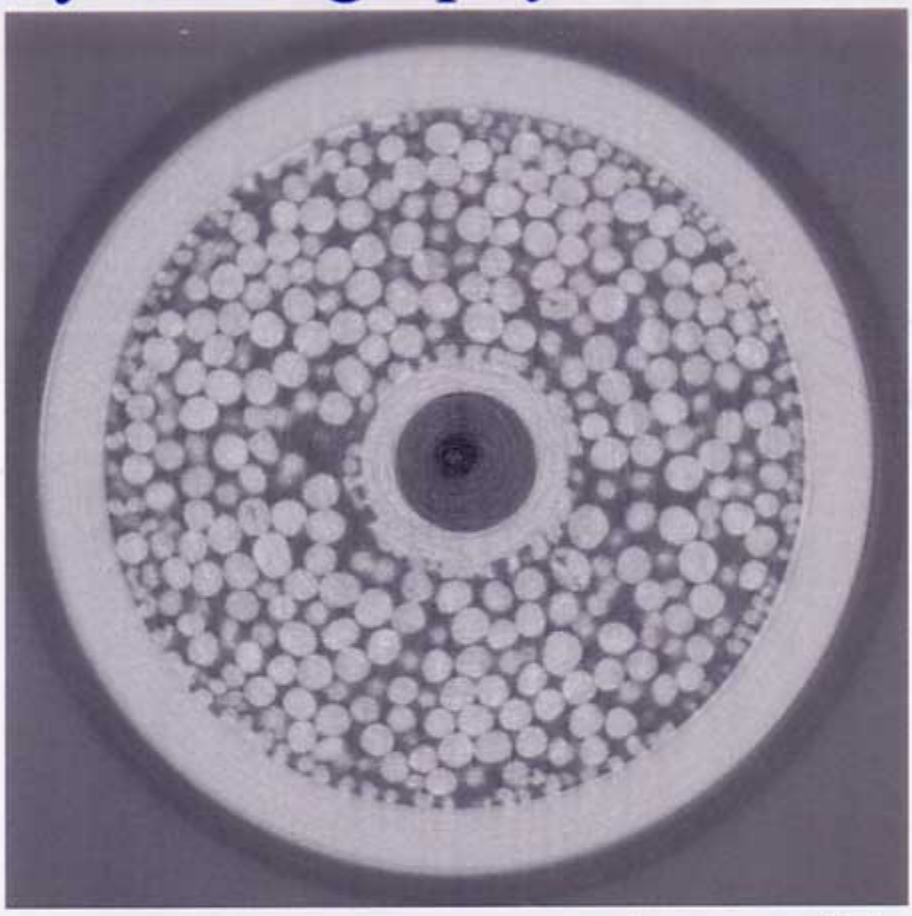

Mustard Seeds (Poppy seeds on walls)

Shear-Induced Dilation

Velocity $\xleftrightarrow{\text{Feedback}}$ Density

(Boundary Conditions)

Density Profile

- Velocity, height dependence
- Material property dependence
- Time evolution

Mustard Seed Density Profile

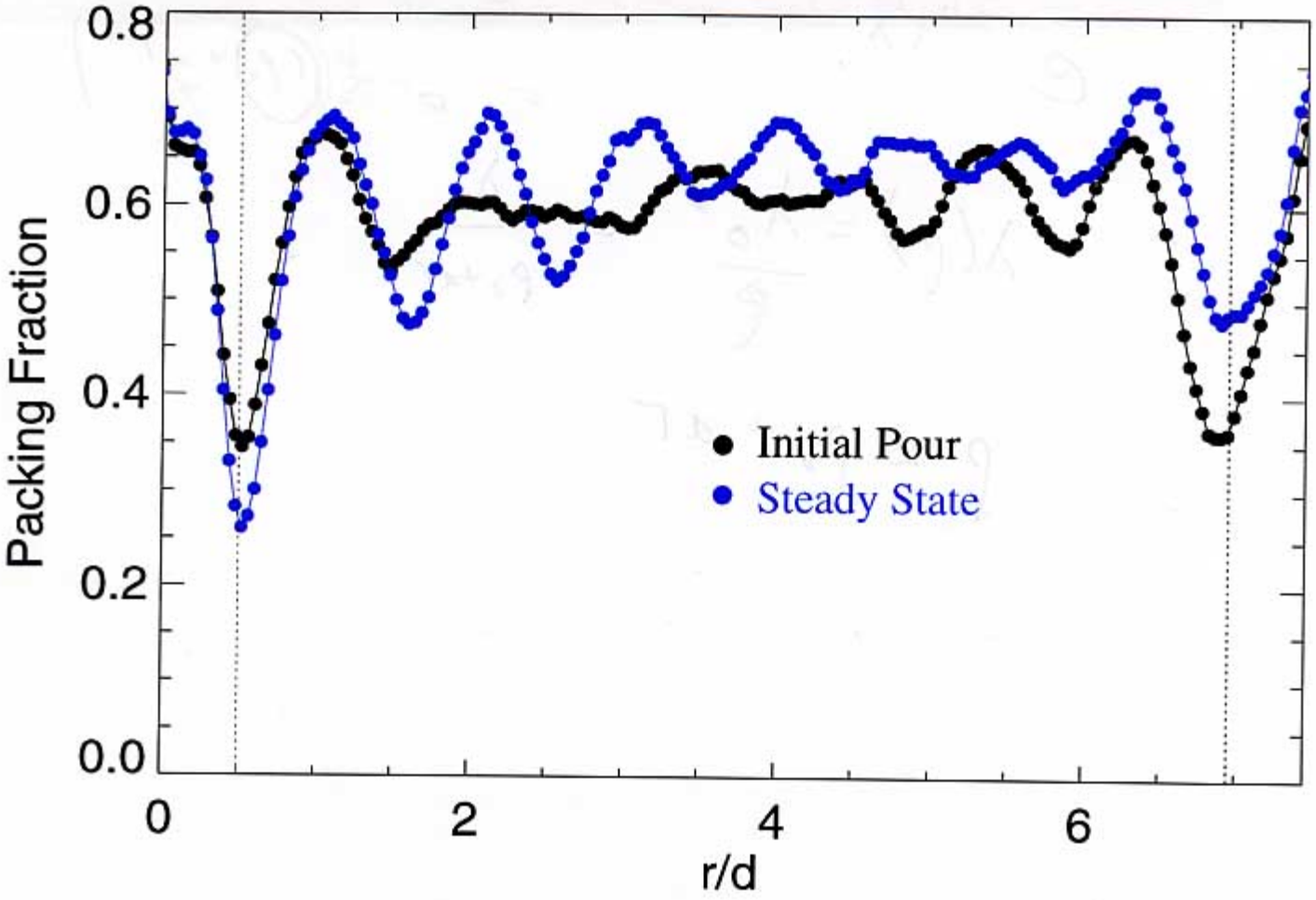

Initial Pour

- Slight layering

Steady State

- Pronounced layering
- Dilation in primary shear zone
- Densification away from primary shear zone

Poppy Seed Density Profile

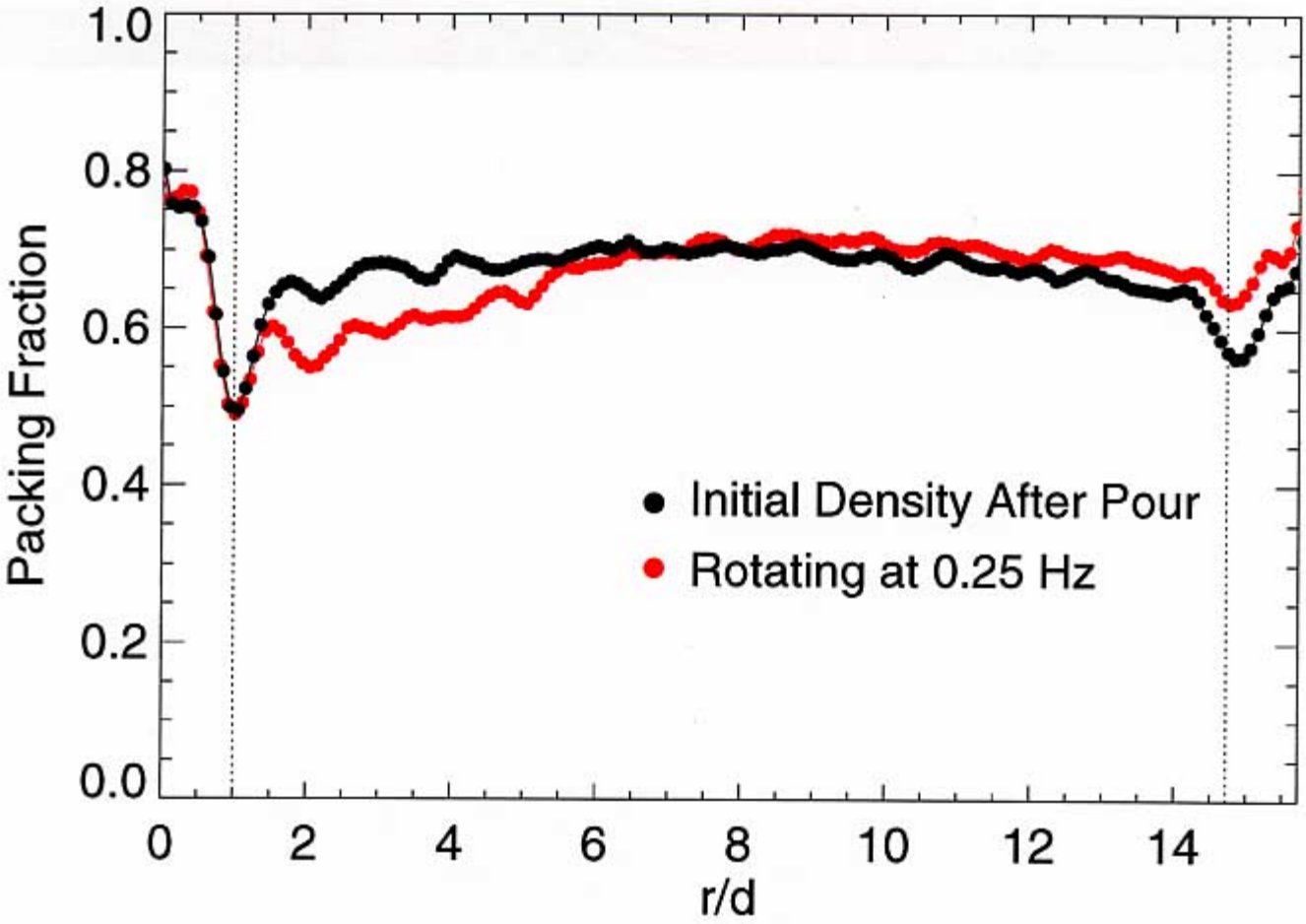

After Pour

- Slight ordering near walls
- Slight dilation near walls

During Shear

- Dilation in primary shear zone
- Compaction away from primary shear zone
- Ordering is enhanced
- Seeds align with flow

High Speed Video of Bottom Surface

Mustard Seeds

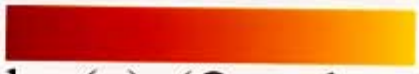

log(v) (Over last 200ms)

Purpose

- Boundary Effects
  - Friction
  - Ordering
  - Reduced dimension
- Fluctuations, Correlations

Observations

Small r	Large r
Layering	Intermittant Flow
Smooth Flow	Correlated Flow
	Radial Flow

High Speed Video of Bottom Surface

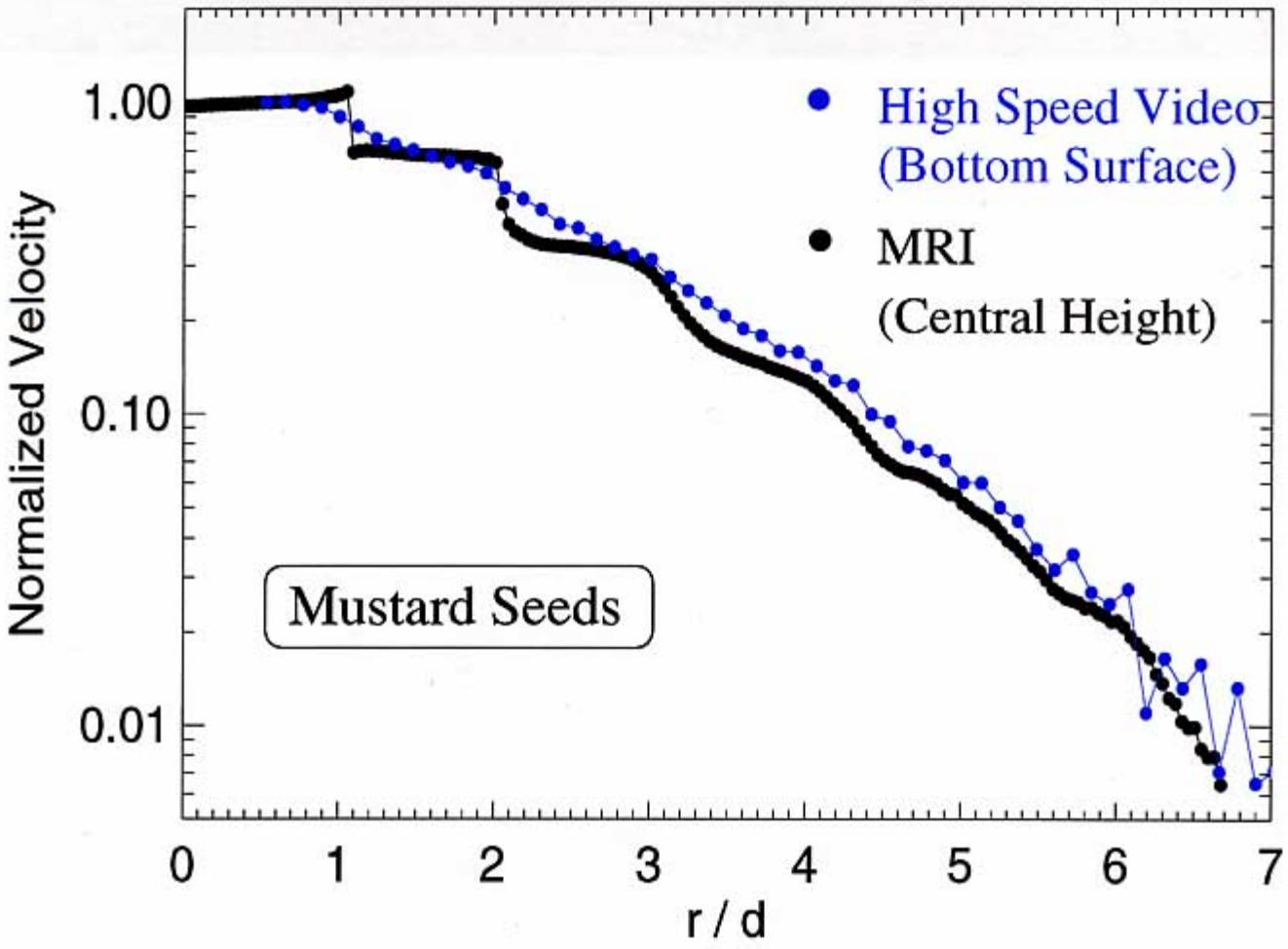

Results

- Boundary resembles bulk

Particle Tracking

- Fluctuations
- Correlations

D. Howell and R. P. Behringer, in *Powders & Grains '97*, editted by R. P. Behringer and J. T. Jenkins, 1997, p337.

Kinematics of a two-dimensional granular Couette experiment at the transition to shearing

C. T. Veje*
PMMH, Ecole Supérieure de Physique et de Chimie Industrielle, 10 Rue Vauquelin, 75231 Paris Cedex 05, France

Daniel W. Howell and R. P. Behringer
Department of Physics and Center for Nonlinear and Complex Systems, Duke University, Durham, North Carolina 27708-0305

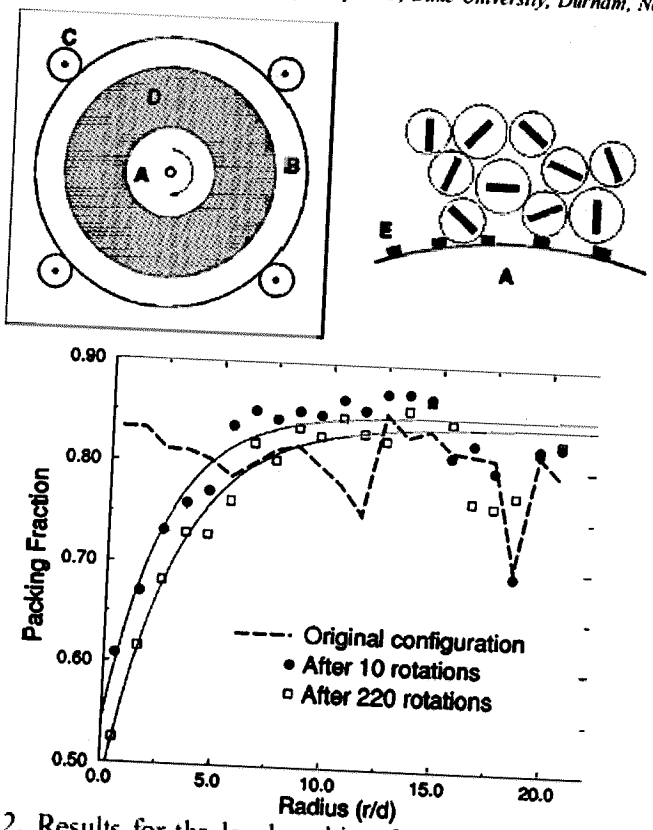

FIG. 2. Results for the local packing fraction after 10 and 220 rotations. The dashed line is the initial configuration. In this case, $\gamma=0.788$. Solid curves show least squares fits to the form $\rho=A-B\exp(-Cr/d)$. Since we are only looking at a quarter of the total cell the area under each curve need not be the same. Most of the relaxation has occurred after 10 rotations: the coefficient C is essentially the same for 10 and 220 rotations. Notably, however, some variation in the packing structure at large r (filling the gap in density near $r=18$) occurred even after very long times—between 20 and 40 rotations—corresponding to a displacement of the shearing wheel by ~2200 to ~4400 disk diameters.

Stress Fluctuations in a 2D Granular Couette Experiment: A Continuous Transition

Daniel Howell and R. P. Behringer
Department of Physics and Center for Nonlinear and Complex Systems, Duke University, Durham, North Carolina 27708-0305

Christian Veje

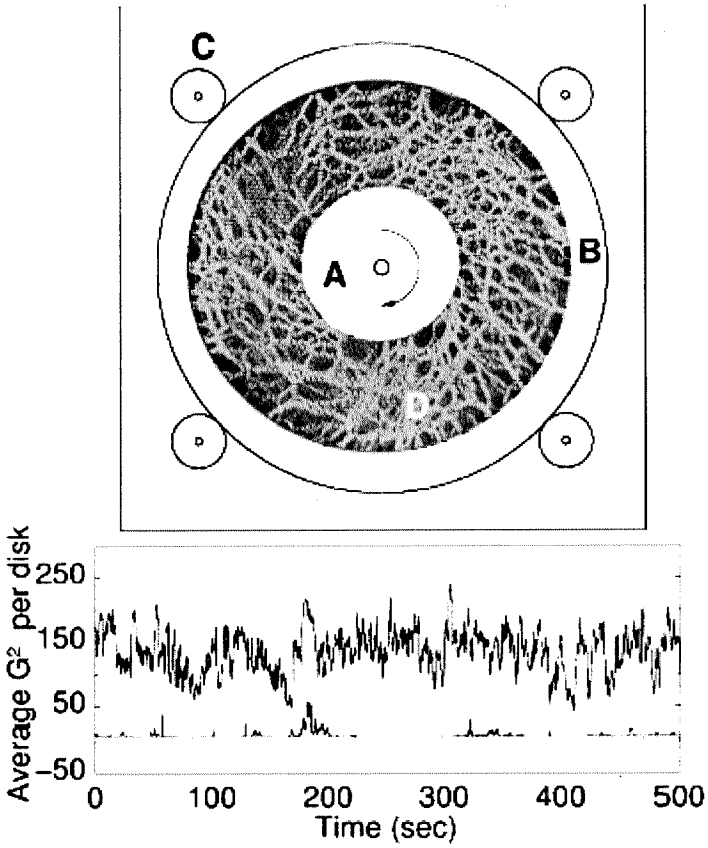

γ = packing fraction.

FIG. 1. Top: image of stress chains from the present experiment using photoelasticity overlaid on a schematic of the apparatus. Bottom: representative time series for stress fluctuations integrated over ~1/10 of the disks. The lower trace is just above γ_c at $\gamma = 0.777$, and the upper trace has $\gamma = 0.803$.

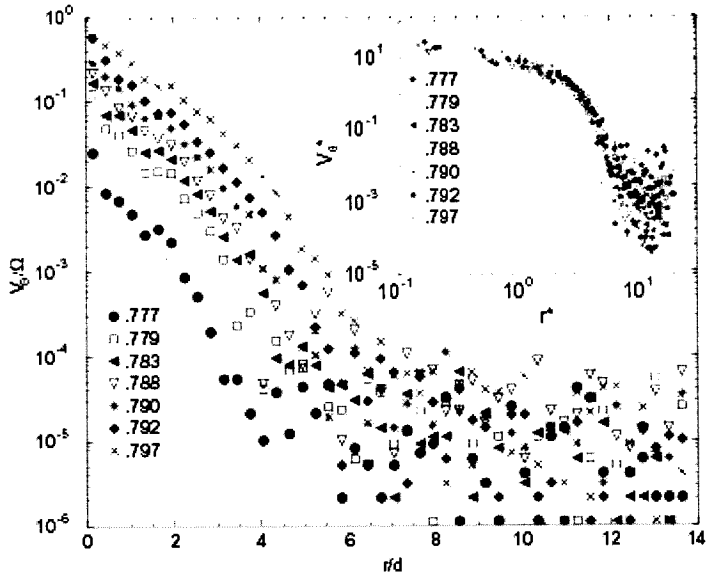

FIG. 2. Mean angular speed of disks normalized by the shearing rate, Ω, V_θ/Ω, vs distance r from the shearing wheel for various γ's, showing critical slowing down. Inset: Scaled data showing collapse.

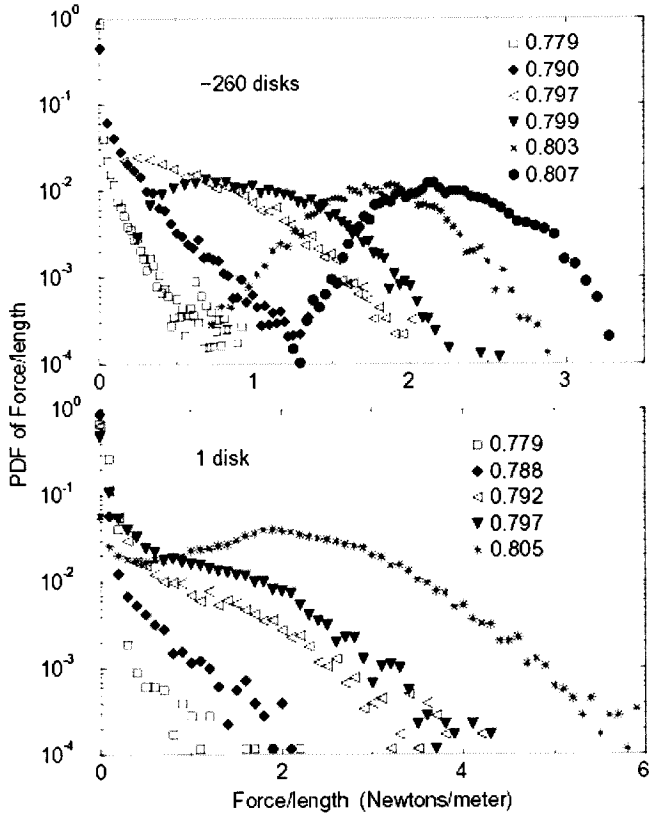

FIG. 4. Distribution for various packing fractions, γ. Top: force per particle for collections of ~260 particles at a time; bottom: for one particle at a time.

Comparison of Velocity Profiles

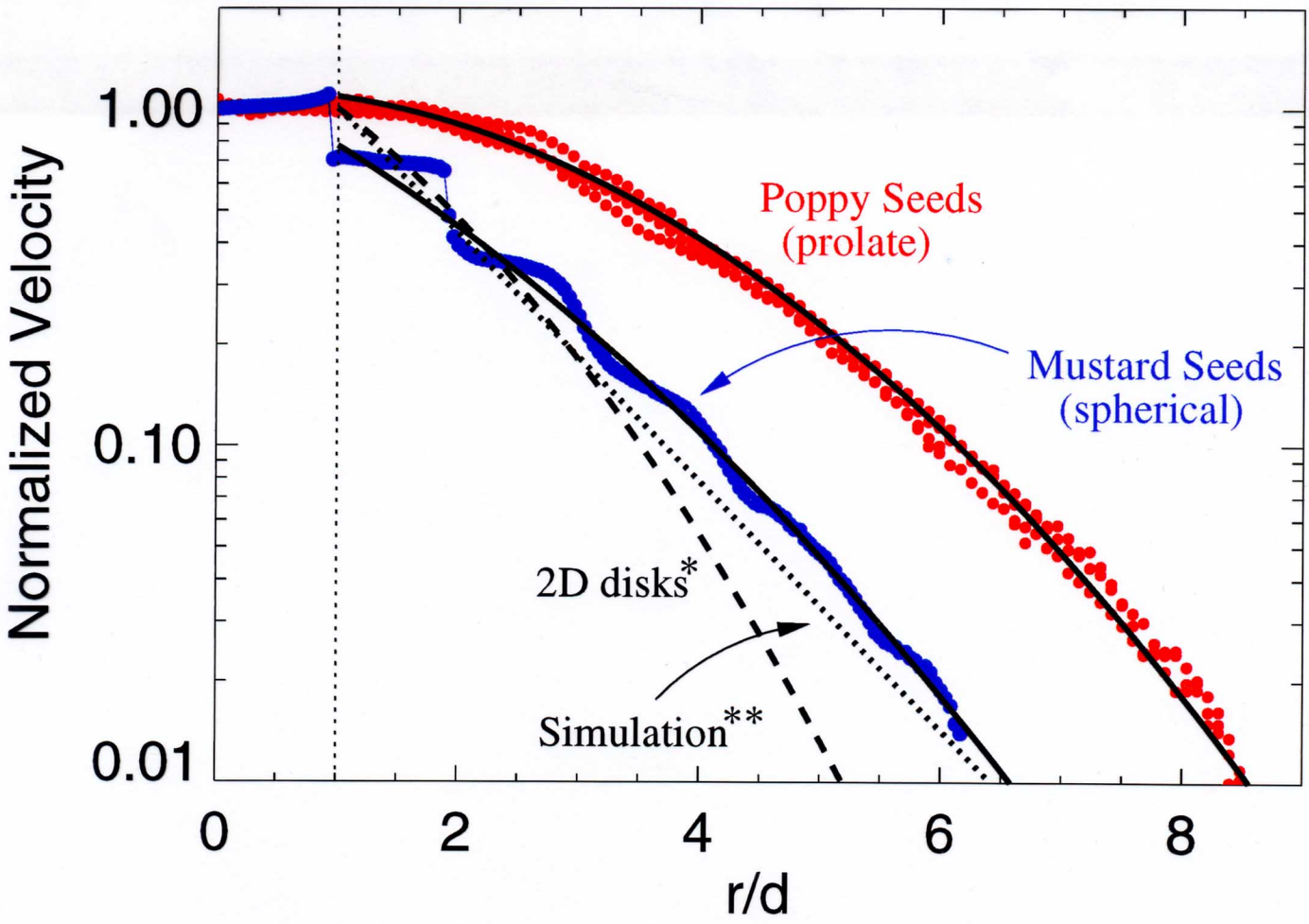

$$v(r) = V_0 \exp(-\mathrm{B}(r/d) - \mathrm{C}(r/d)^2)$$

Poppy Seeds	B = 0,	$\mathrm{C} = 0.10 \pm 0.02$
2D Disks*	$\mathrm{B} = 0.42 \pm 0.10$,	$\mathrm{C} = 0.11 \pm 0.01$
Mustard Seeds	$\mathrm{B} = 0.50 \pm 0.15$,	$\mathrm{C} = 0.05 \pm 0.02$
MD Simulation**	$\mathrm{B} \approx 0.85$,	C = 0

* C. T. Veje, D. W. Howell, and R. P. Behringer, Phys. Rev. E **59**, 739 (1999).

**C. T. Veje, et al, in *Physics of Dry Granular Media*, editted by H. J. Herrmann, H.-P. Hovi, and S. Luding, 1998, p237.

Flow in granular material: Conclusions

Perched precariously between liquid and solid

Density must decrease for flow:
vibrations
shear force

$\Rightarrow$ Feedback between shear and density

Flow occurs in Shear Bands
Profile sensitive to microstructure

MRI and X-ray micro-tomography:
high-resolution, non-invasive
velocity and density in shear band

Particle Dynamics in Sheared Granular Matter

W. Losert,[1] L. Bocquet,[2,3] T. C. Lubensky,[2] and J. P. Gollub[1,2]

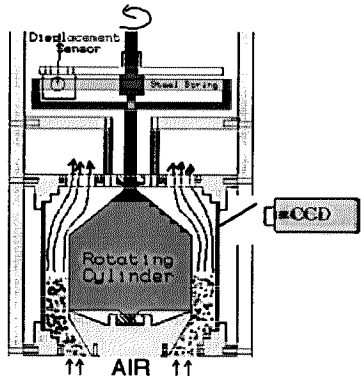

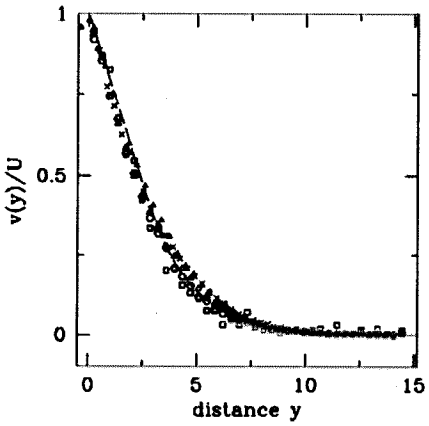

FIG. 2. Mean particle velocity (normalized by the shear rate) as a function of distance from the inner cylinder (in particle diameters). The respective shear rates U (in Hz) are 0.004 (hexagons), 0.04 (squares), 0.01 (open triangles), 0.4 (crosses). The solid triangle is the velocity profile at $U = 0.01$ Hz *without* air flow. The normalized velocity profile is independent of shear rate and shear dynamics (intermittent or steady motion). The dashed line is the solution of Eqs. (2) and (3), with $\delta = 4.7d$, $y_w = 2.8d$, and $\alpha = 0.4$ (see text for details).

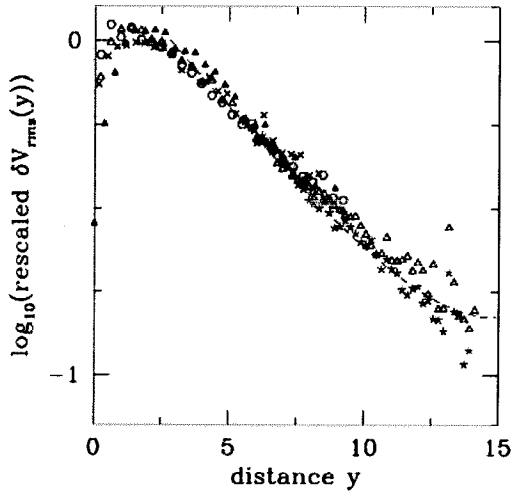

FIG. 3. rms velocity fluctuations perpendicular to the shear direction. Fluctuations decrease roughly exponentially far from the inner cylinder, but more slowly than the mean flow. The rms fluctuations are rescaled (shifted vertically) such that all experimental points fit on the same master curve. The dashed line is the theoretical result (see text), with a decay length $\delta = 4.7d$ and a boundary position $y_w = 2.8d$.

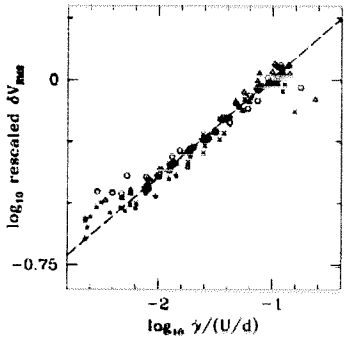

FIG. 4. Connection between the local rms velocity fluctuations and local shear rate (same symbols as for Fig. 2). Local fluctuations are found to increase approximately as a power law of the local velocity gradient, with a power of 0.4 (dashed line).

$$\eta \sim (\rho_c - \rho)^{-1.75}$$

Medical CT	Microtomography (Advanced Photon Source at Argonne National Labs)
Resolution	
0.5 mm	1 μm
Image size	
512 x 512	2000 x 2000 (set by camera)
Energy	
100 keV (broad spectrum)	1 - 100 keV (white or mono ΔE = 1 eV)
Method	
Stationary or spiral scan	Stationary beam: rotate sample
Acquisition time	
>0.3 s/slice	1 s/volume (600 x 600 x 60)
Advantages	
Stationary sample Large sample size	High spatial resolution High flux (fast) Energy tunable (optimize contrast) Monochromatic (high precision for density measurements)
Disadvantages	
Low contrast on low absorption matter	Must rotate sample Max. sample width 50 mm (or need to translate)

X-RAY IMAGES OF DENSITY WAVES IN A HOPPER OF FLOWING SAND

ROUGH

SMOOTH SAND

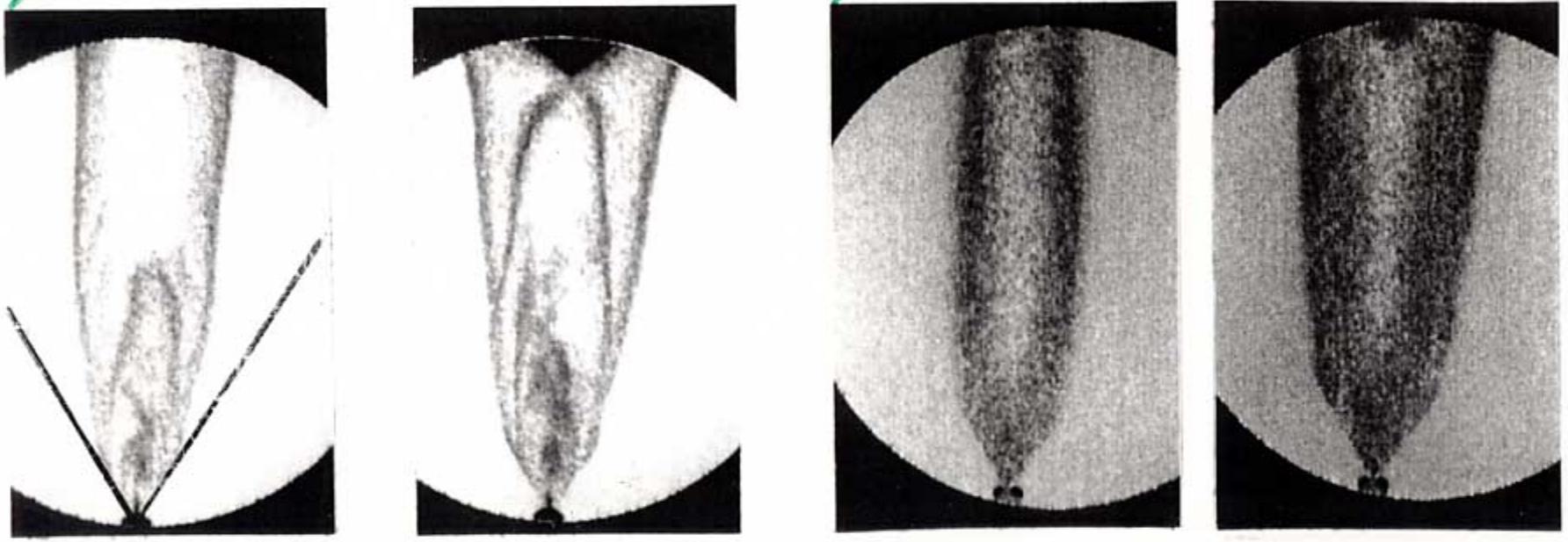

(a) 11.56 (b) 14.896 (c) 11.563 (d) 21.564

G.W. BAXTER, R.P. BEHRINGER, T. FAGGERT, AND G.A. JOHNSON, PHY. REV. LETT. 62, 2825 (1989).

Granule-by-granule reconstruction of a sandpile from x-ray microtomography data

G. T. Seidler,[1,2,*] G. Martinez,[1] L. H. Seeley,[1] K. H. Kim,[1] E. A. Behne,[1] S. Zaranek,[1] B. D. Chapman,[1] S. M. Heald,[2,3] and D. L. Brewe[1,2]

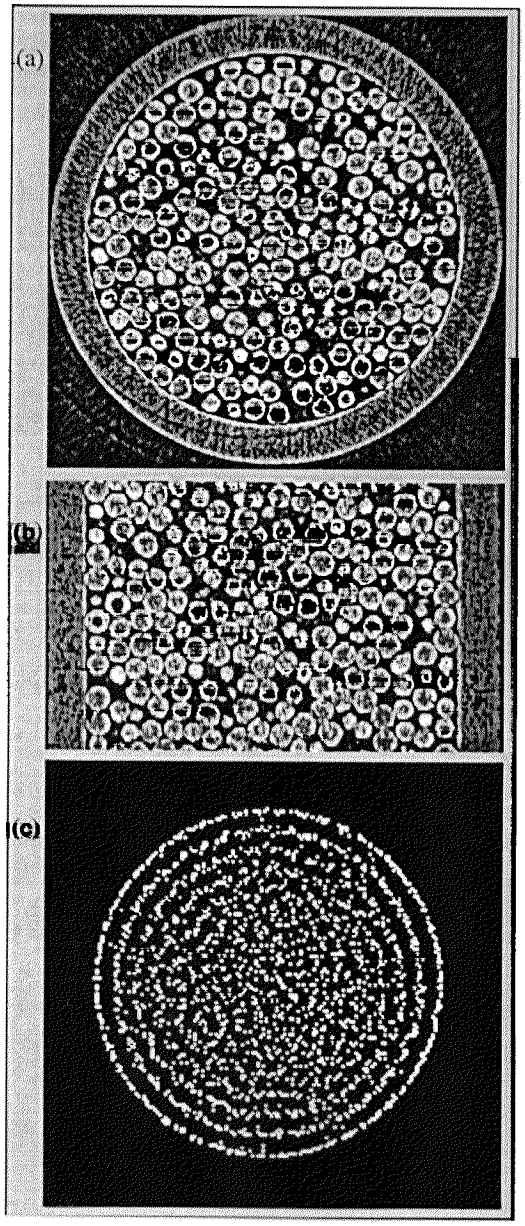

FIG. 1. Two perpendicular cuts through the full 3D tomograph of a granular bed consisting of mean diameter $D=63\ \mu$m spherical glass beads in a 1.0-mm inner-diameter glass cylinder. (a) A cut perpendicular to the cylinder axis. (b) A cut parallel to the xz plane. (c) A projection down the cylinder axis of the granule centers as determined by the 3D Hough transform. See the text for details.

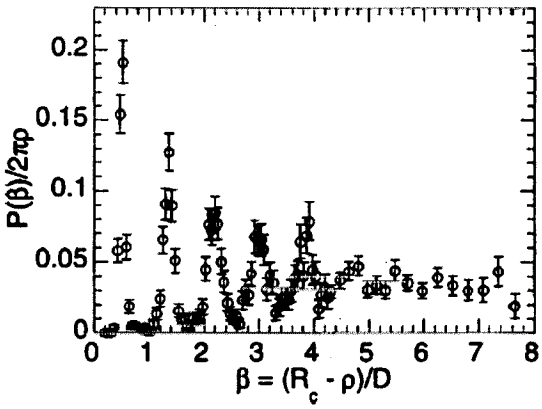

FIG. 2. The normalized cylindrical density function for sphere centers as a function of distance β from the cylinder wall in units of the mean granule diameter D.

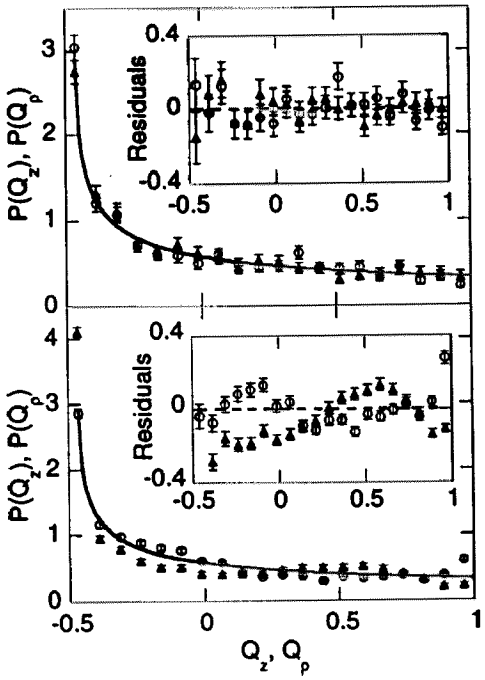

FIG. 5. The probability density functions (PDFs) for the nematic order parameters with respect to the vertical and cylindrical radial directions. The solid line shows the expected behavior for isotropic bonds with respect to the directors; see the text for details. Top: The PDFs for bonds in **G**. Bottom: The PDFs for bonds outside of **G**. Insets: The residuals between the data and the expected behavior for isotropy. Note that the extreme residual for $P(Q_{\vec{\rho}}=-0.5)$ is not included in the bottom inset.

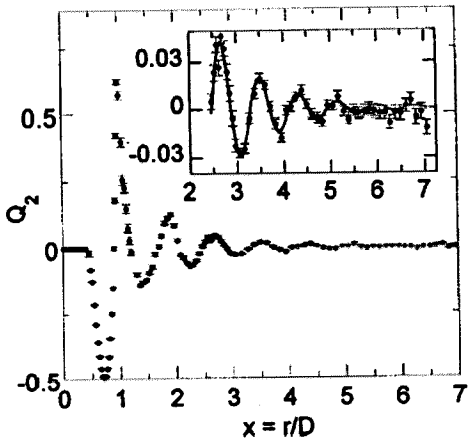

FIG. 6. The bond orientational correlation function $Q_2(x)$ for bonds contained in the subsample **G**. Inset: A least squares fit of Eq. (3) to the region $x>2.5$. See the text for details.

RELAXATION OF θ IN A STATIONARY DRUM WITH DIFFERENT VIBRATION INTENSITIES.
GLASS BEADS

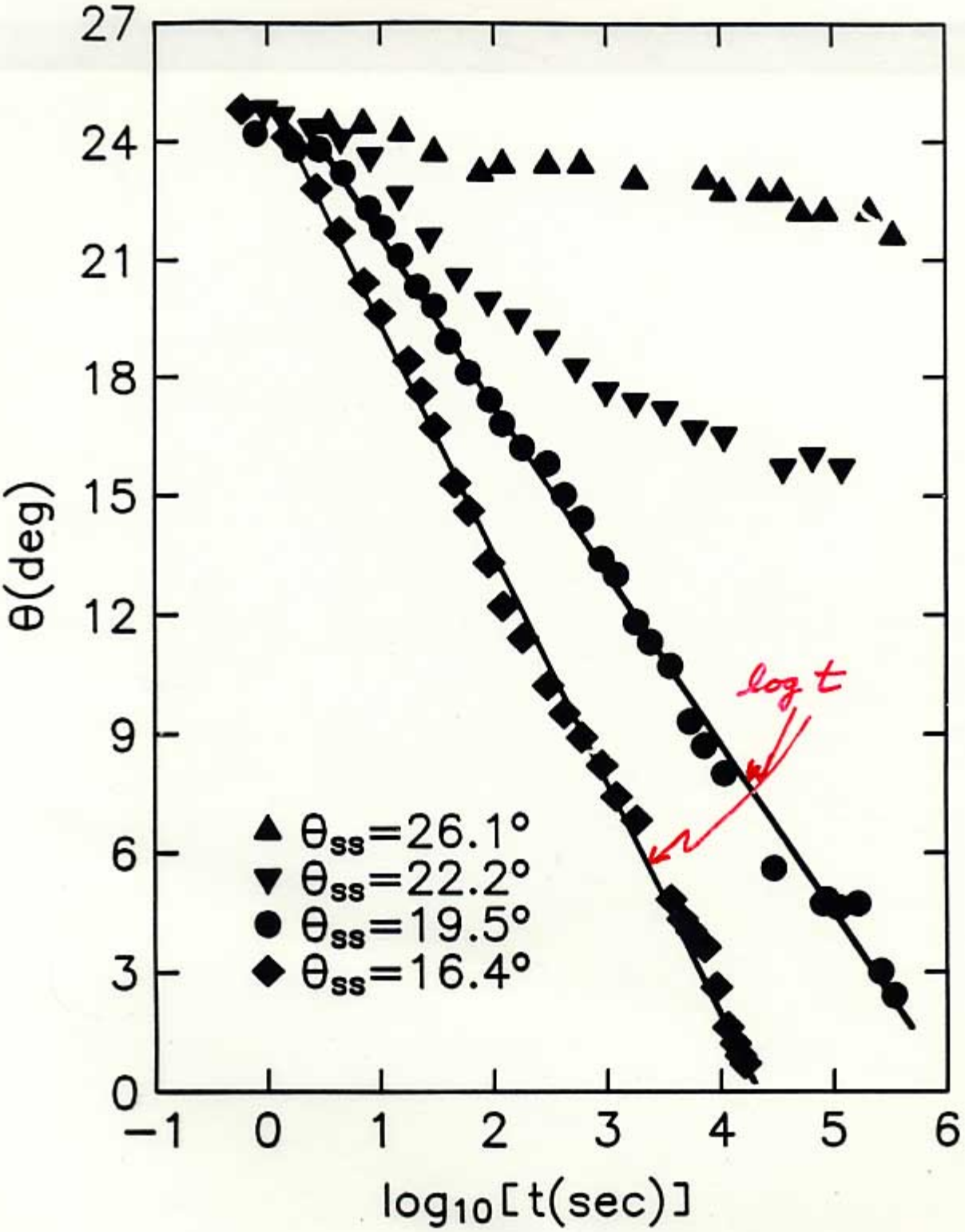

H. M. JAEGER, C-h. LIU, & S.R.N.

MODEL FOR LOGARITMIC RELAXATION

Analogy with electrical conduction:

$$j = \sigma(T)\ E.$$

In rotating drum:

$j \rightarrow d\theta/dt$ and

$E \rightarrow \theta$.

$\sigma(T)$ is determined by diffusion of particles over barriers, $U(r)$. Effective barrier height, posed by neighboring grains of sand, changes as θ is varied: $U \approx U_o - U_1(\theta - \theta_r)$.

Mechanical vibrations produce an effective temperature, T_{eff}.

$$d\theta/dt = - A\ \theta\ \exp[\beta\ (\theta - \theta_r)]$$

where $A = A_o\ \exp[-U_o/kT_{eff})$ and $\beta = U_1/kT_{eff}$.

Solving for θ:

$$\theta = \theta_r - (1/\beta)\ \ln\ (\beta A \theta_r t + 1).$$

From Avalanches to Fluid Flow: A Continuous Picture of Grain Dynamics Down a Heap

P.-A. Lemieux and D. J. Durian

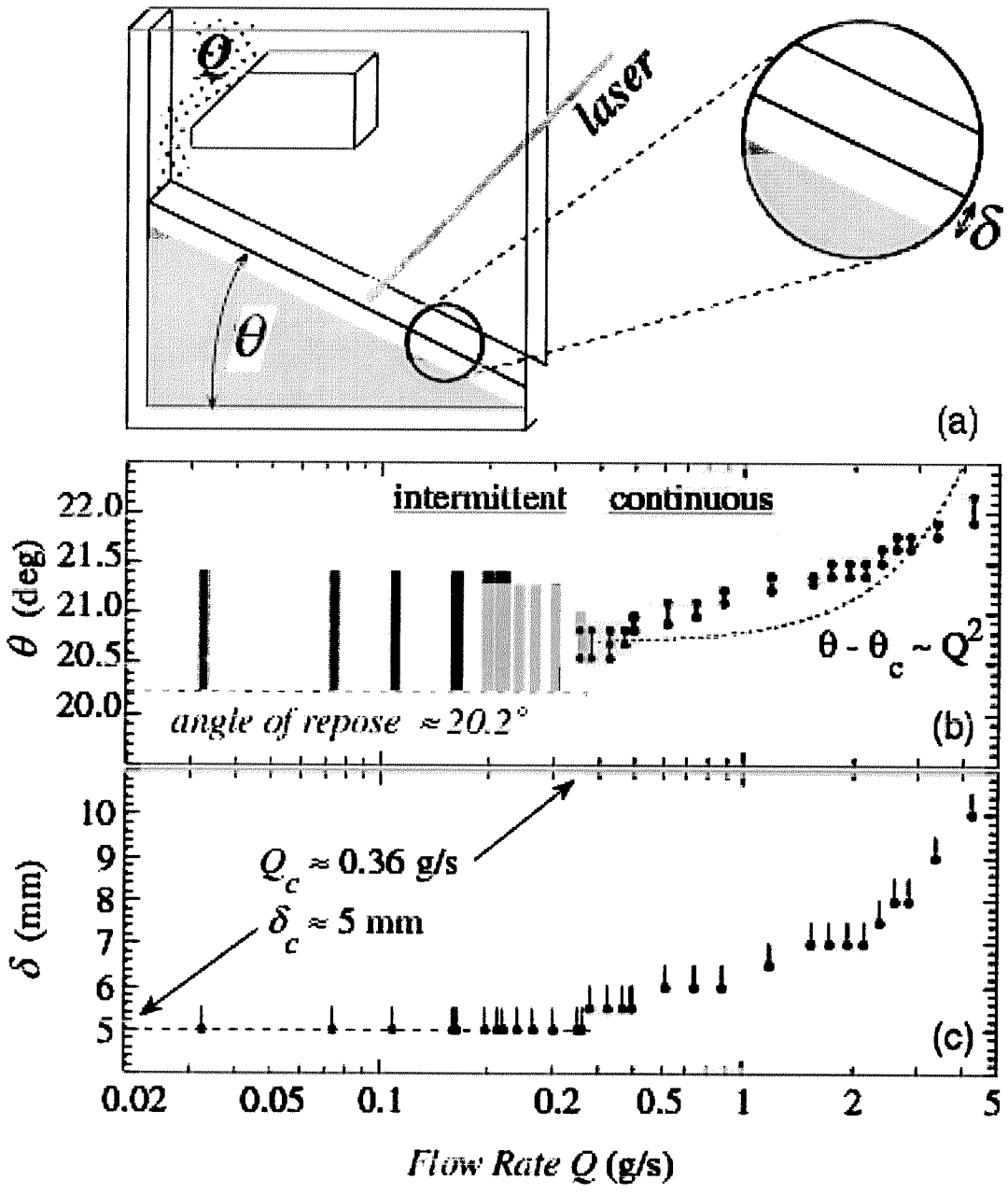

FIG. 1. The experimental setup (a), and two macroscopic measures of the response vs mass flow rate: (b) heap angle and (c) layer thickness. Note that the data do not agree with the modified-Bagnold model prediction $\theta - \theta_c \propto Q^2$.

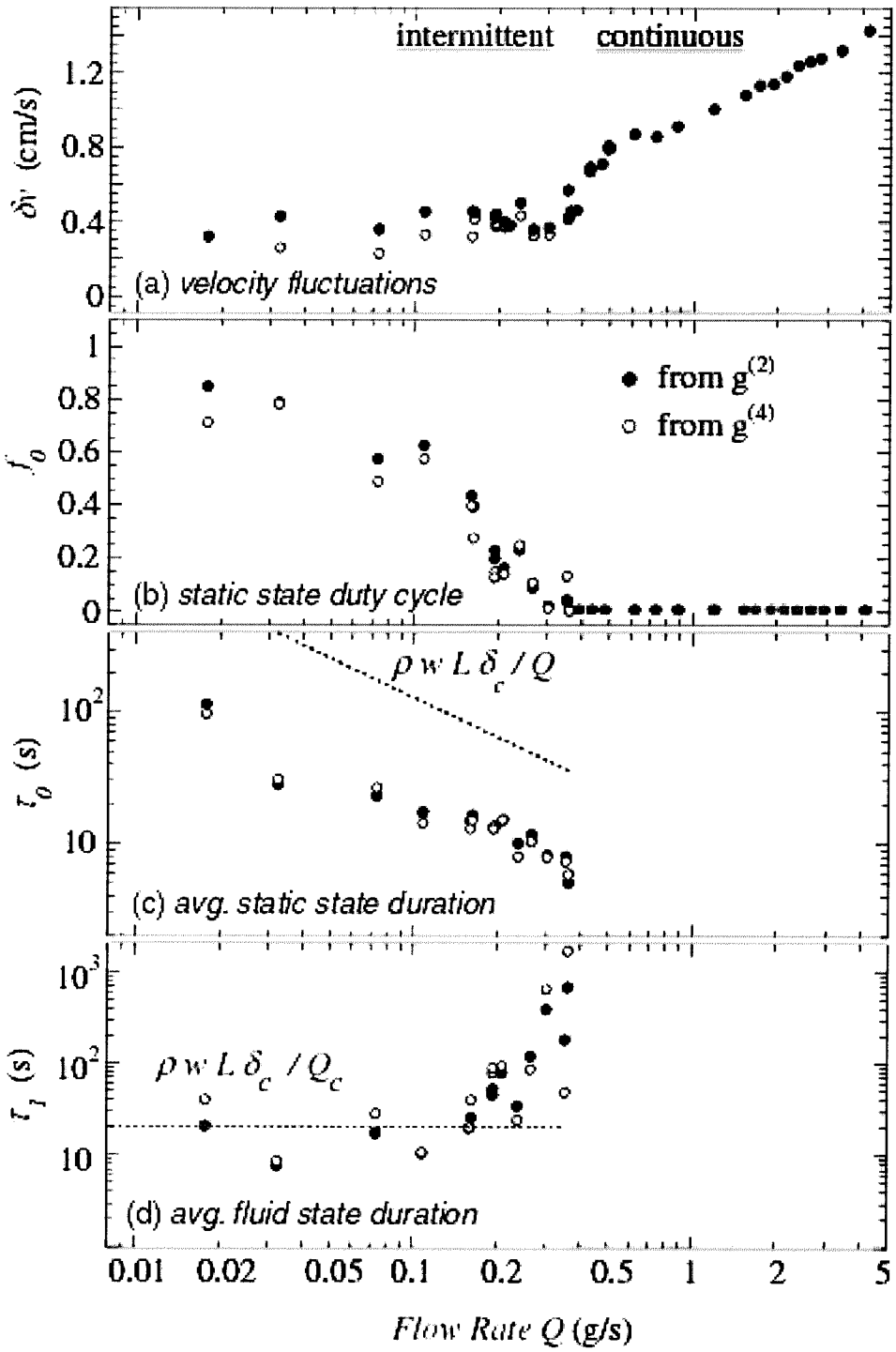

FIG. 3. Grain dynamics vs mass flow rate: (a) velocity fluctuations, (b) fraction of time spent static, (c) average time spent static, and (d) average time spent flowing. Consistent results are obtained from second- and fourth-order correlation data using Eqs. (1) and (2), respectively.

Surface Waves

Douady, S., S. Fauve et al., Europhysics Lett. **8**, 621 (1989).
Melo, F., P. Umbanhowar, and H. L. Swinney, Phys. Rev. Lett. **72**, 172 (1993); **75**, 3838 (1995).
Metcalf, T., J. B. Knight and H. M. Jaeger, preprint.
Pak, H. K., and R. P. Behringer, Phys. Rev. Lett. **71**, 1832 (1993).
Wassgren, C. R., C. E. Brennen, and M. L. Hunt, (preprint).

Why do surface excitations exist in sand?

What is their dispersion relation?

Are they the same or different from surface waves in liquids (Faraday crispations)?

Are they waves?

S. DUADY, S. FAUVE... EUROPHYSICS LETT. 8, 621 (1989).

5 - THE STANDING WAVE REGIME

When the acceleration is increased further, time-dependent instabilities of the free surface develop. They consist of localized waves that propagate in an erratic fashion. However, there exist intervals in the excitation amplitude and frequency, where a standing surface wave is parametrically amplified at half the excitation frequency, and forms a perfectly ordered pattern (see figure 3).

RECTANGULAR CONTAINER.

Fig. 3 - Photograph of the standing surface wave ($\nu = 20$ Hz, $\Gamma = 3.5\,\Gamma_c$).

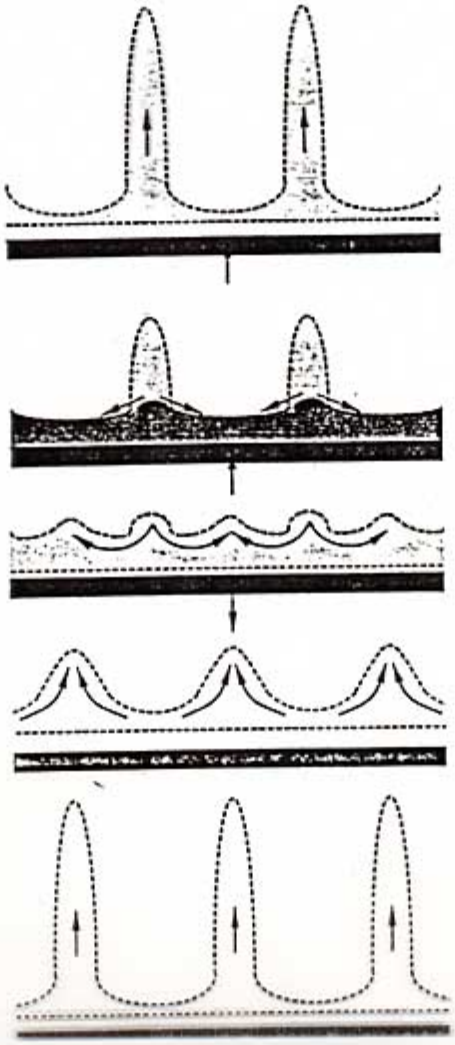

H.K. PAK AND R.P. BEHRINGER PHYS. REV. LETT. 71, 1832 (1993).

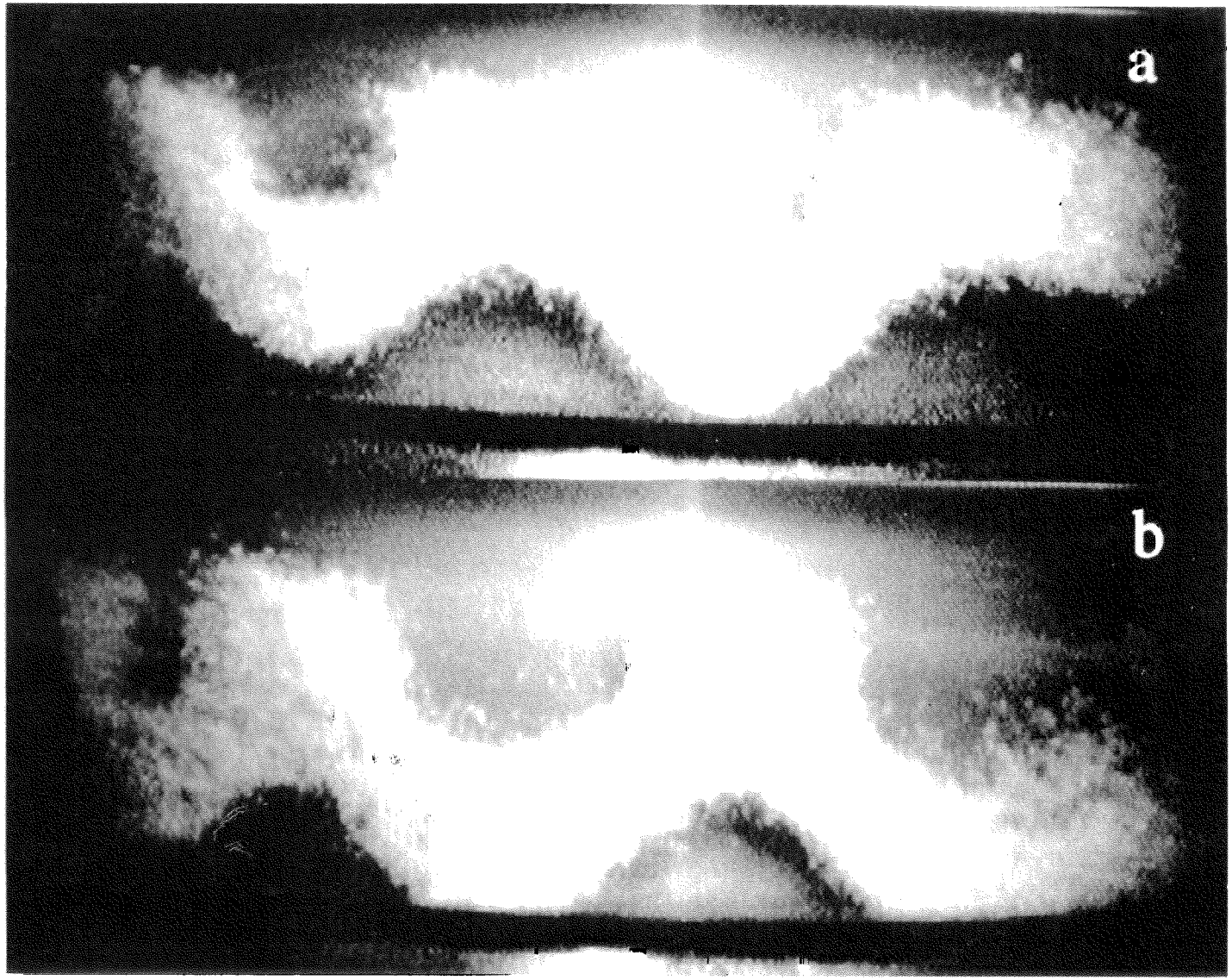

Standing waves for granular material in an annulus subject to vertical vibration. Parts a and b are separated in time by a half wave period which is a full excitation period.

F. MELO, P. UMBANHOWAR, AND H.L. SWINNEY
PHYS. REV. LETT. 75, 3838 (1995)

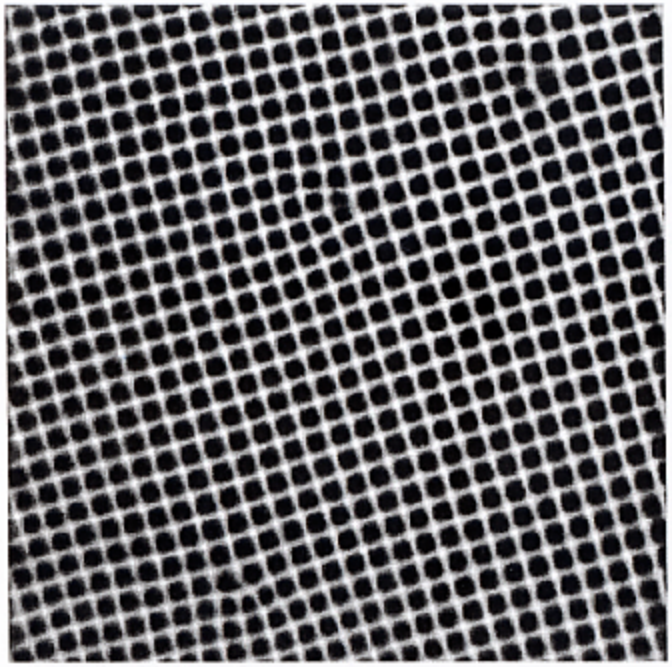

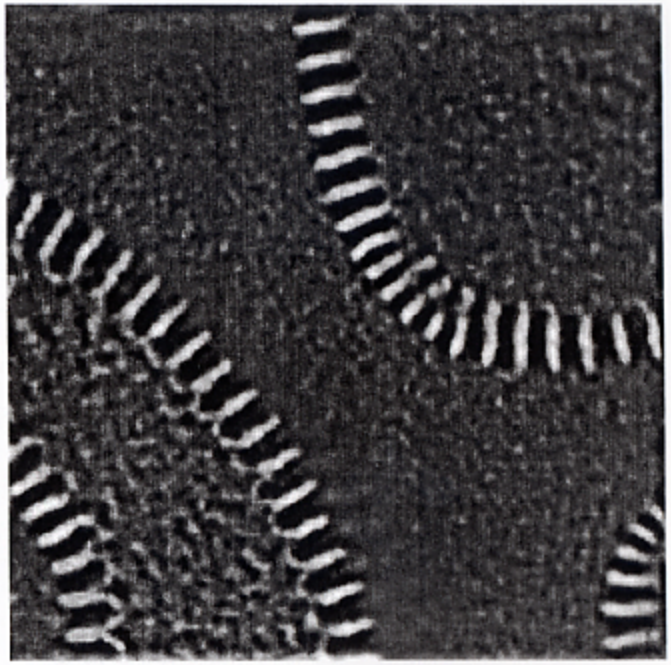

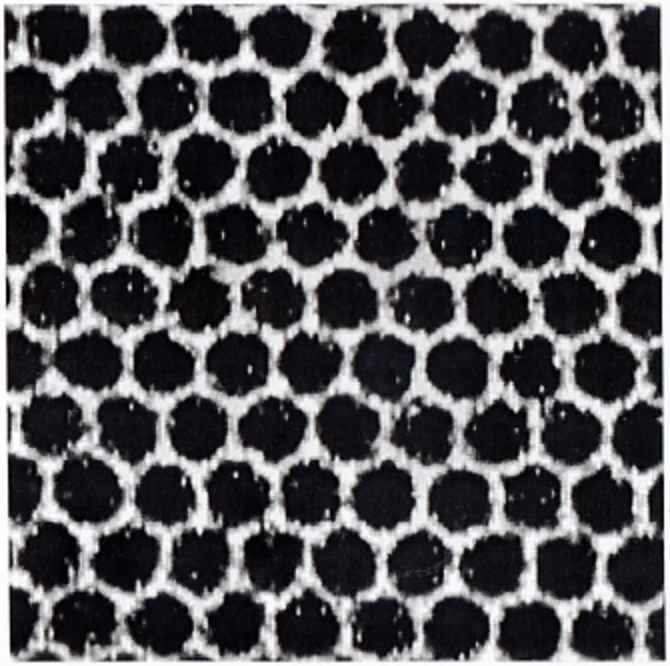

HEXAGONAL PATTERN ← 2 WAVE MIXING.

PHASE DIAGRAM, DISPERSION RELATIONS.

$\lambda \propto 1/f^2$

Localized excitations in a vertically vibrated granular layer

Paul B. Umbanhowar*, Francisco Melo† & Harry L. Swinney*

LETTERS TO NATURE

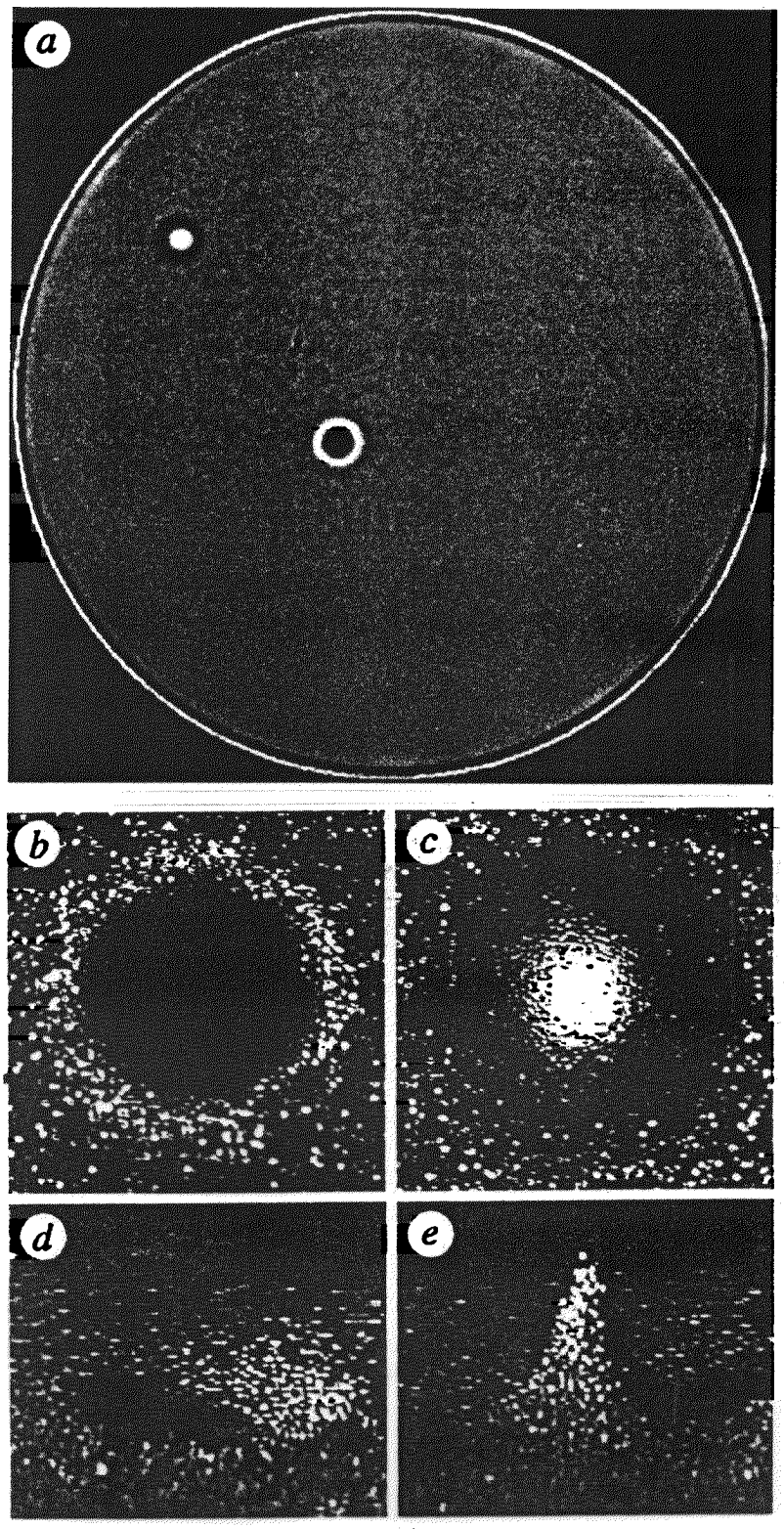

Patterns in 3D Vertically Oscillated Granular Layers: Simulation and Experiment

C. Bizon,* M. D. Shattuck, J. B. Swift, W. D. McCormick, and Harry L. Swinney†
Center for Nonlinear Dynamics and Department of Physics, University of Texas, Austin, Texas 78712
(Received 13 June 1997; revised manuscript received 15 September 1997)

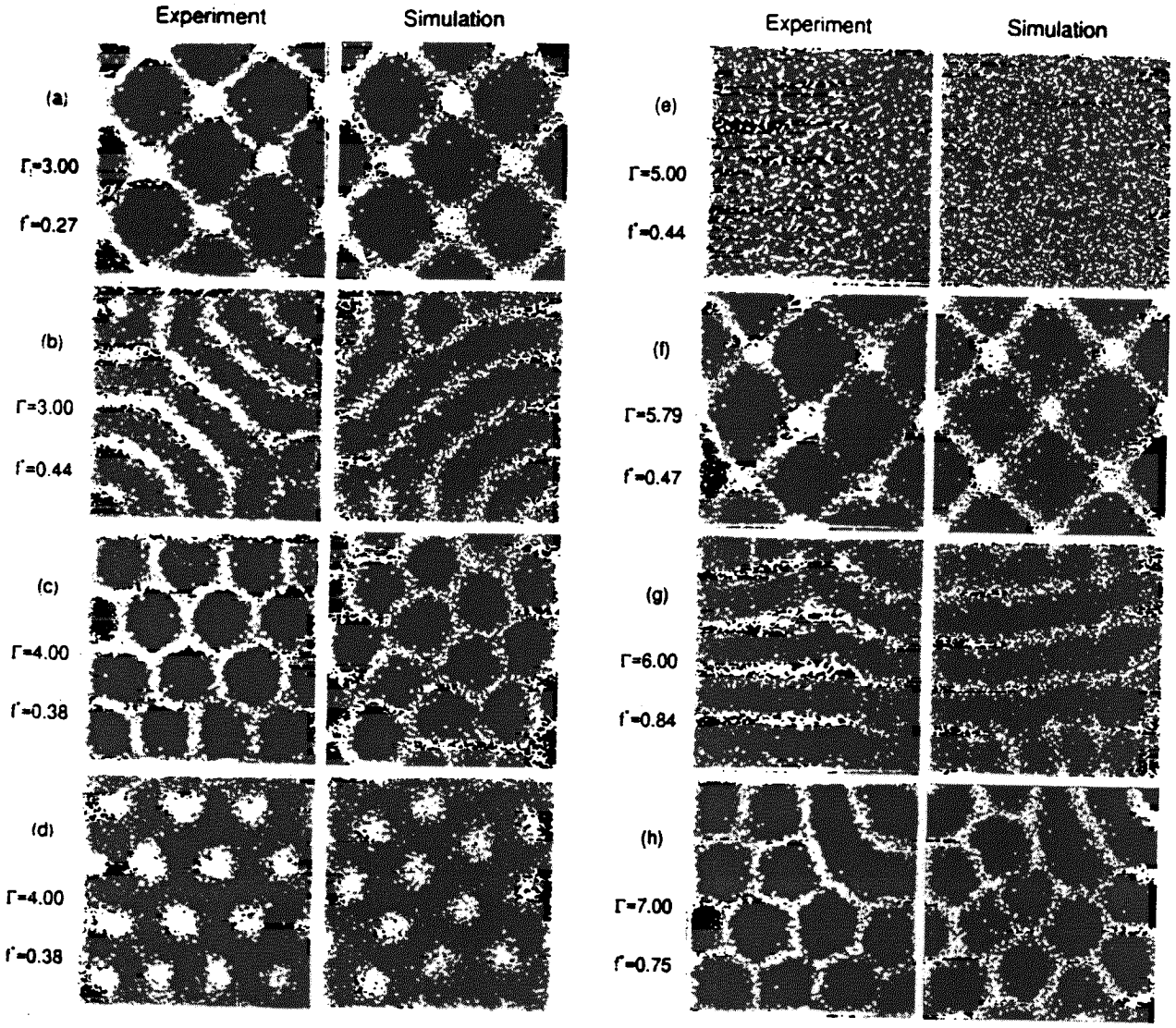

FIG. 1. Standing wave patterns: (a) squares, (b) stripes, (c) and (d) alternating phases of hexagons, (e) flat layer, (f) squares, (g) stripes, and (h) hexagons. Patterns (a)–(e) oscillate at $f/2$, (f)–(h) at $f/4$. The dimensionless layer depth N is 5.42. The brightness indicates the height of the layer. The experiments use lead spheres sieved between 0.5 and 0.6 mm.

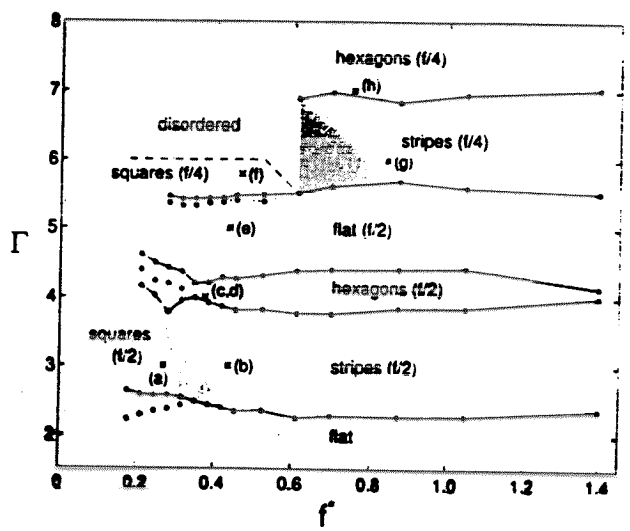

T. METCALF, J.B. KNIGHT, H.M. JAEGER.

28 grams ($^{7}/_{64}$") 0.5 mm glass beads
13 Hz shaking, 2 g RMS acceleration, 12 Torr vacuum

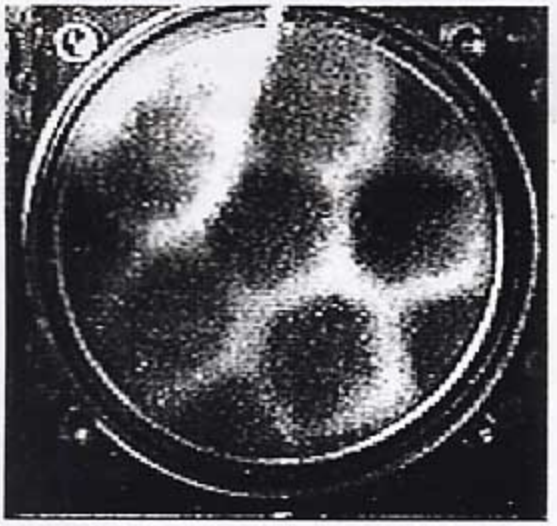

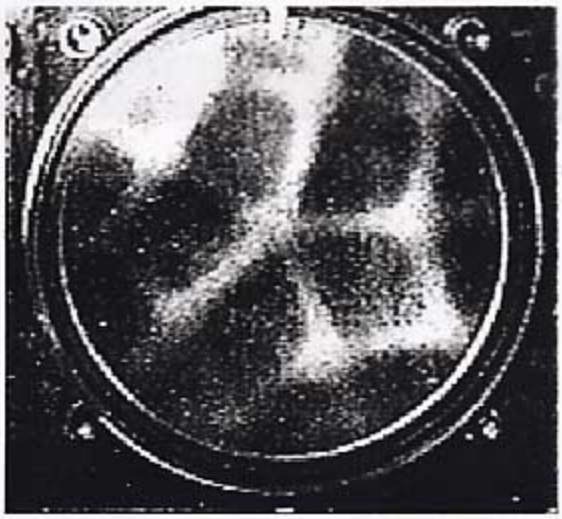

PENTAGONAL

ROLE OF AIR.

0.5mm glass beads, $^{1}/_{8}$" deep, 15 Hz, 1.8 g RMS acceleration

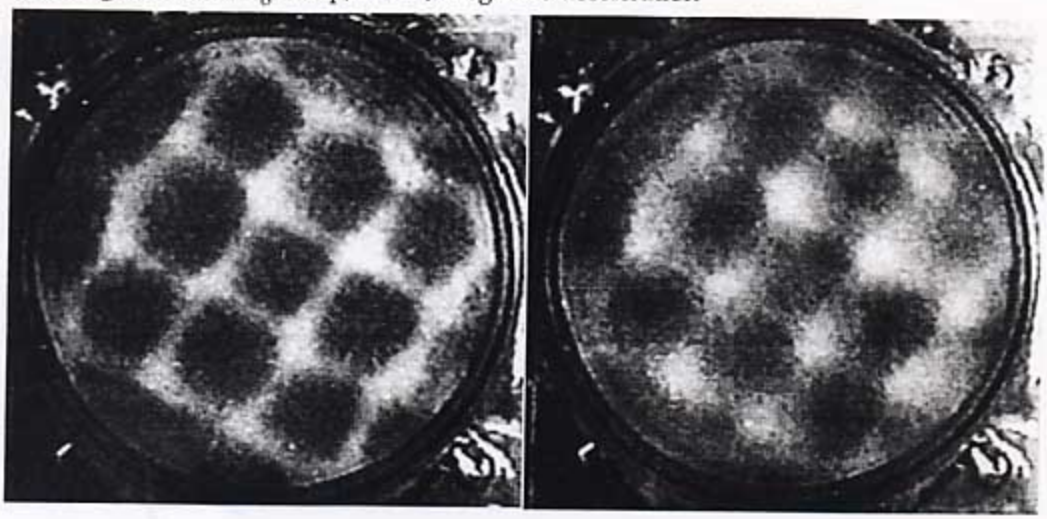

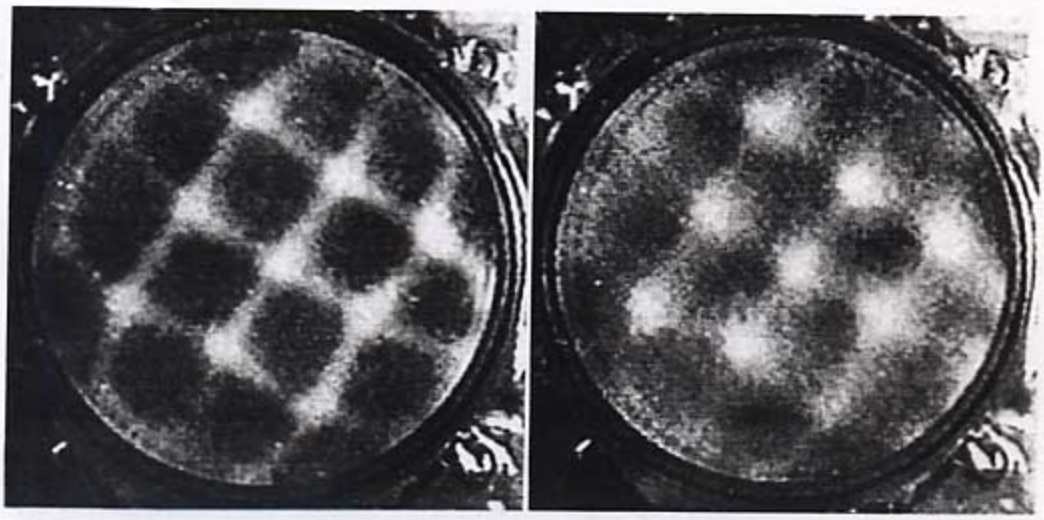

H. M. JAEGER, J. B. KNIGHT, C.-h. LIU, AND S. R. NAGEL
MAT. RES. SOC. BULL. 19, 25 (1994).

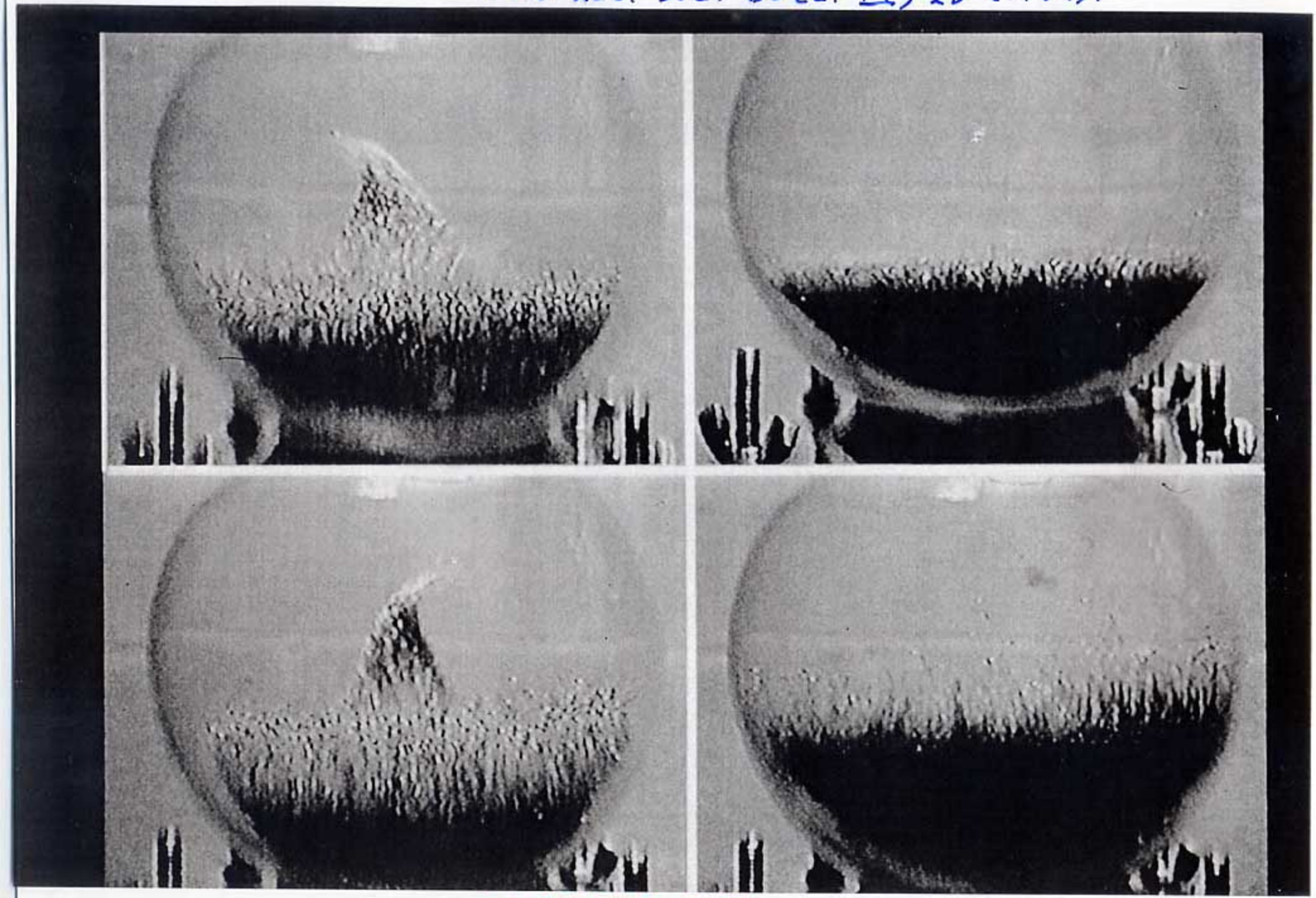

3- DIMENSIONAL

Inelastic Gases - Inelastic Collapse

What happens to a gas of inelastic particles?

It loses energy during collisions (coefficient of restitution).

It forms CLUMPS (i.e., clusters).

It also can have INELASTIC COLLAPSE.
(McNamara and Young)

It forms STRUCTURES that are long and thin.
(Goldhirsch and Zanetti)

What is the relation of Collapse and Clustering?

Can the existence of clustering be predicted by hydrodynamics?

Does inelastic collapse have any "real" consequences?

Inelastic Gases

Energy lost during each collision

$\Rightarrow$ **clusters**

and collapse (McNamara and Young, Zhou and Kadanoff, Grossman, Mungan and Constantin)

Leads to structures

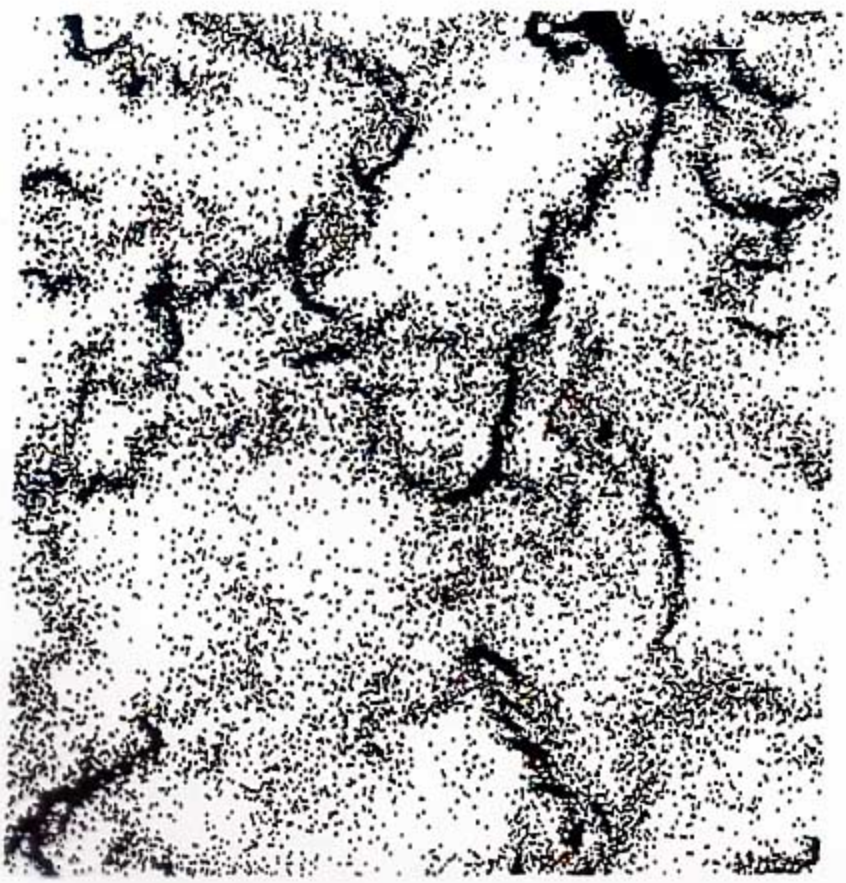

Goldhirsch and Zanetti

Velocity Fluctuations in a Homogeneous 2D Granular Gas in Steady State

Florence Rouyer* and Narayanan Menon†

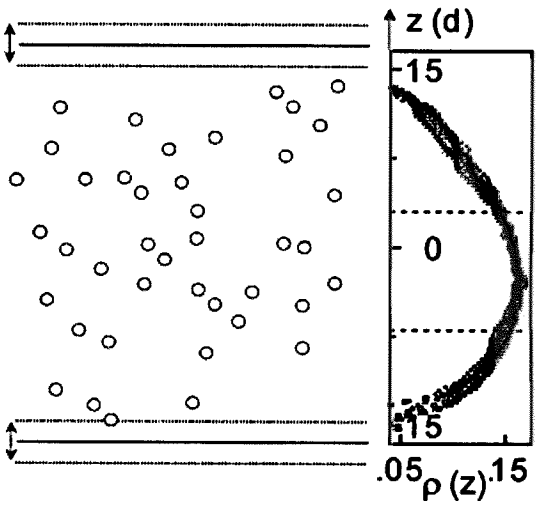

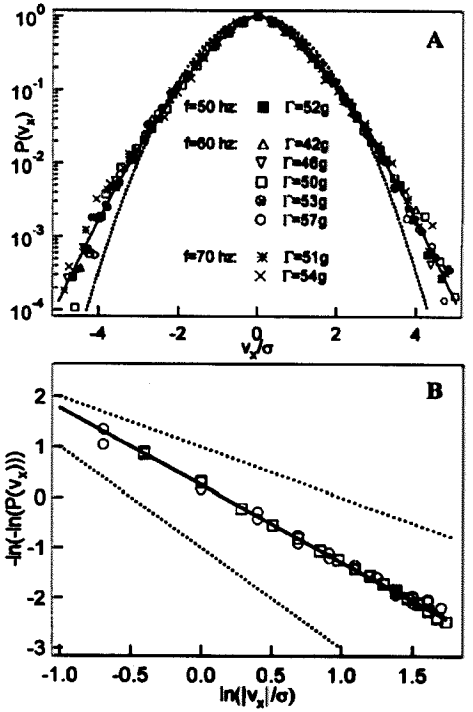

FIG. 2. (a) $P(v_x/\sigma)$. the histogram (normalized to be 1 at maximum) of scaled horizontal velocity v_x/σ for $\rho = 0.15$ for different values of f and Γ in a rectangular cell. v_0 is varied from 1.1 to 1.6 m/s and A from 1.6 to $3.2d$. σ varies from 0.40 to 0.62. The dotted line is a Gaussian: $\exp[-\frac{1}{2}(v_x/\sigma)^2]$. it overestimates small velocities and underestimates large velocities. (b) $-\ln\{-\ln[P(v_x/\sigma)]\}$ vs $\ln(|v_x|/\sigma)$ for $\rho = 0.15$ in a rectangular cell (squares), and in a circular cell (circle). The slope of the linear fit (solid line) is -1.52. The dotted lines with slopes equal to -1 and -2 correspond to an exponential and a Gaussian.

Size Separation:
The Convection Connection

BRAZIL NUT EFFECT:

If you shake things up, the big nuts rise to the top.

(Big nuts rise to the top in a container of mixed nuts.)

What drives size separation?

Local rearrangements (such as avalanching)? (Williams, Rosato, Jullien, Duran)

But then how is shaking different from thermal agitation?

Convection drives size separation.

What drives convection?

Faraday, 1831, thought air flow did.

CONVECTION AND SIZE SEPARATION
IN VIBRATED GRANULAR MATERIALS

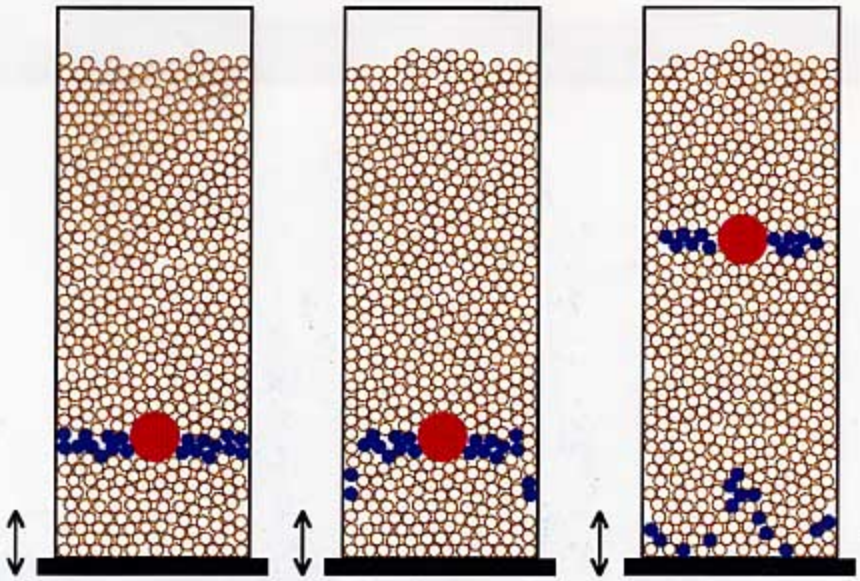

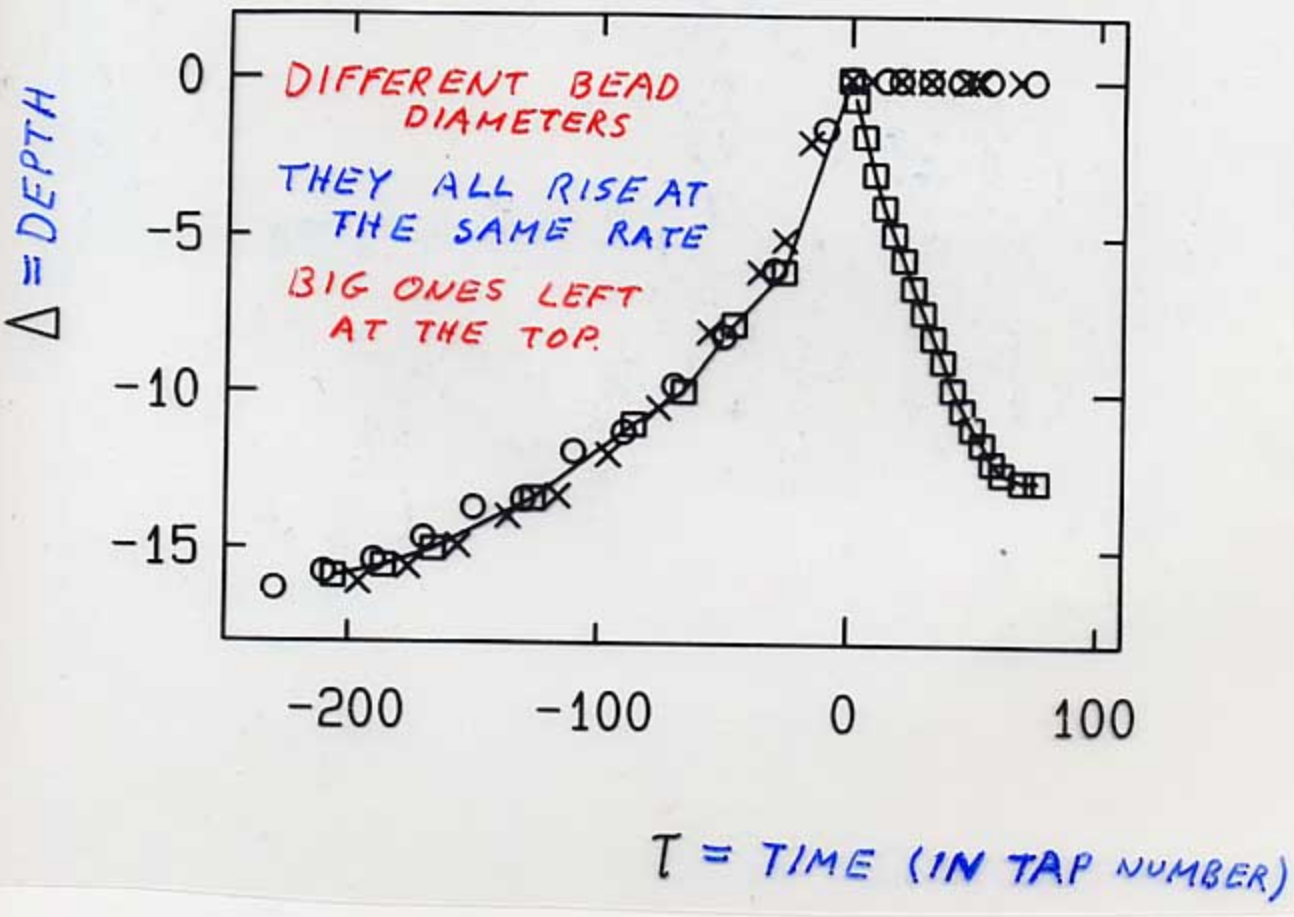

Convection

Tracer Beads allow measurement of slow flows.

Magnetic Resonance Imaging (MRI) allows 3-d probe of convection. (flow profile vs. depth, radius)

Vary boundary conditions:
- **Friction at walls**
- **Slope of walls**
- **Aspect ratio of container**

Vary forcing:
- **Acceleration**
- **Frequency**

VARY Γ

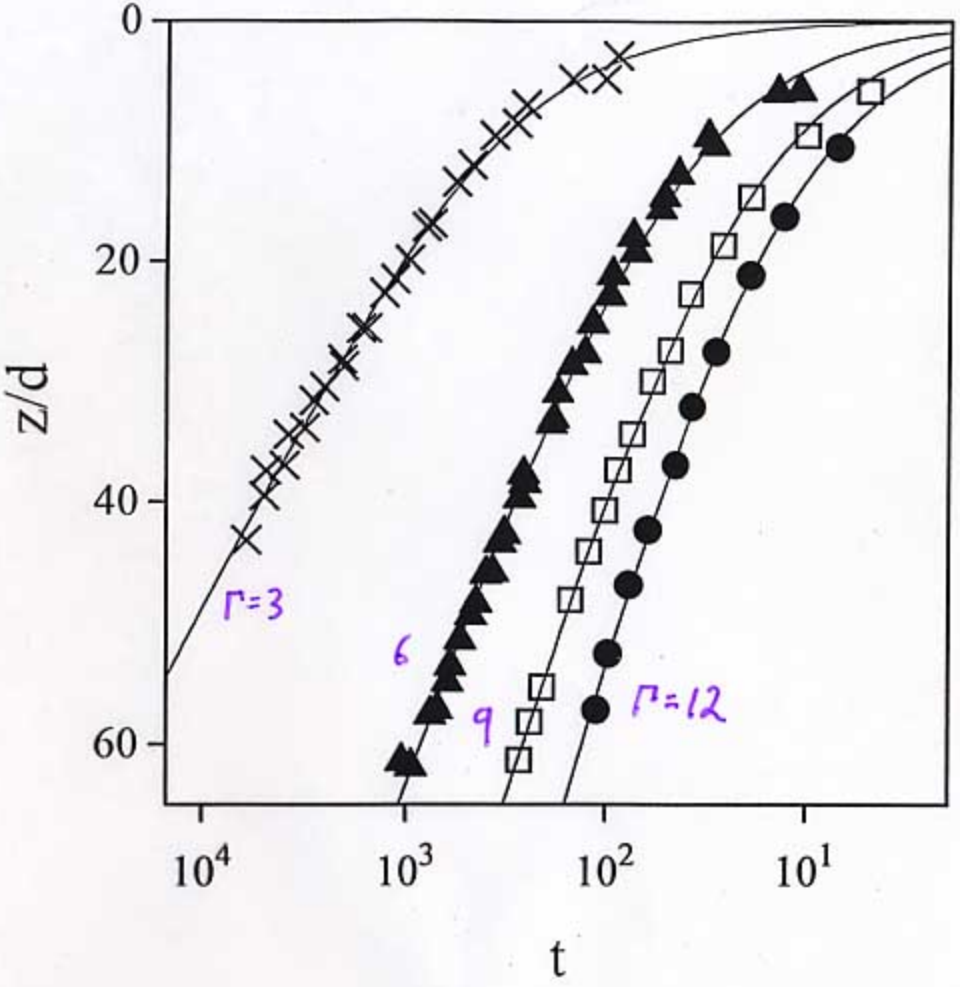

f = 30.5 Hz

VARY f

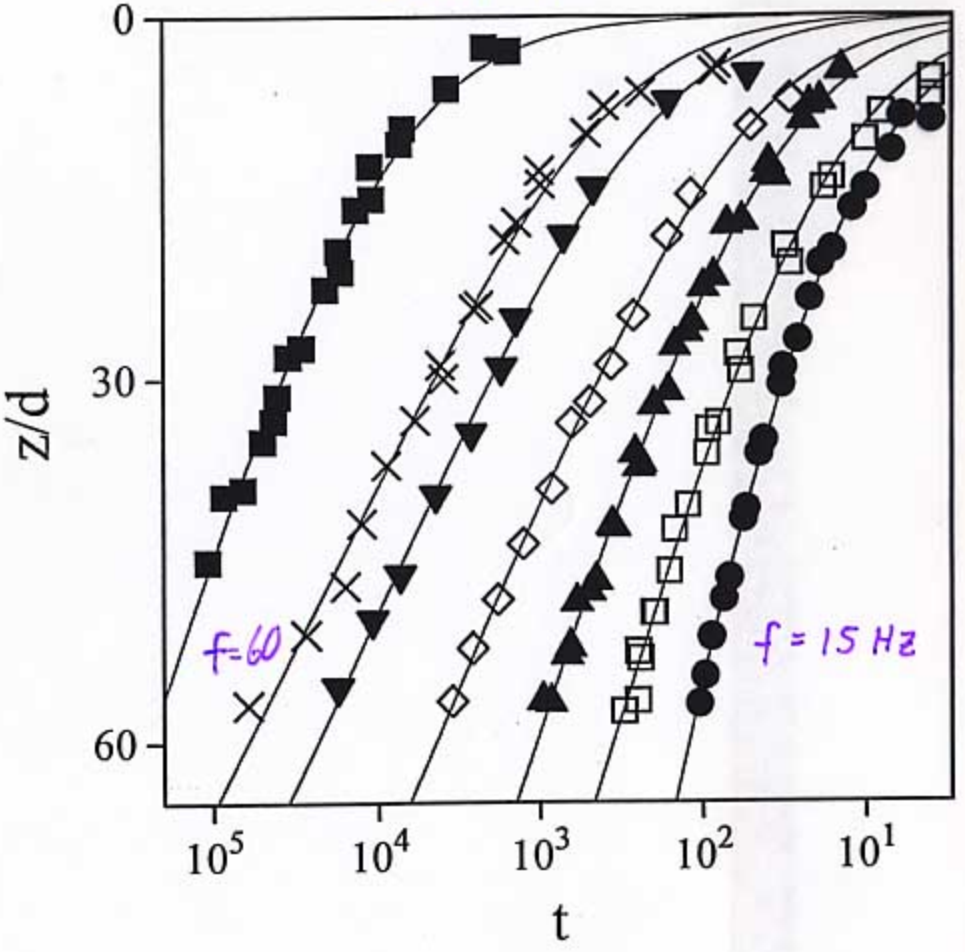

Γ = 6

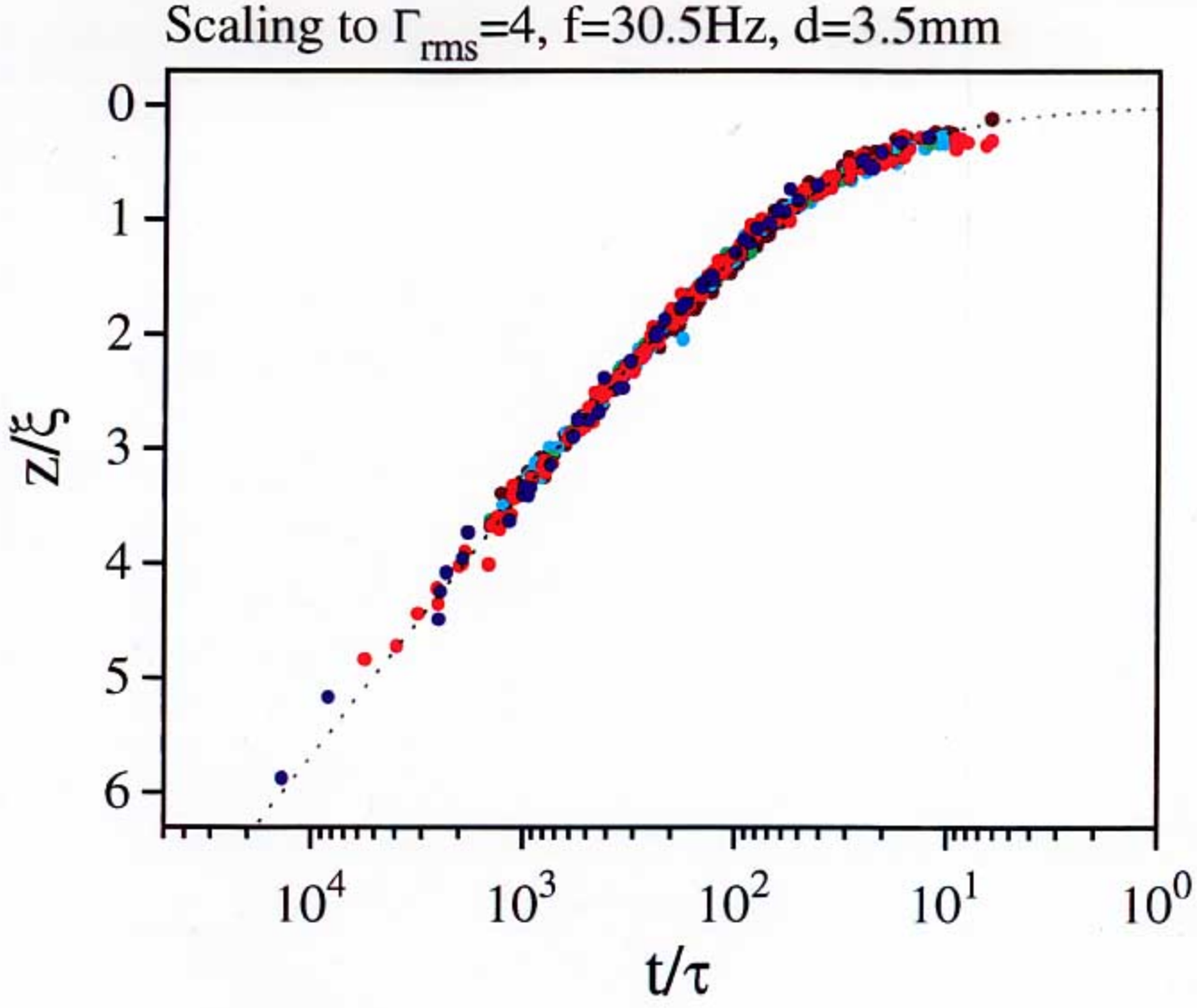

frequency: 10 Hz < f < 100Hz

acceleration : 1.5< Γ_{rms} <9.3 ($\Gamma_{rms} \alpha Af^2$)

waveform: both discrete & continuous

particle diameter: 1.0mm < d < 3.5mm

container diameter: D = 57mm

TIME

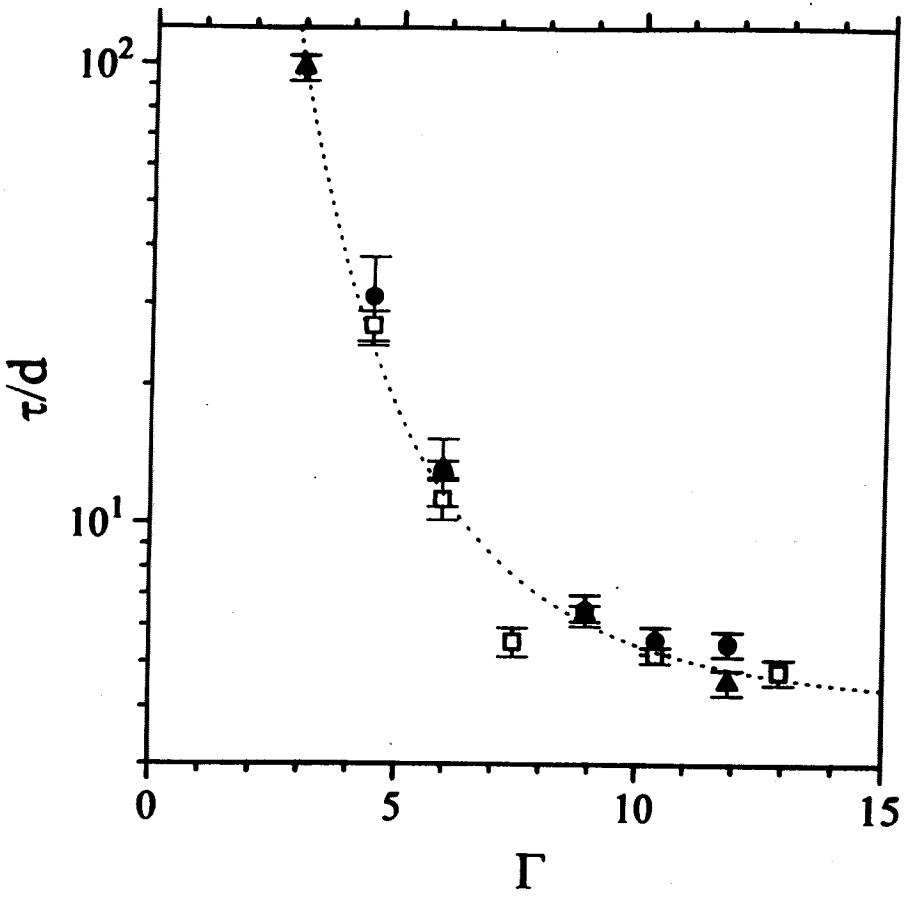

LENGTH

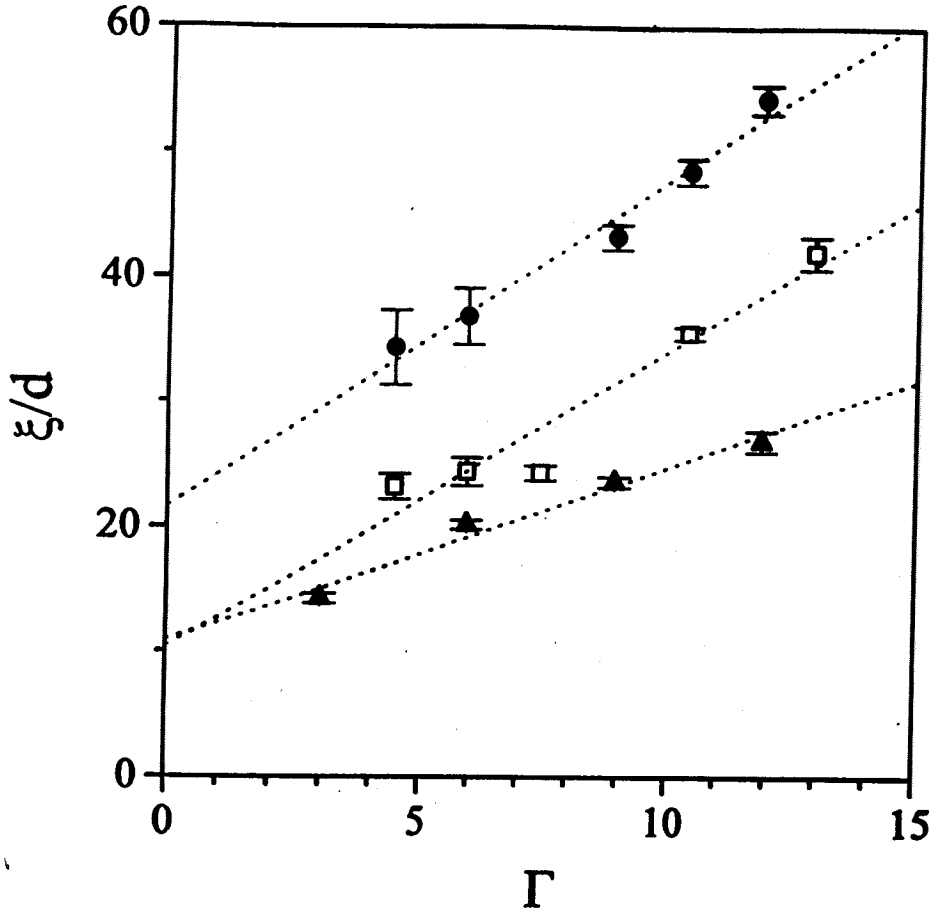

LIKE A GLASS??

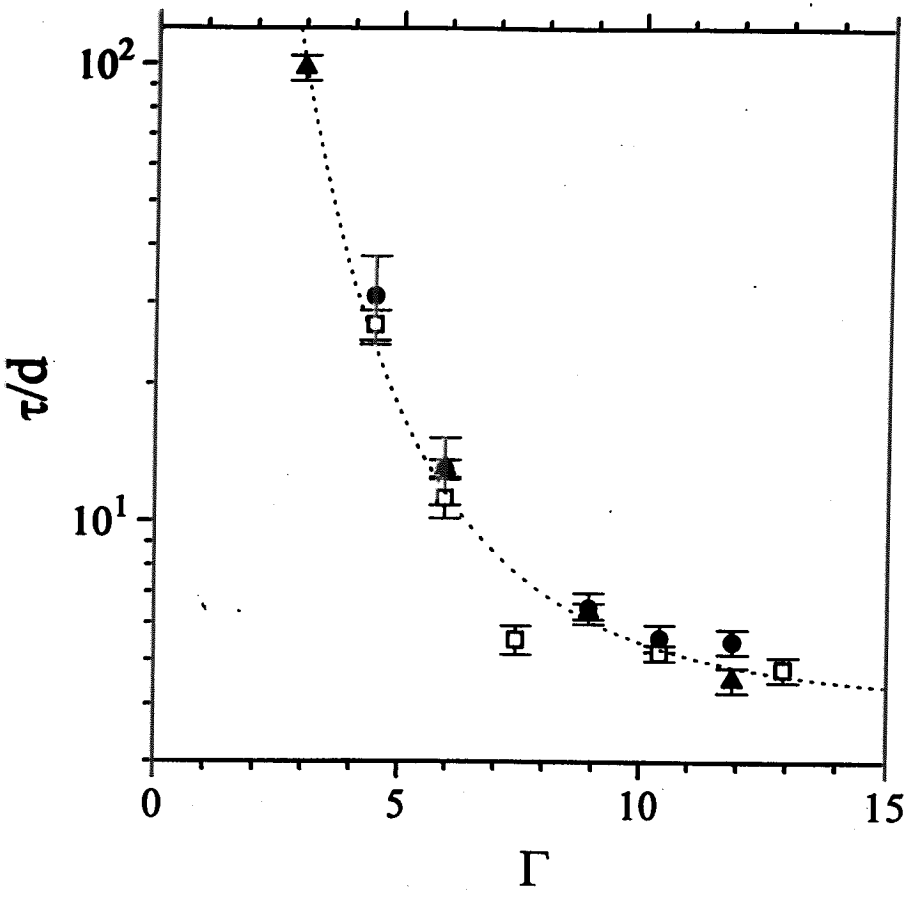
10^2
10^1
τ/d
0
5
10
15
Γ

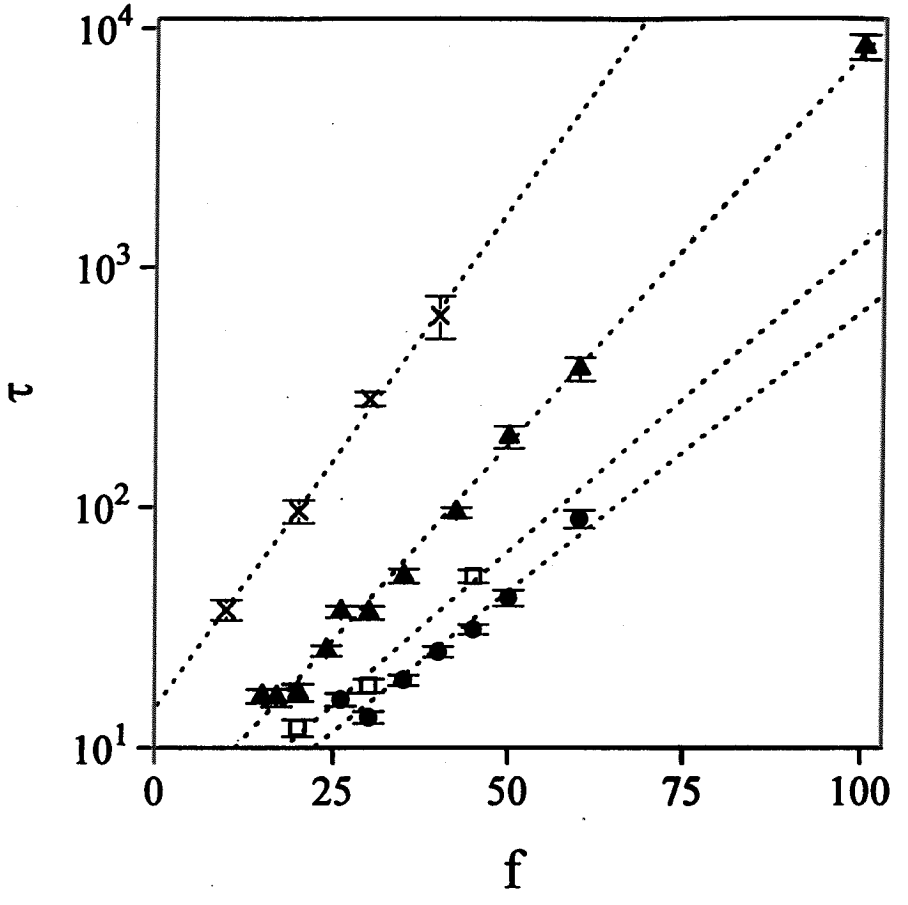
10^4
10^3
10^2
10^1
τ
0
25
50
75
100
f

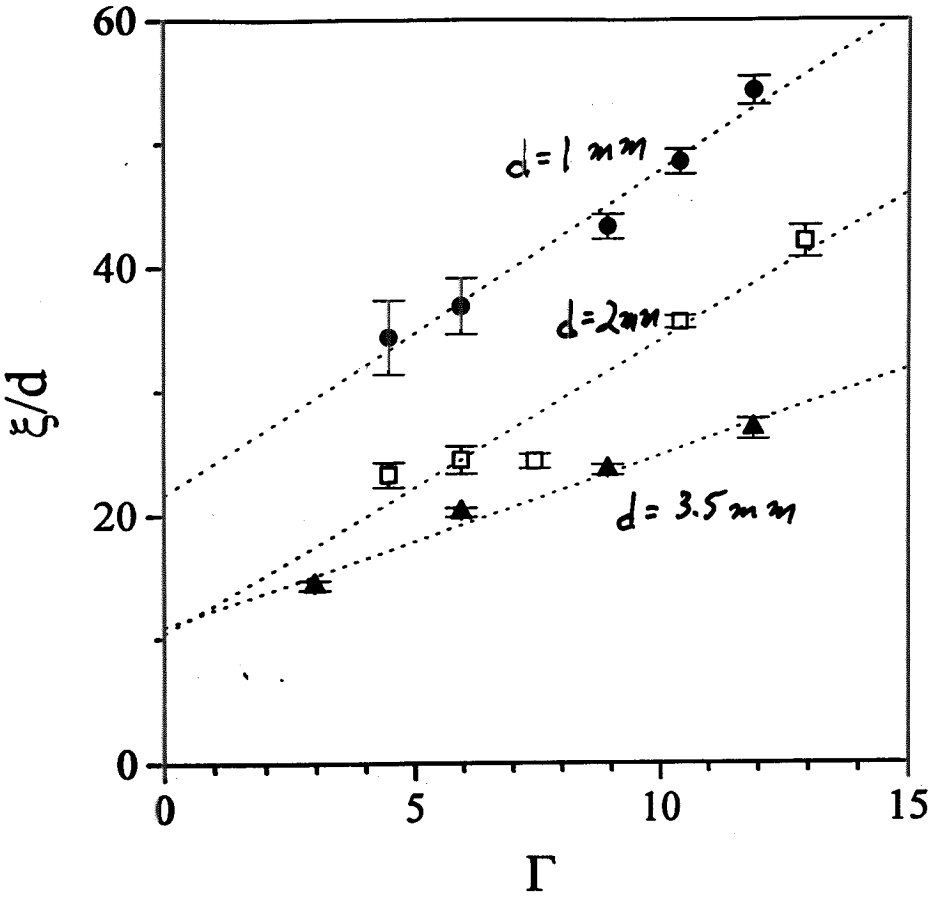

f = 30.5 Hz

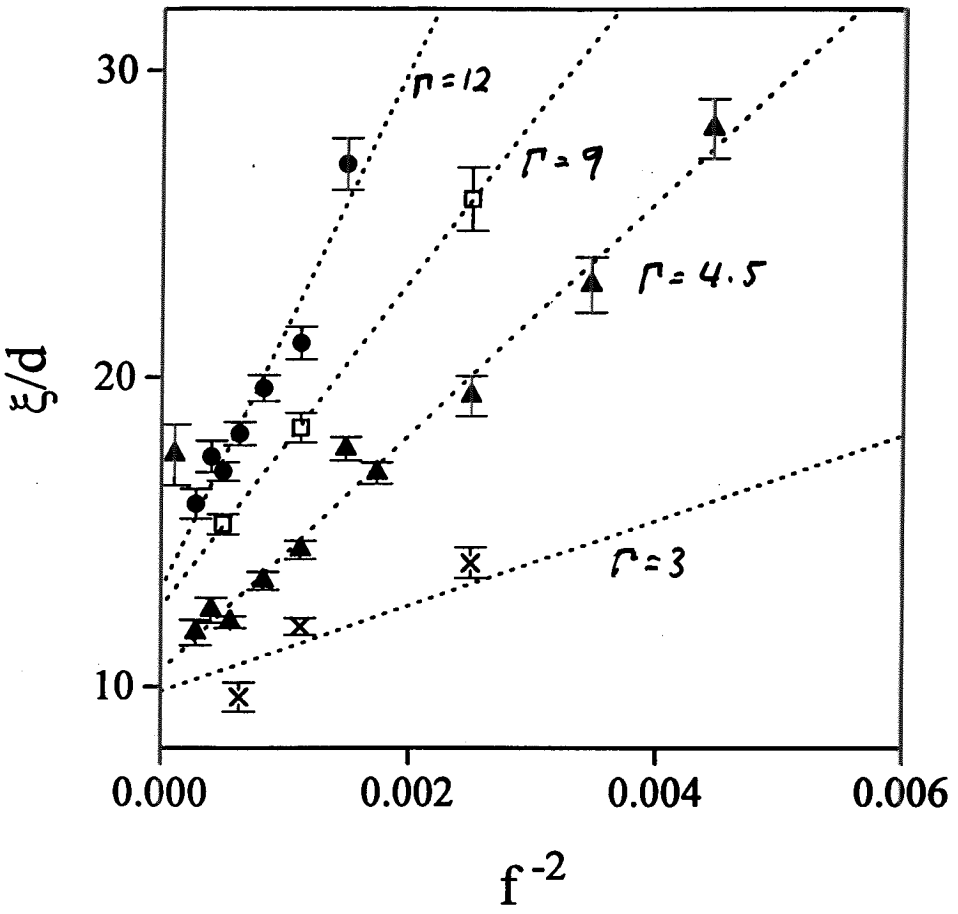

Γ = 3, 4.5, 9, 12

d = 3.5 mm

Magnetic Resonance Imaging of Convection Rolls

Ehrichs, Jaeger, Karczmar, Knight, Kuperman and Nagel

[MRI techniques first used on granular avalanches by Nakagawa et al., *Experiments in Fluids*, 16, 54 (1993).]

MRI: non-invasive probe maps flow patterns in interior of container.

Determine flow profiles quantitatively.

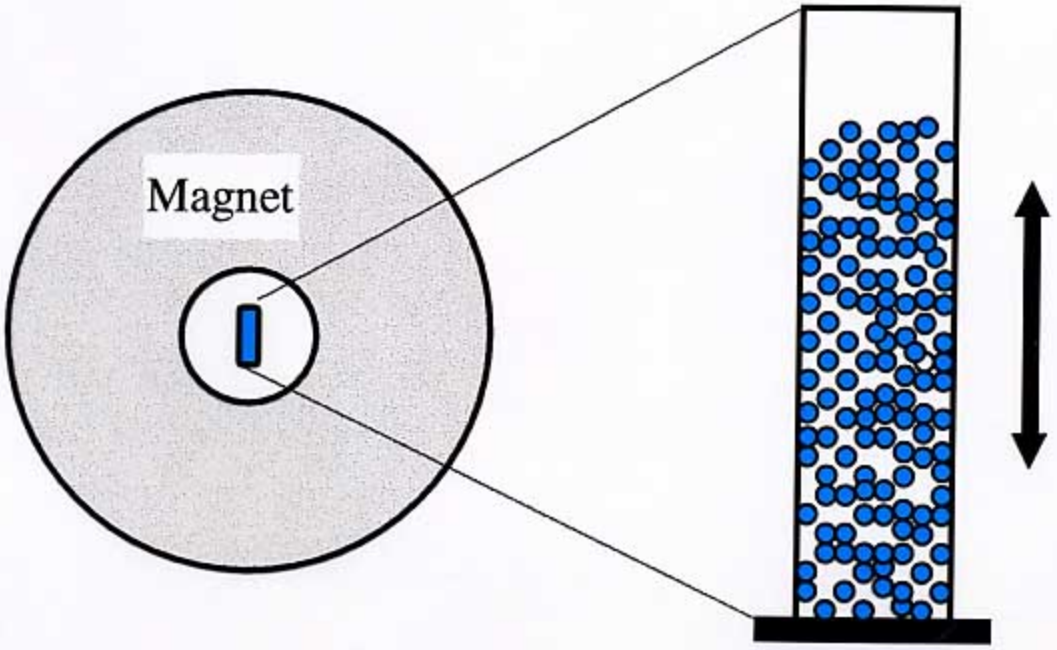

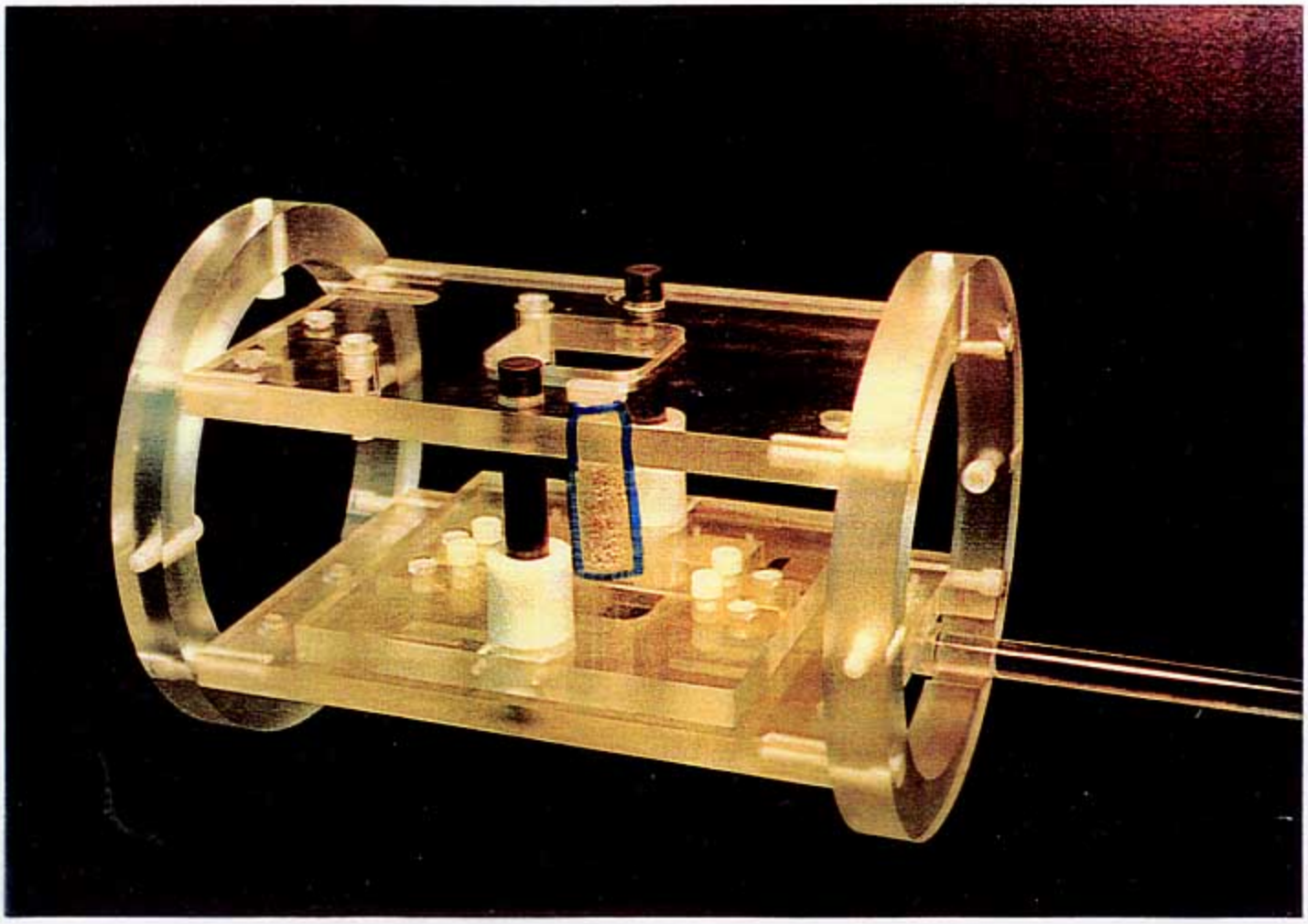

Coffee Beans Rise to the Top

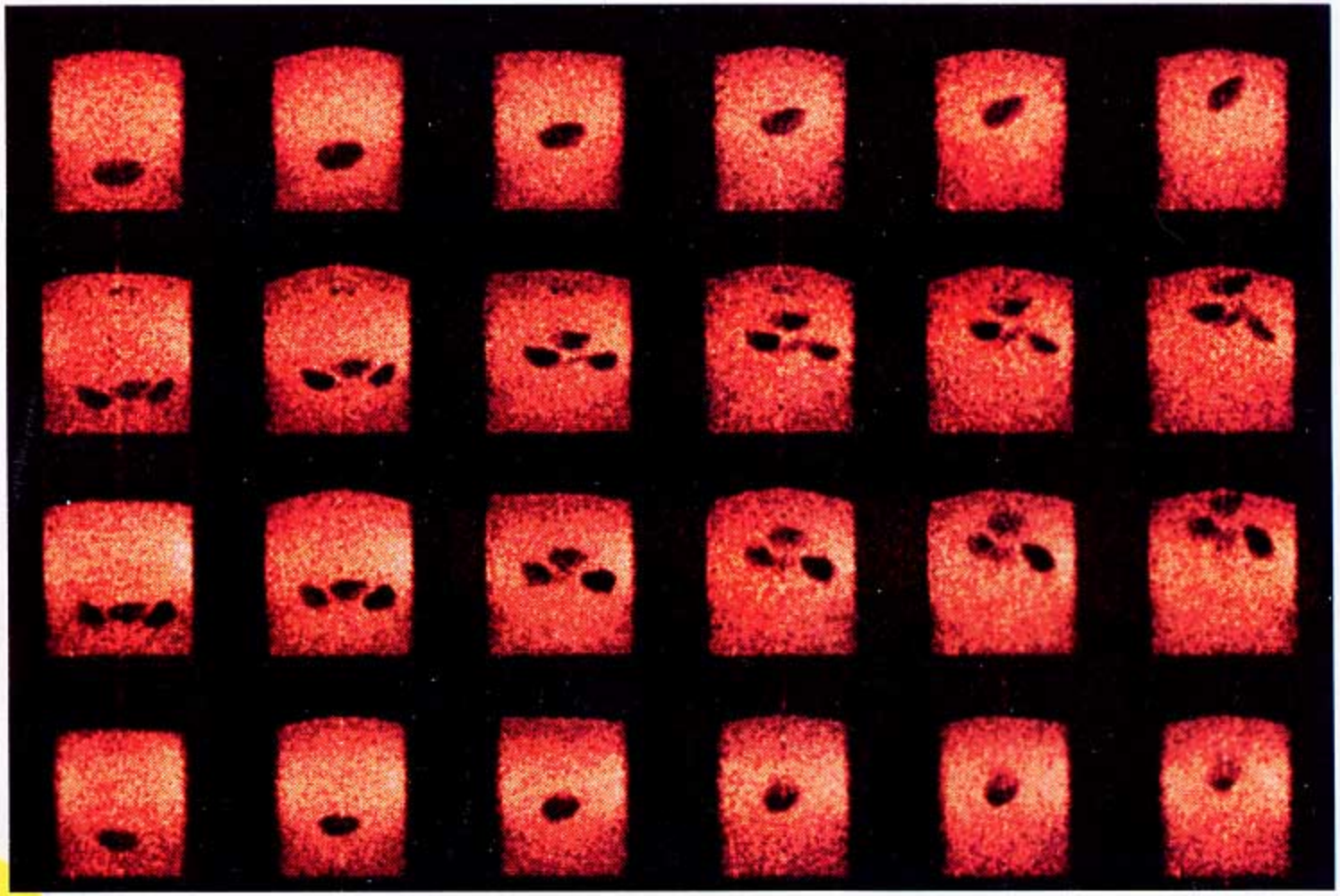

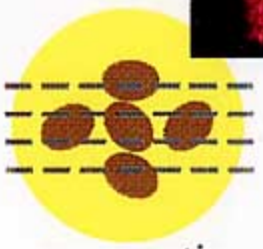

cross section

time (taps) ⟶

Spin Tagging

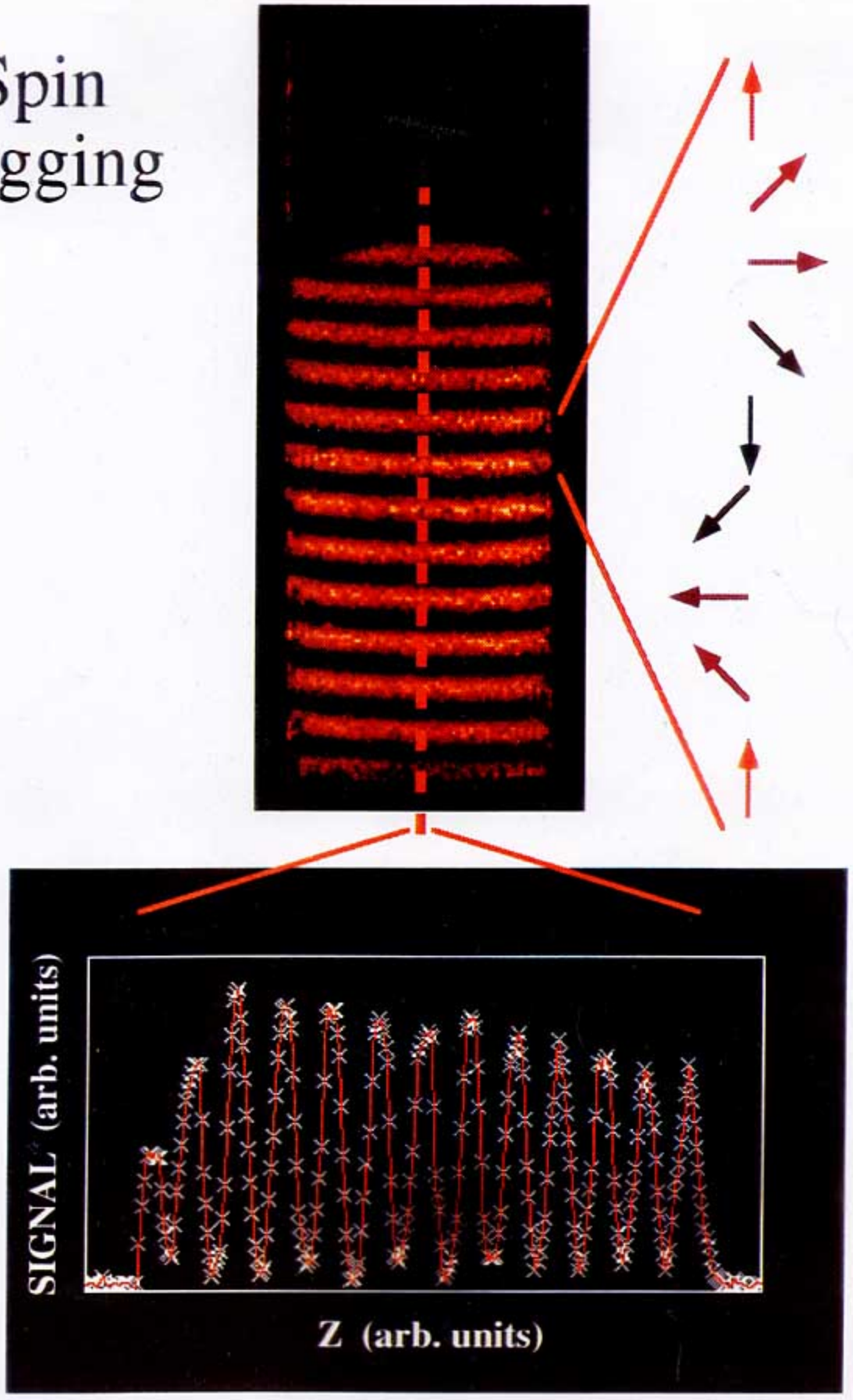

$T_1 \sim 200$ ms

$\Gamma = 6$

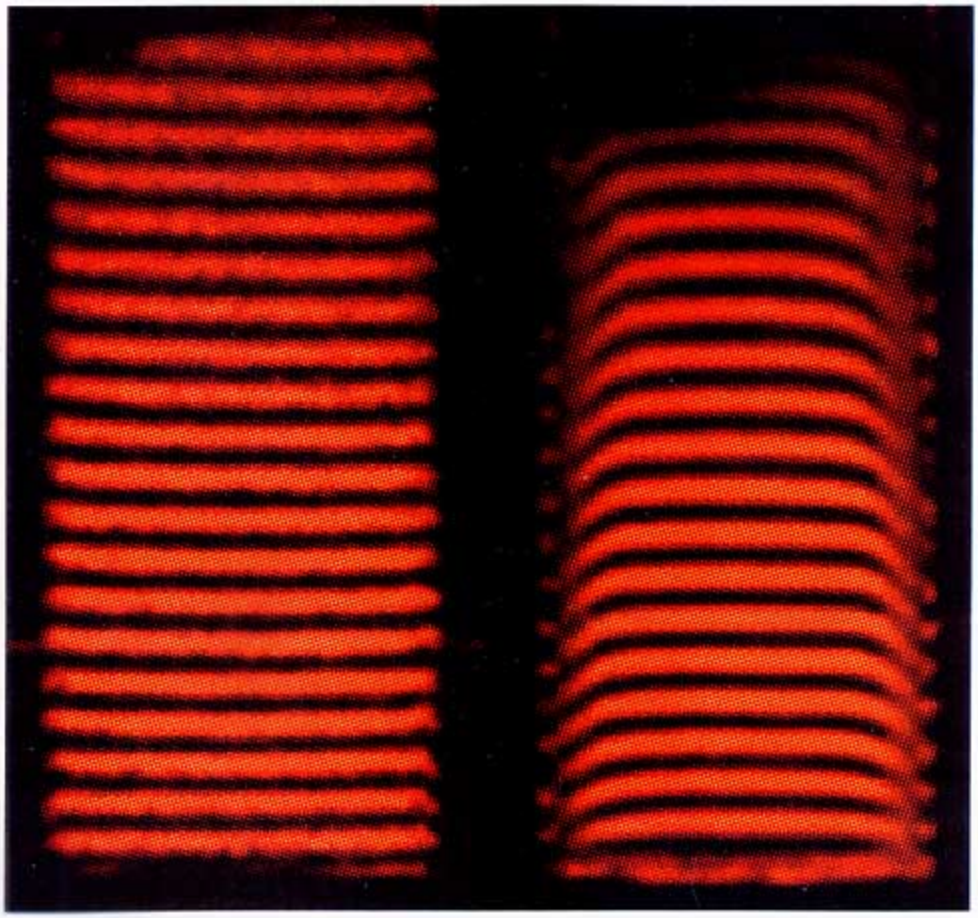

← 25 mm →

SEEDS GLUED TO WALL

Control Image (0g)

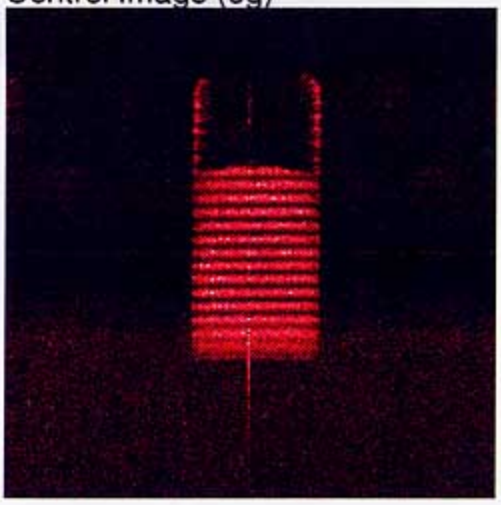

3g

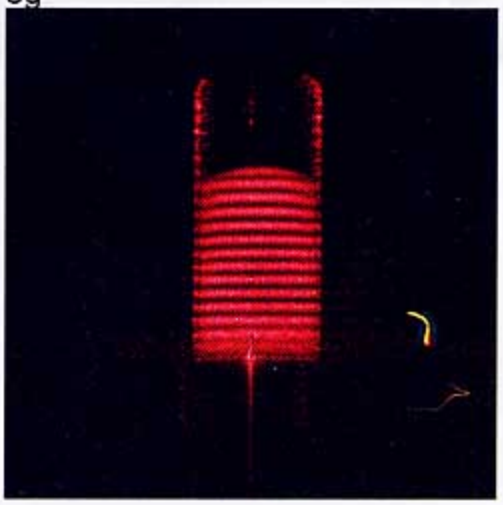

4g

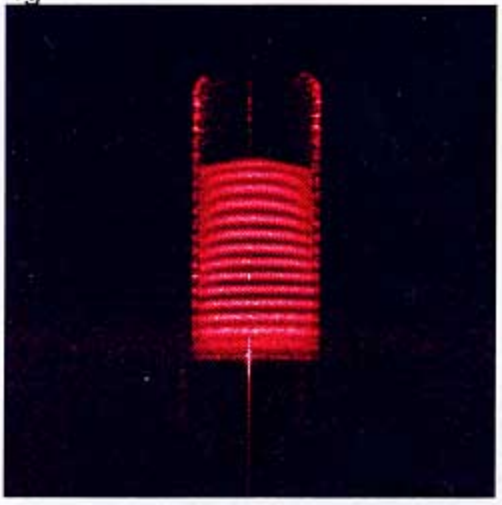

5g

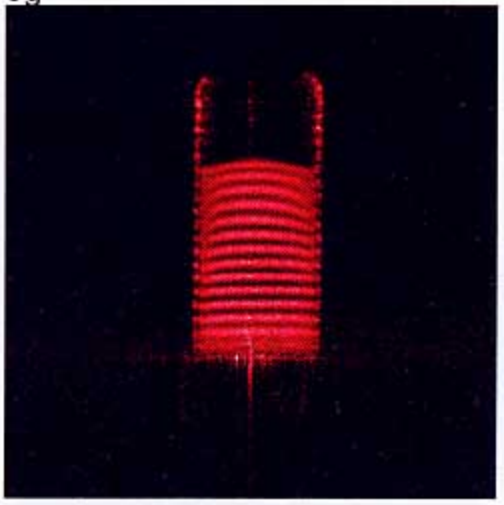

6g

8g

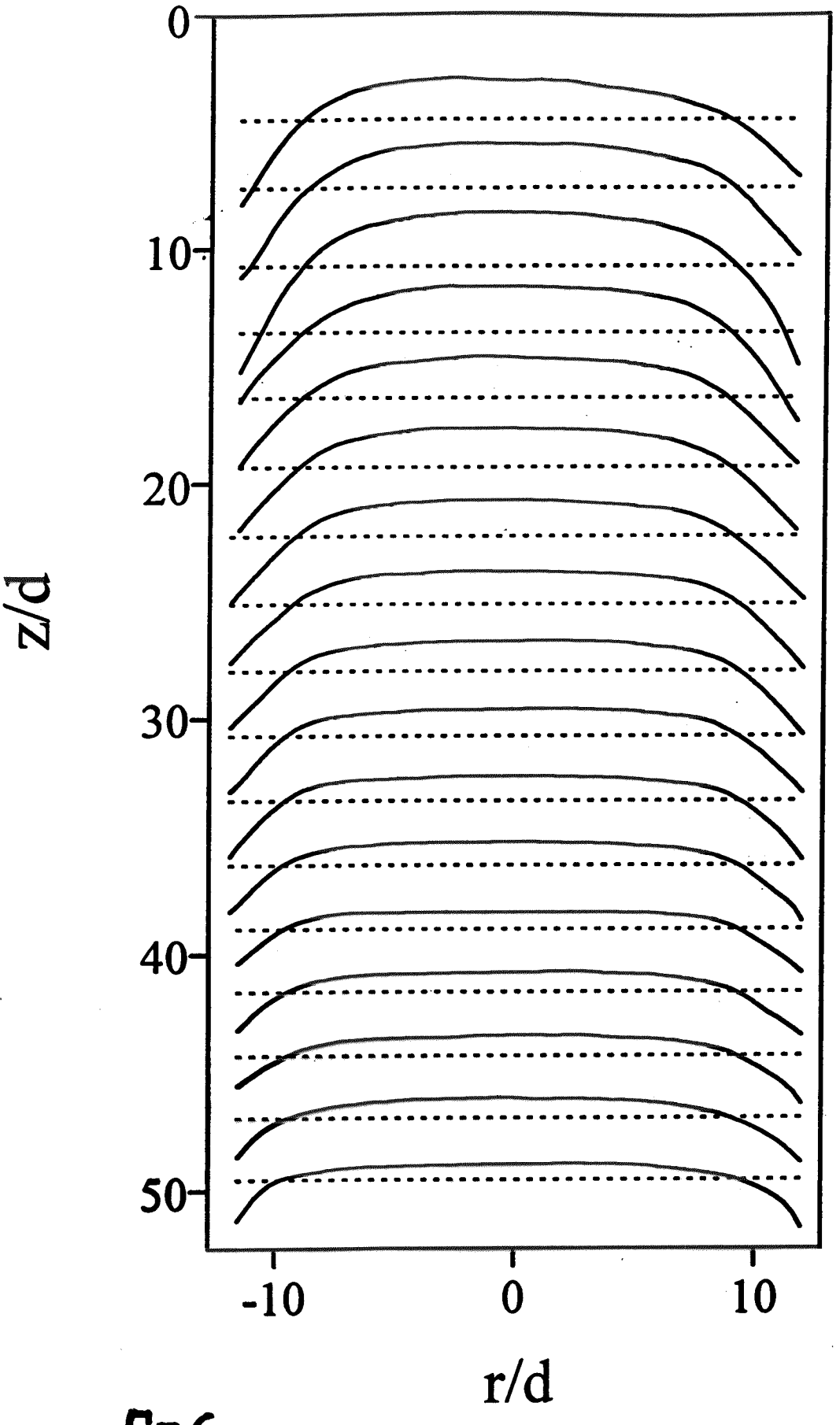

Γ=6

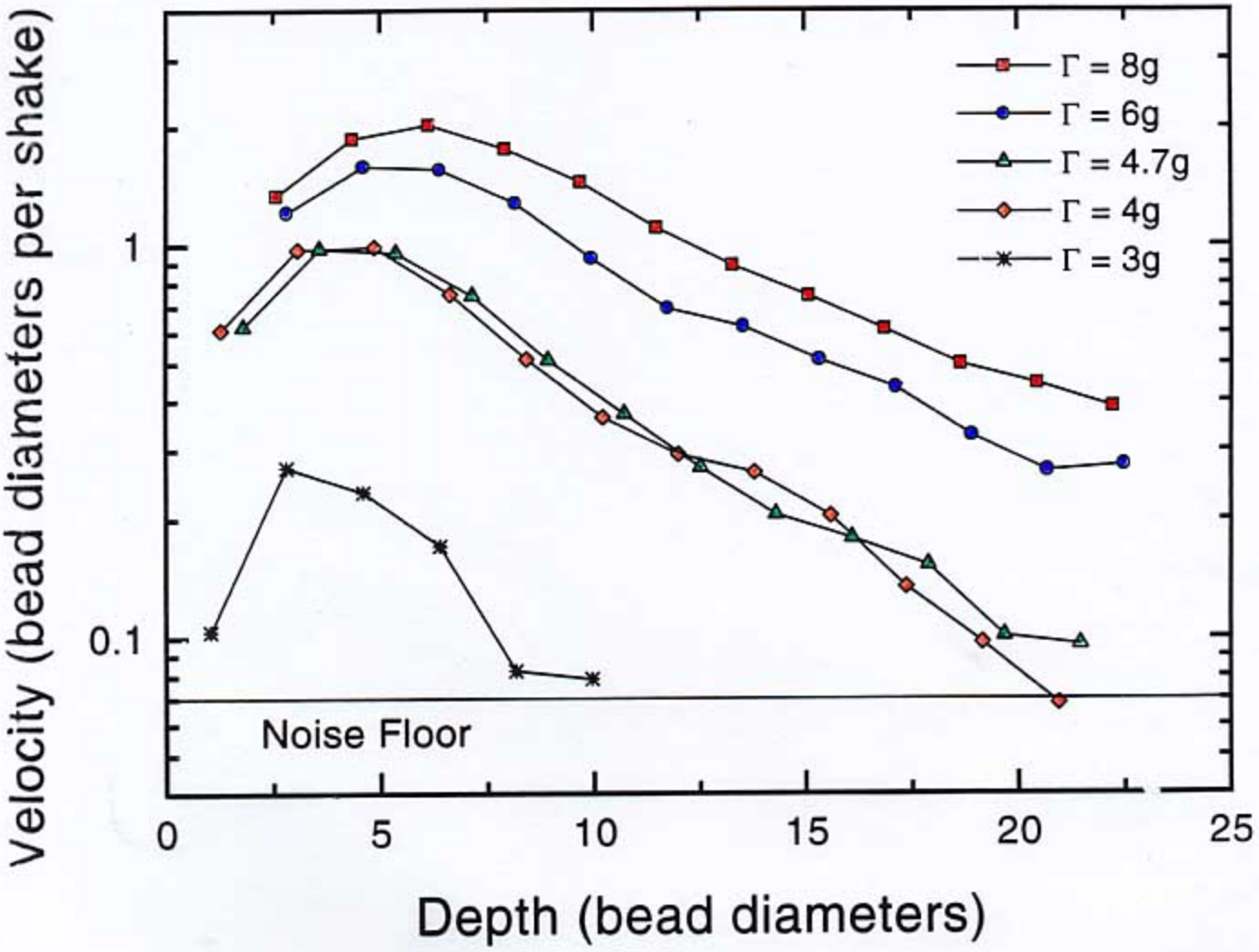

$\text{VELOCITY} \propto e^{-\text{DEPTH}/\xi}$

Velocity at 3 Depths ($\Gamma = 6$)

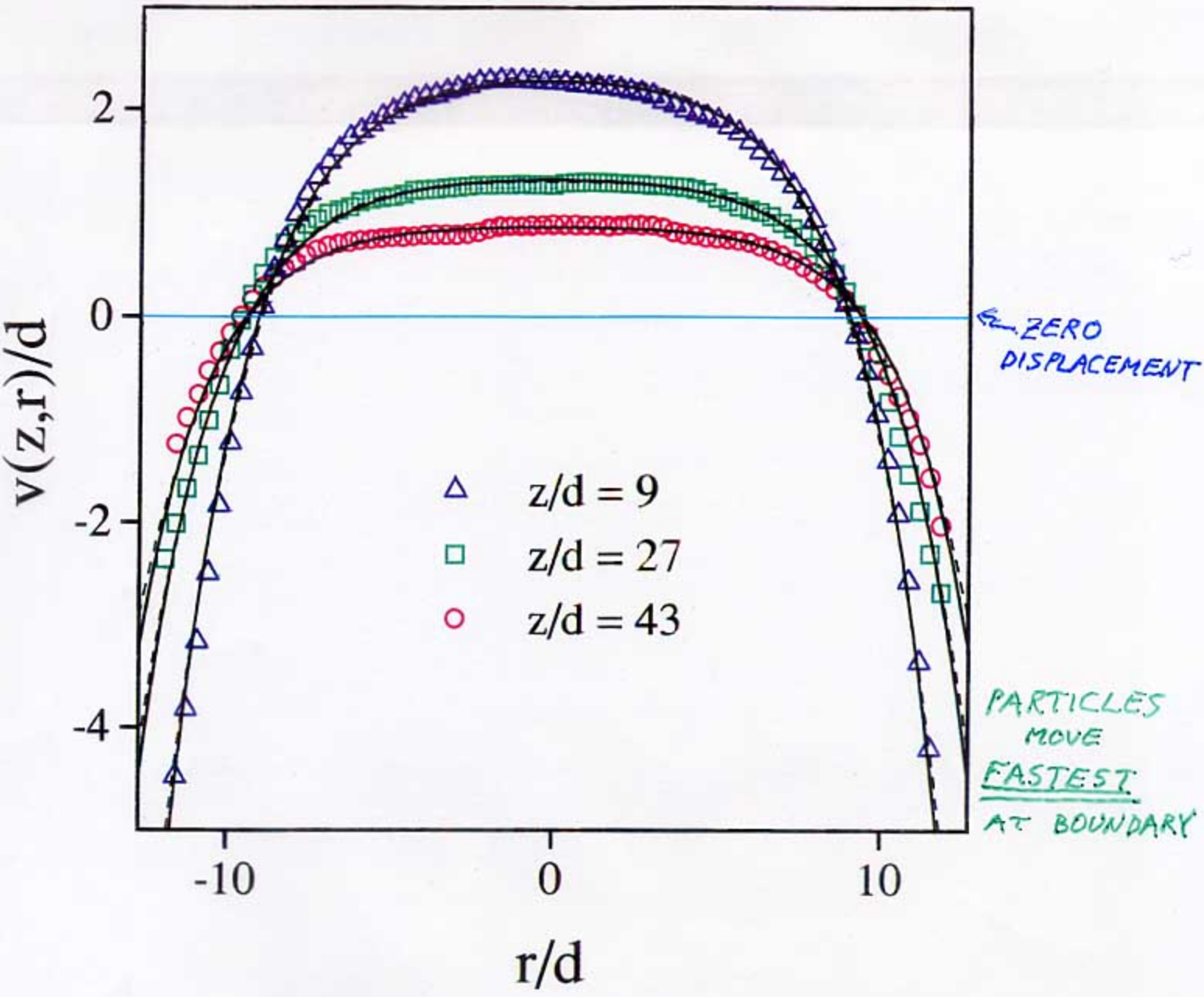

——— $v(r,z) \propto \cosh(r/r_c)$

- - - - - - $v(r,z) \propto I_0(r/r_c)$

or

$$v_z(r) = v_o[1 + A(1-\cosh(r/r_c))]e^{-z/\xi}$$

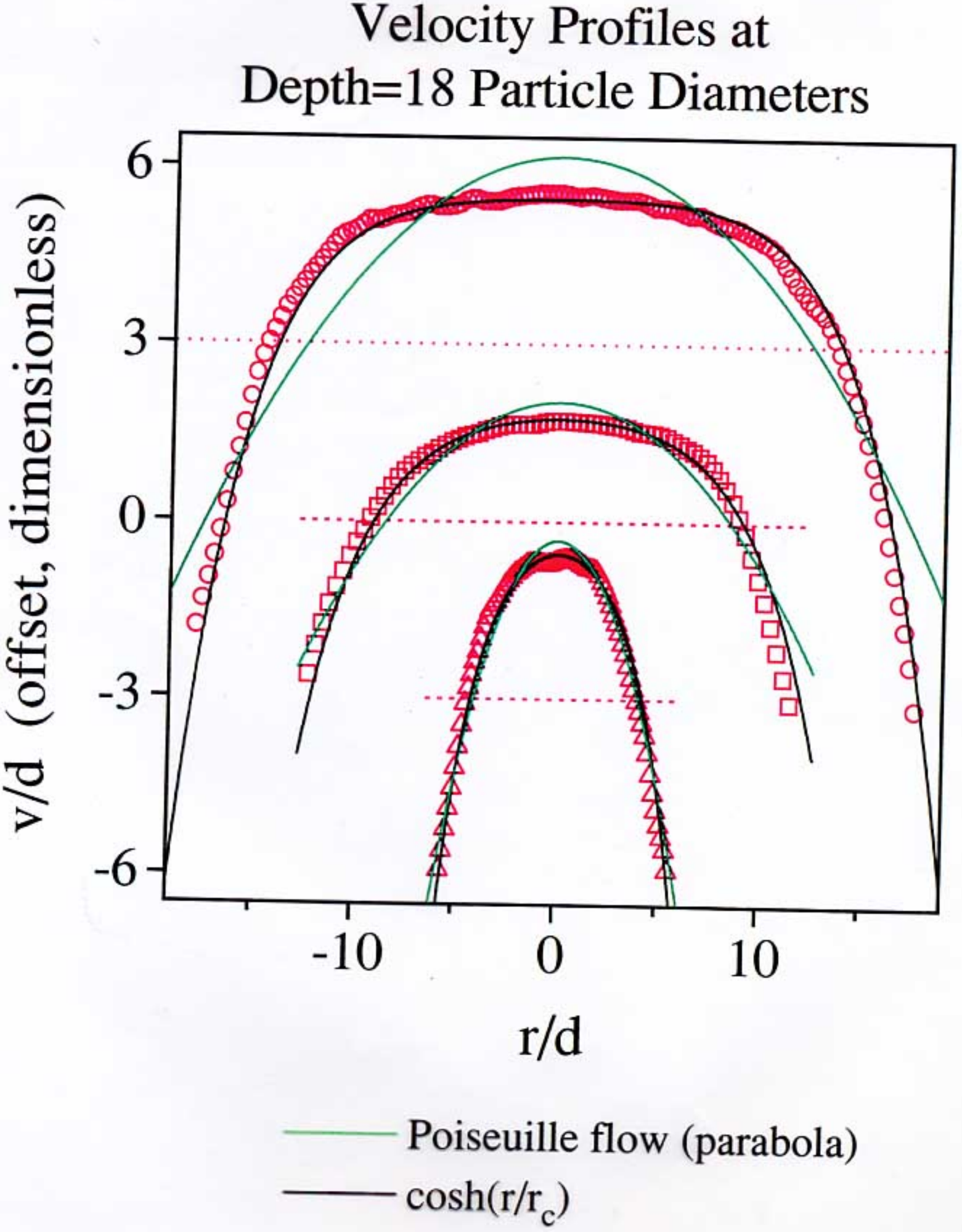
Velocity Profiles at
Depth=18 Particle Diameters
v/d (offset, dimensionless)
6
3
0
-3
-6
-10
0
10
r/d
Poiseuille flow (parabola)
cosh(r/r_c)

Conclusions

- Depth Dependence of Velocity (Tracer Beads, MRI):

$$v(r,z) = \frac{\xi}{\tau}\left(1 - \frac{1}{f\left(R/r_c\right)}\left(1 - I_0\left(r/r_c\right)\right)\right)e^{-\frac{z}{\xi}}$$

  - Equivalently, $I_0 \longrightarrow \cosh$

- Width of the Downward Flow Proportional to Container Size (MRI):

$$w_d \propto R$$

- Acceleration (Γ) and Frequency (f) Dependence of Length (ξ) and Time (τ) Scales (Tracer Beads):

$$\xi \propto \frac{\Gamma}{f^2} \propto A \qquad \tau \propto d\exp\left(\frac{f}{f_0}\right)$$

τ diverges at low Γ

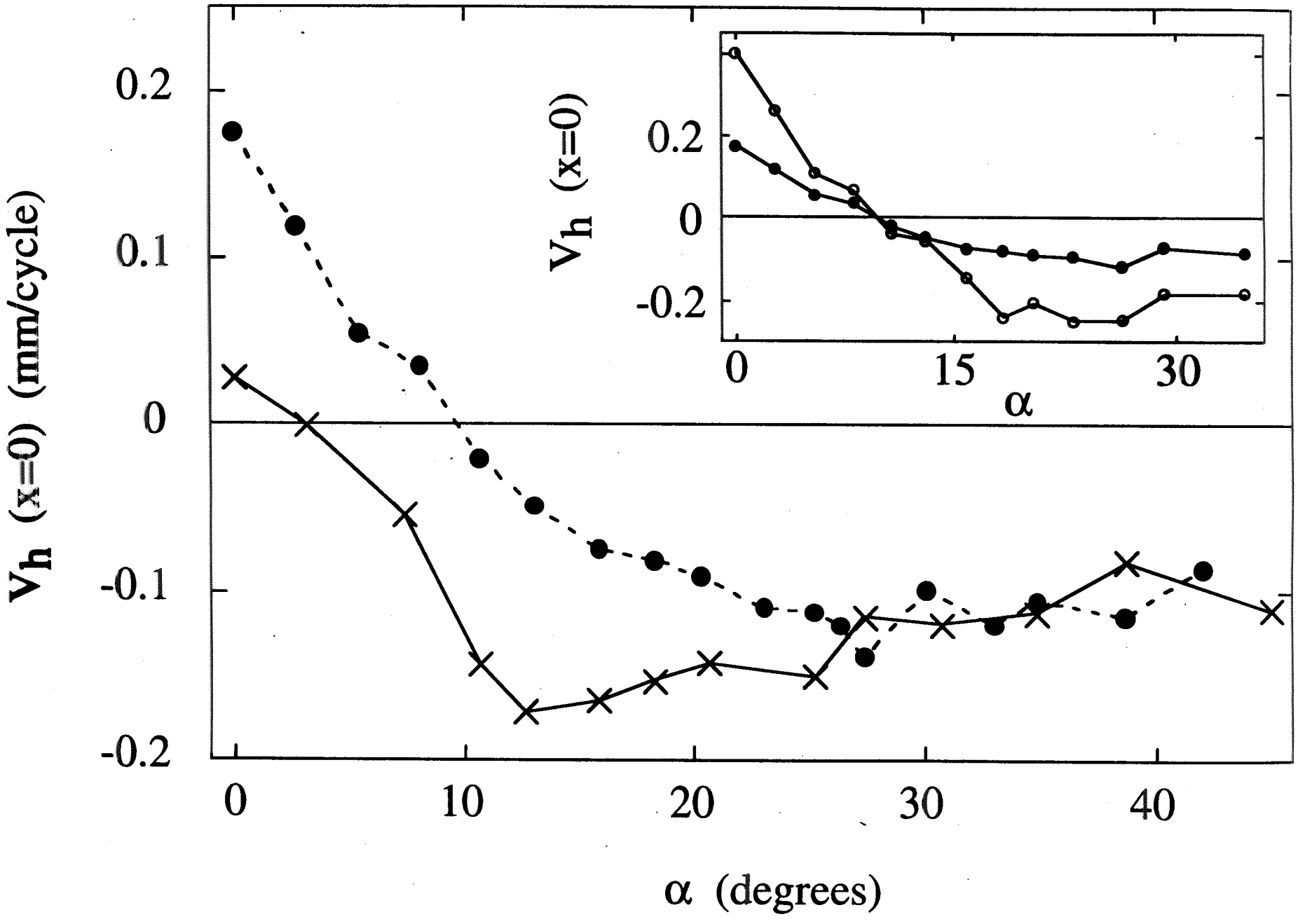
0.2
0.1
0
-0.1
-0.2
0
10
20
30
40
V_h (x=0) (mm/cycle)
α (degrees)
V_h (x=0)
0.2
0
-0.2
0
15
30
α

Intruder in the Dust
Experimental Setup

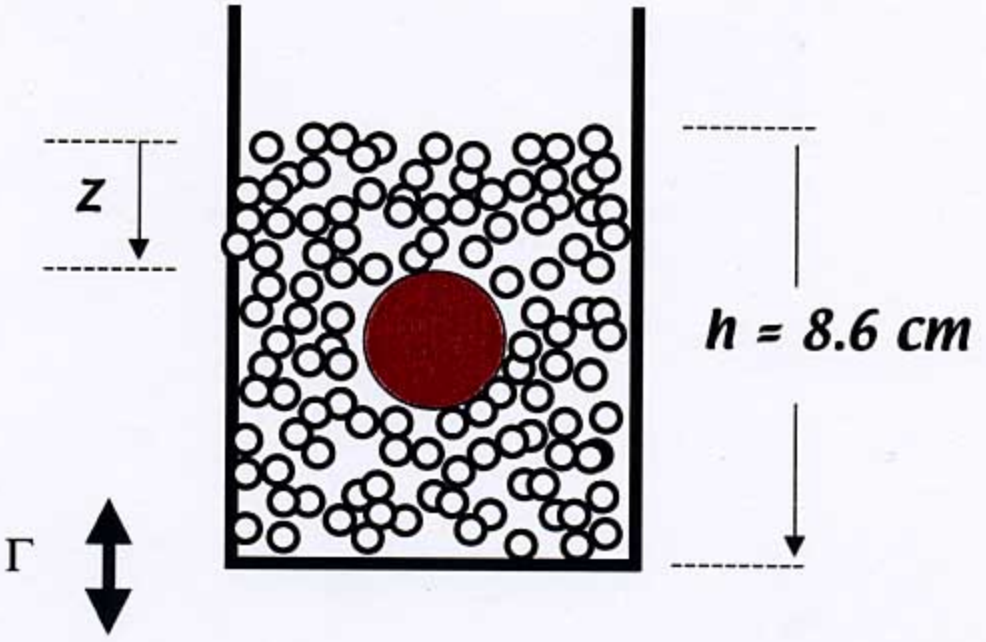

ρ_{medium} = 2.4 g/ml

d = 0.05 cm

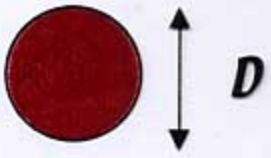

$0.037 < \rho < 7.78$ g/ml

$10 < D/d < 53$

SHINBROT & MUZZIO
LIFFMAN, ET. AL.
HONG, QUINN & LUDING

Rise Times for Intruder

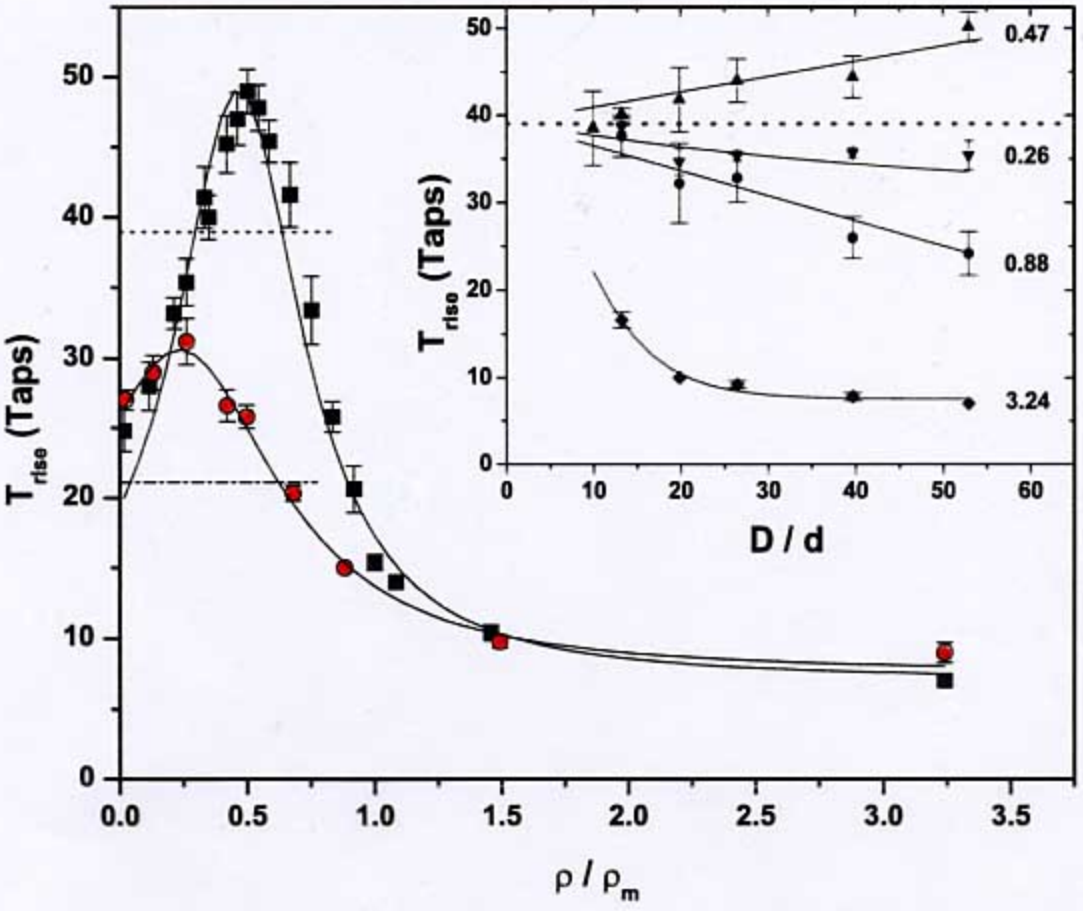

■ AMBIENT PRESSURE

● 50 TORR

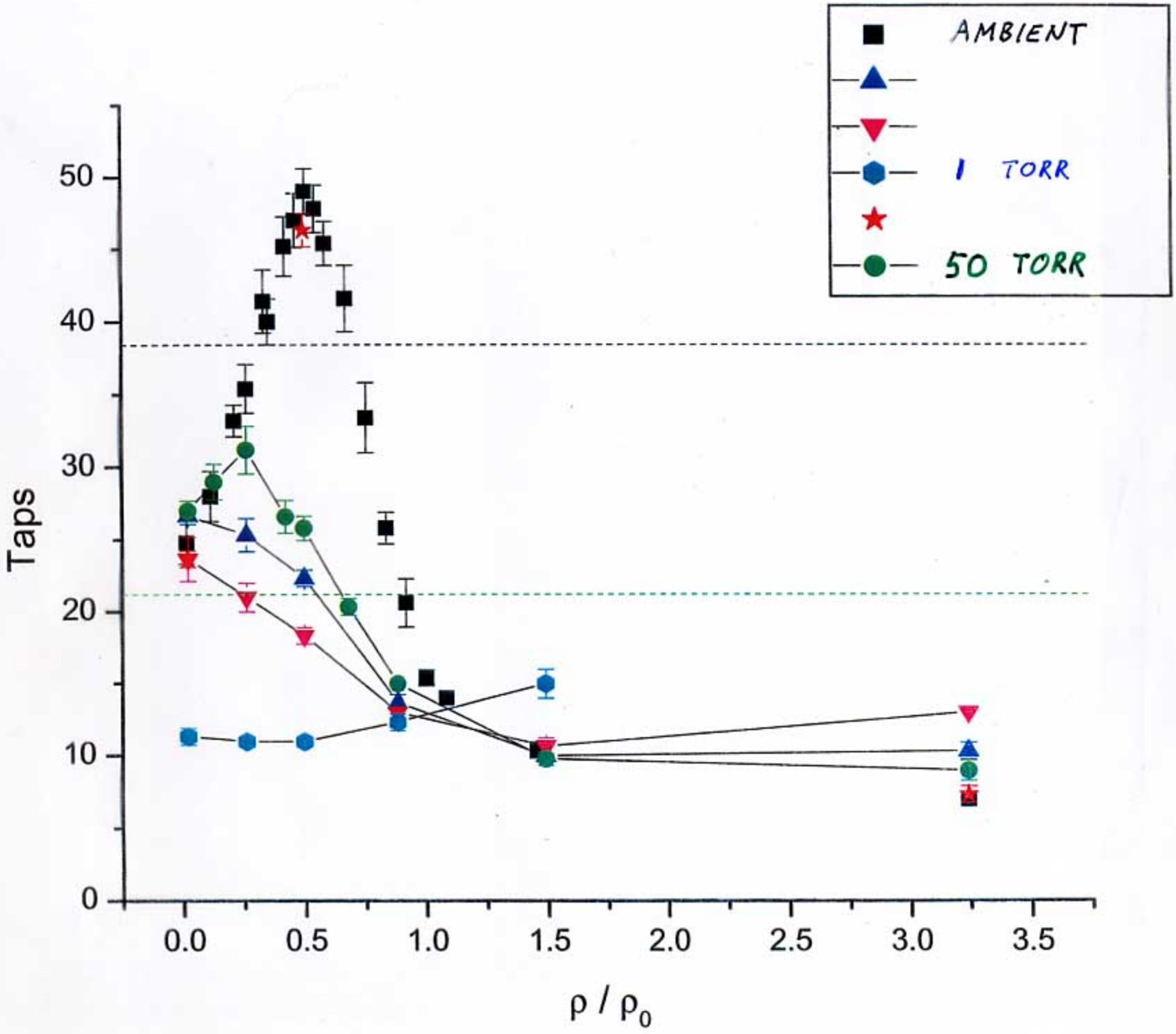
AMBIENT
1 TORR
50 TORR
Taps
0
10
20
30
40
50
0.0
0.5
1.0
1.5
2.0
2.5
3.0
3.5
ρ / ρ0

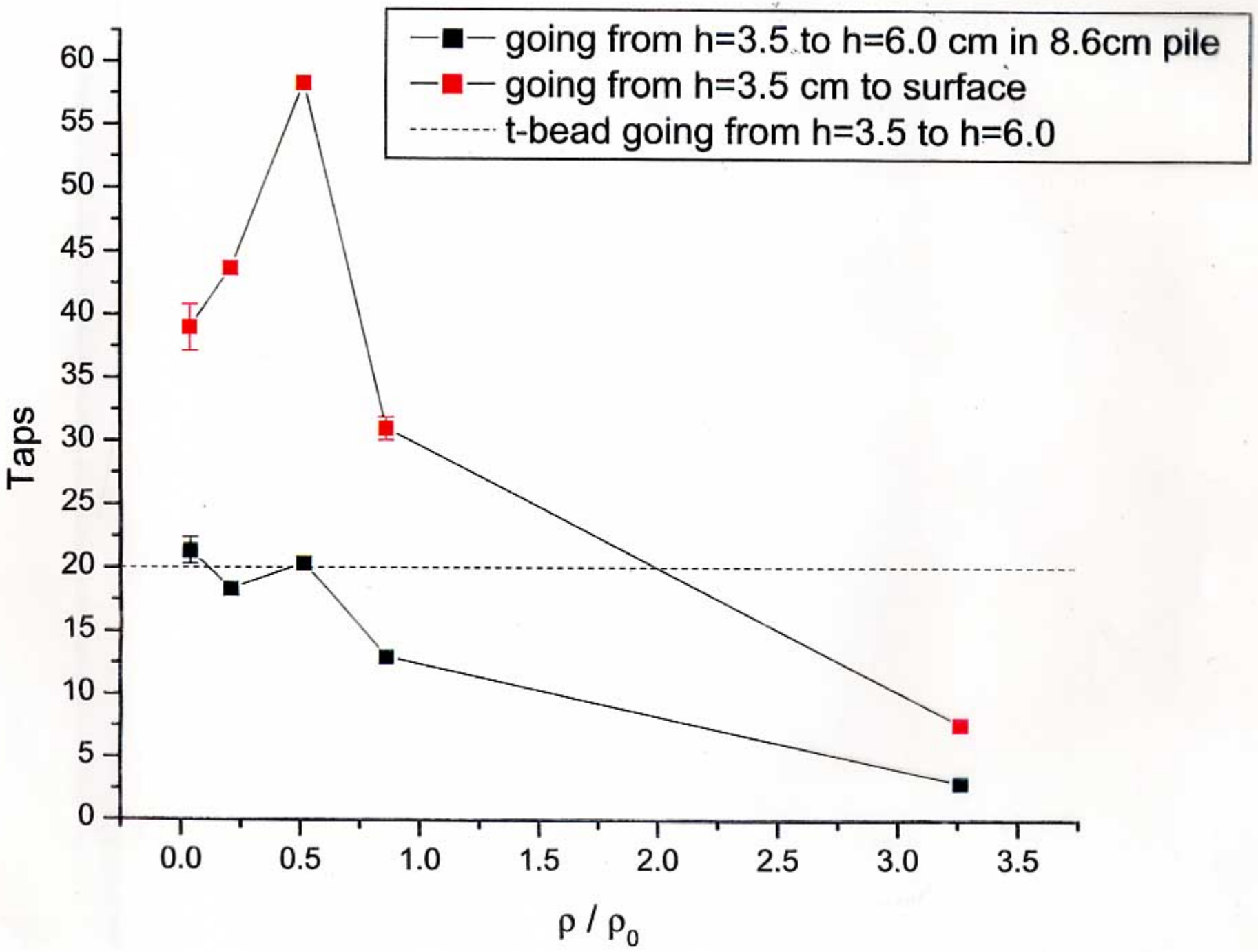
going from h=3.5 to h=6.0 cm in 8.6cm pile
going from h=3.5 cm to surface
t-bead going from h=3.5 to h=6.0
Taps
0
5
10
15
20
25
30
35
40
45
50
55
60
0.0
0.5
1.0
1.5
2.0
2.5
3.0
3.5
ρ / ρ0

Vibrations

Vertical
(gravity breaks symmetry)

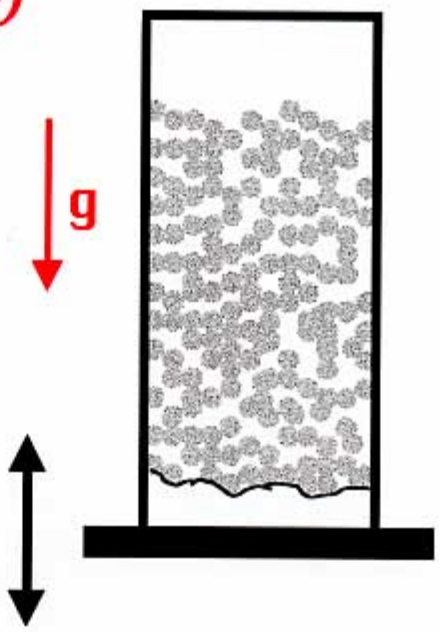

Horizontal
(Symmetry unbroken)
M. Medved

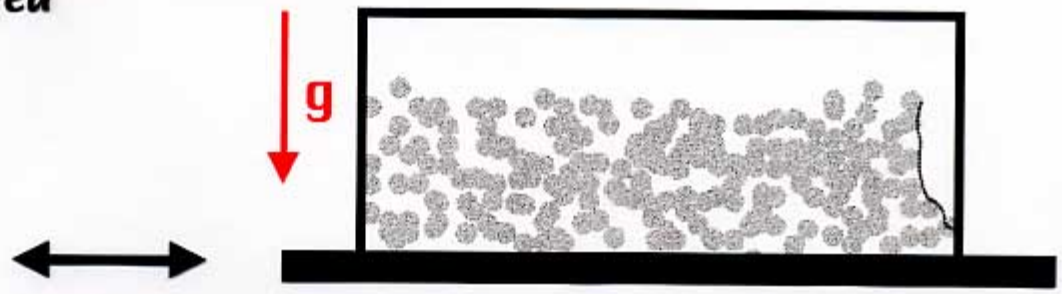

$k_B T \ll mgd \Rightarrow$ vibrations important

Horizontal Shaking

convection streamlines

Note gap

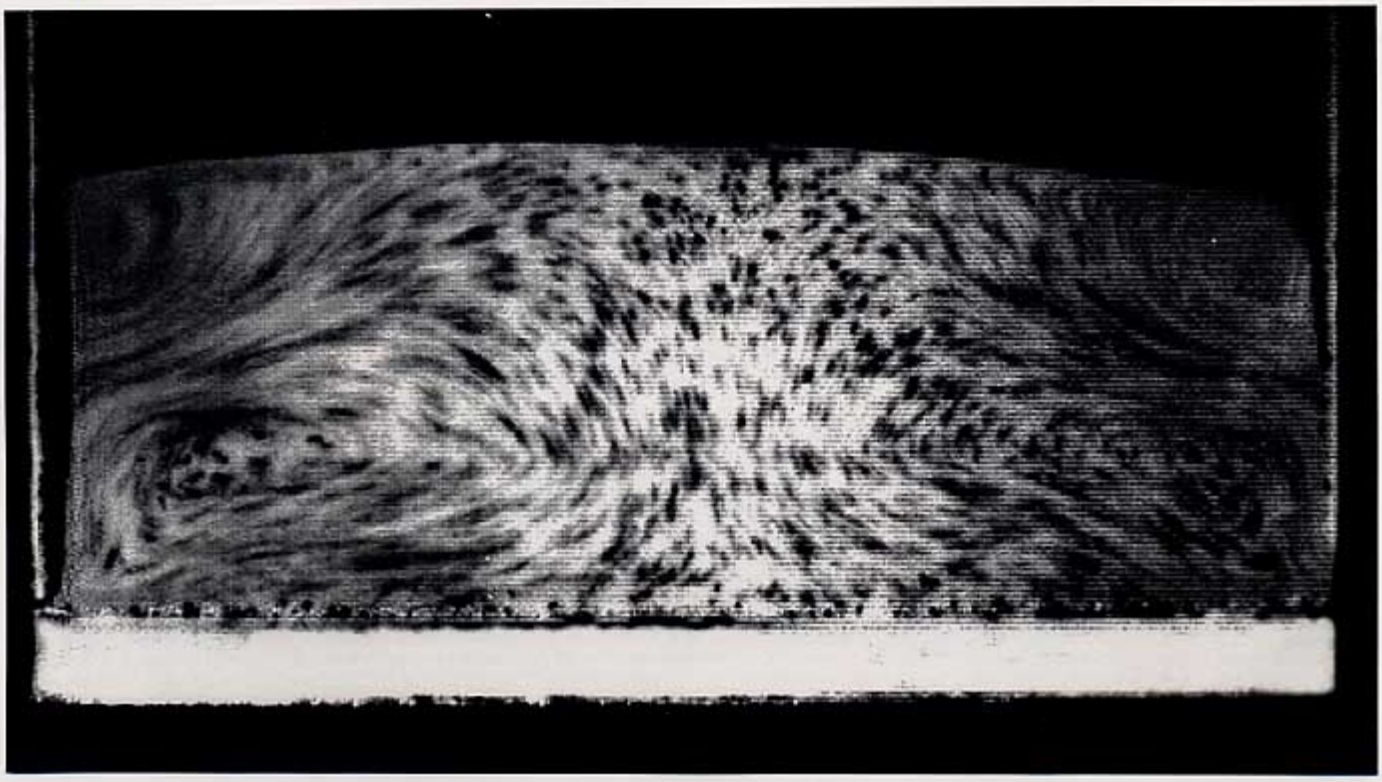

ROUGH WALLS

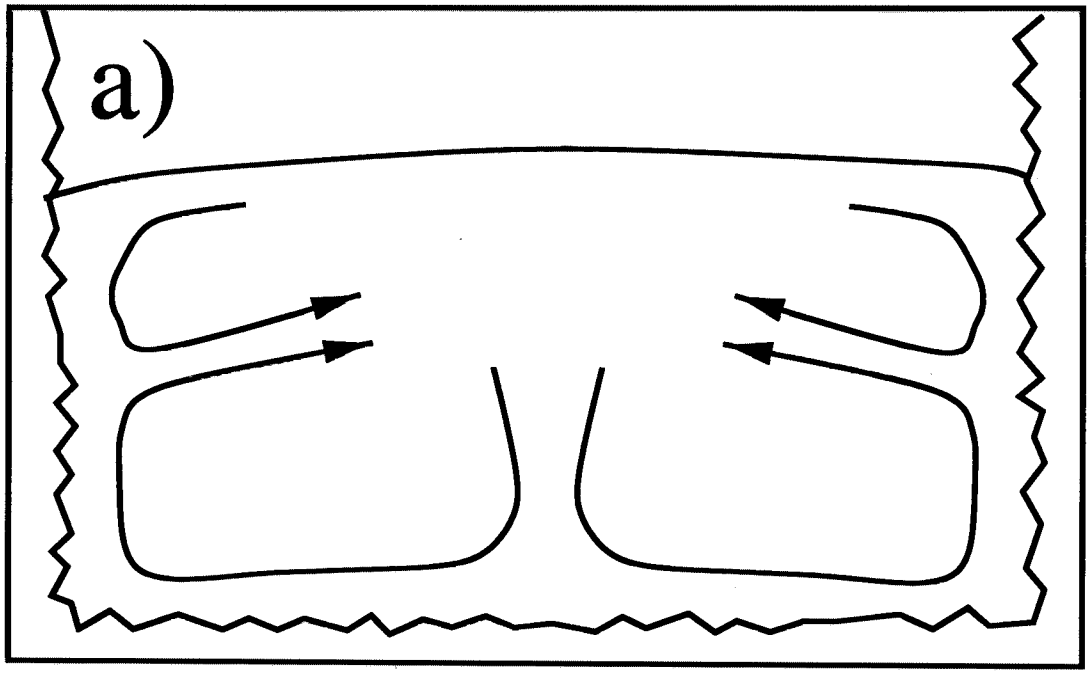

SMOOTH WALLS

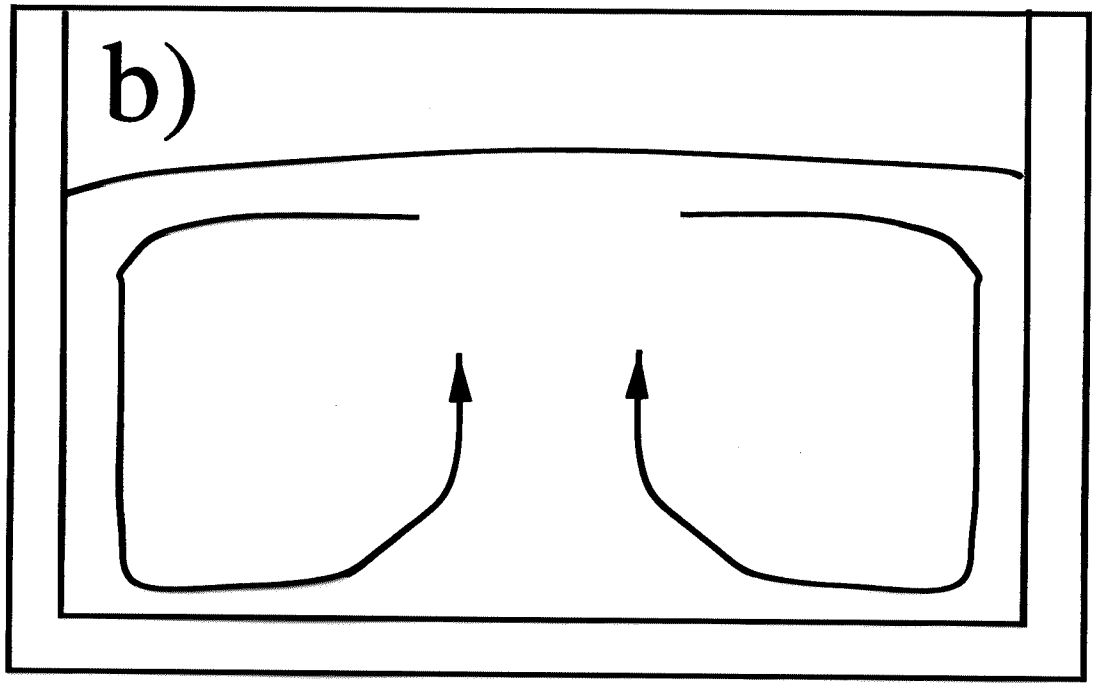

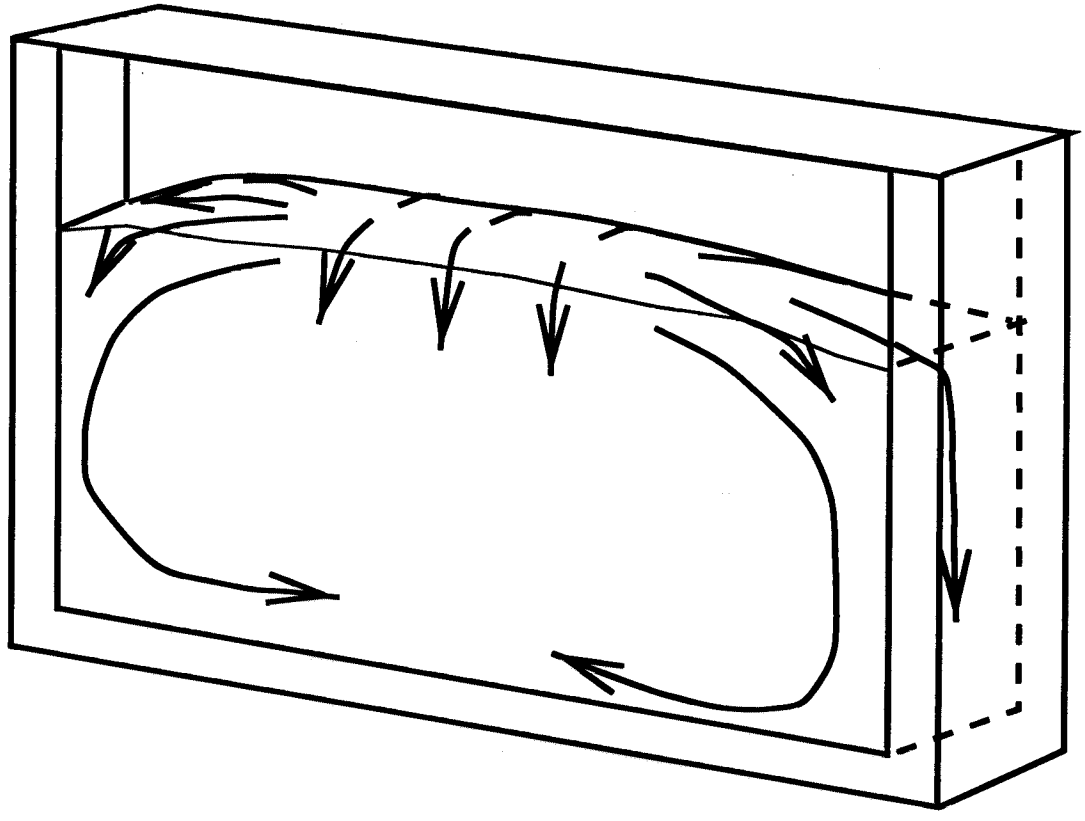

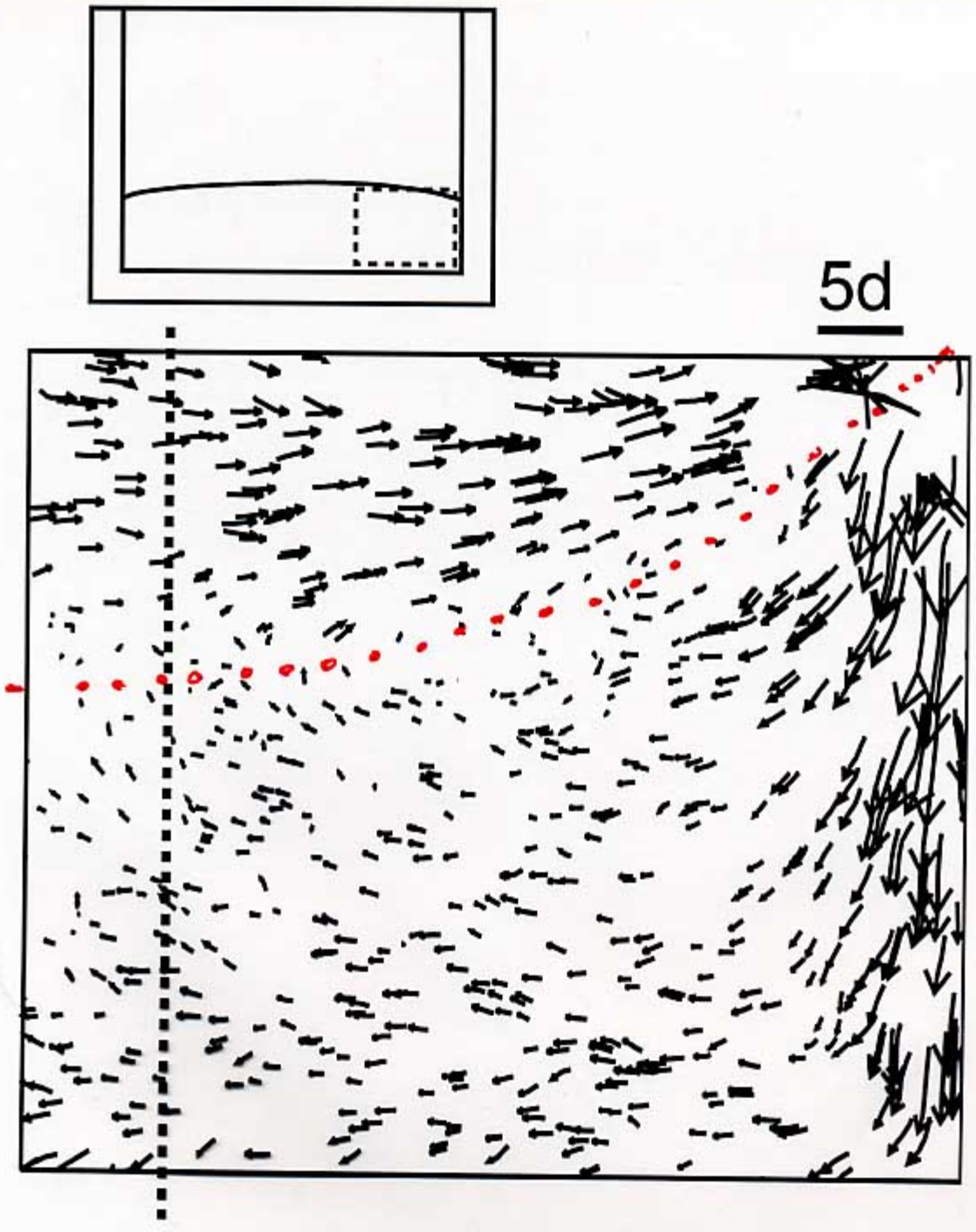
5d
SHEAR
BAND.

Convection in a Slurry

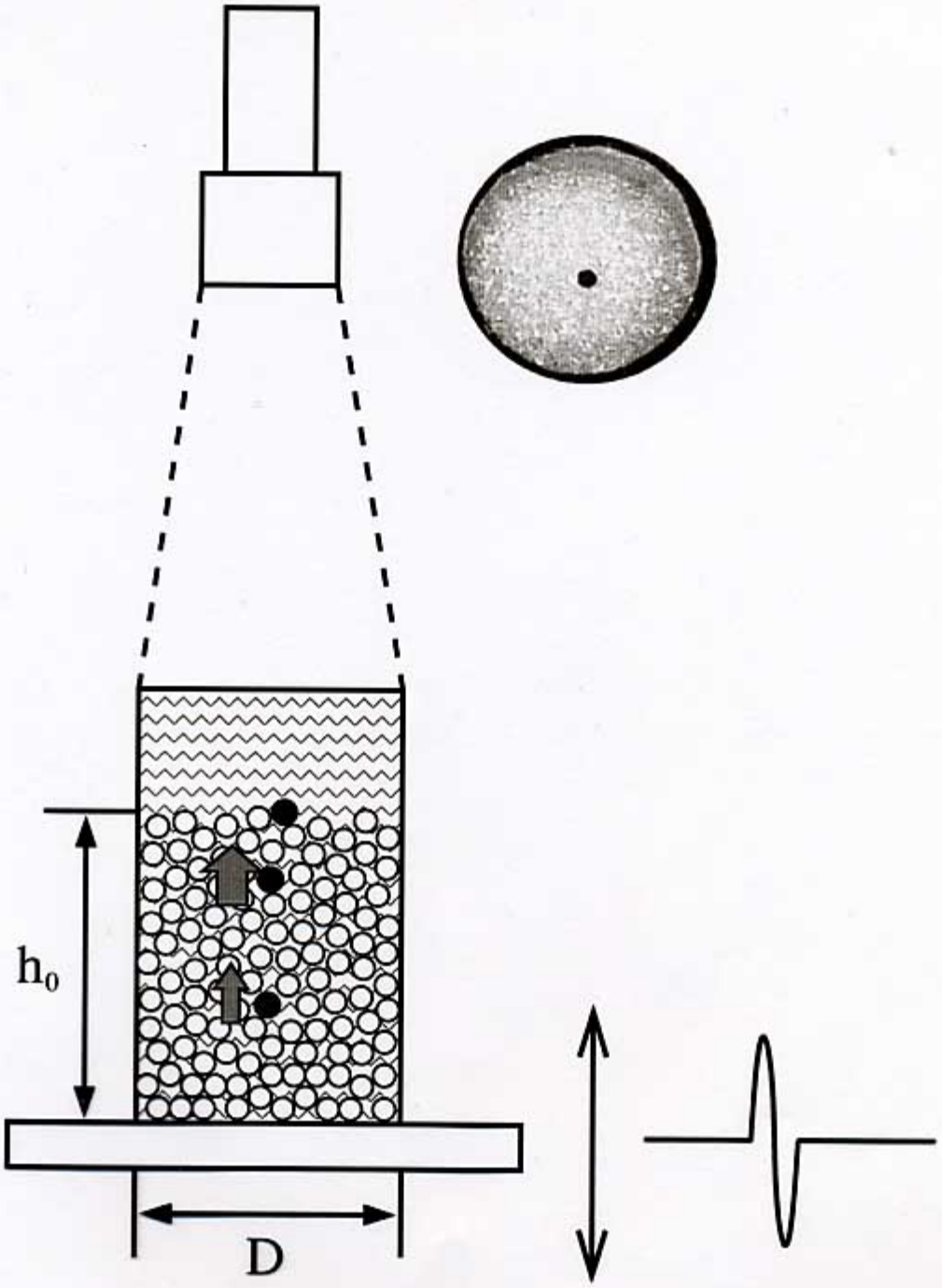

Convective Rise-times for Dry and Wet Material

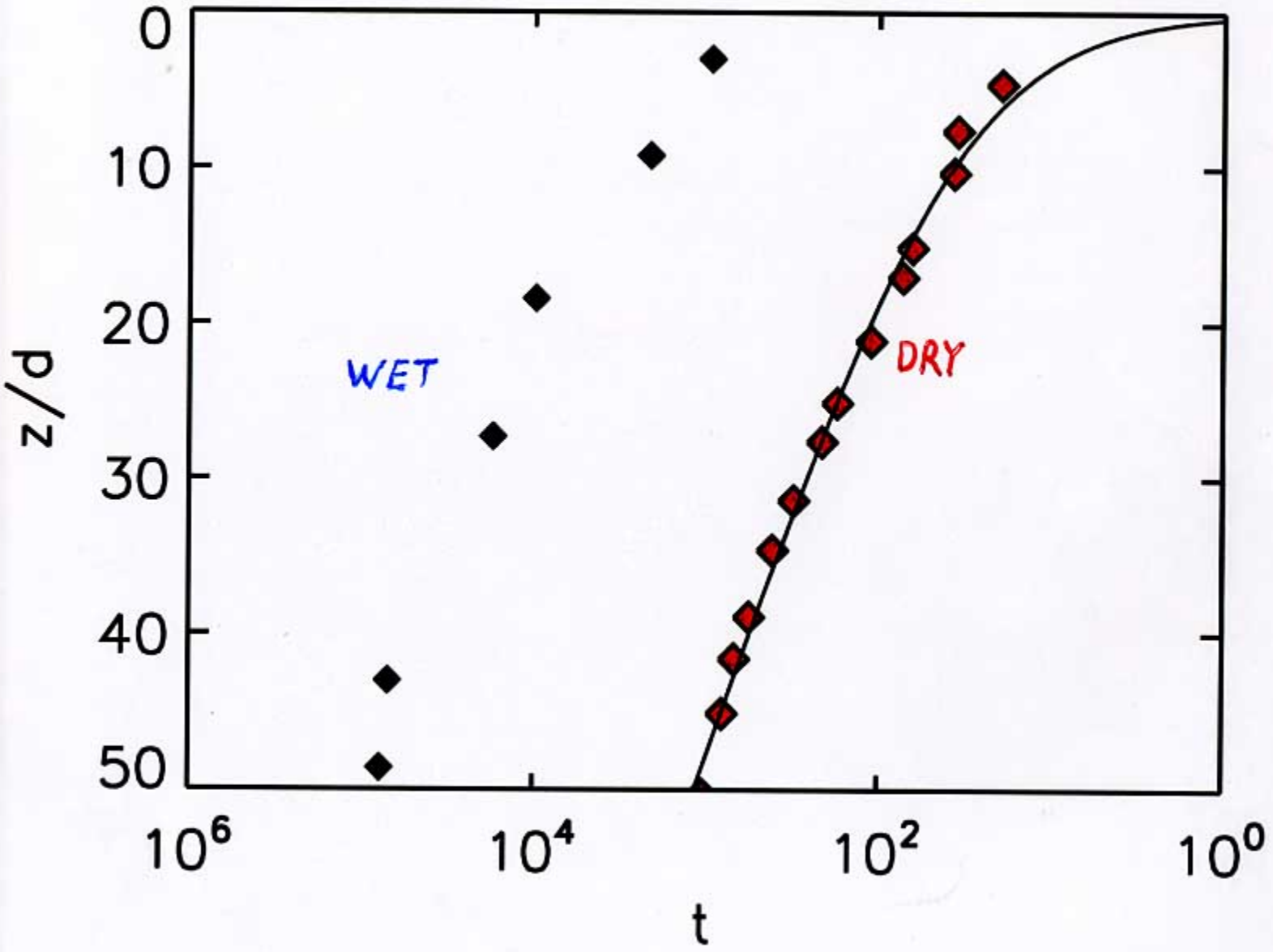

Parameters in Log fit: $z = \xi \ln(1+t/\tau)$

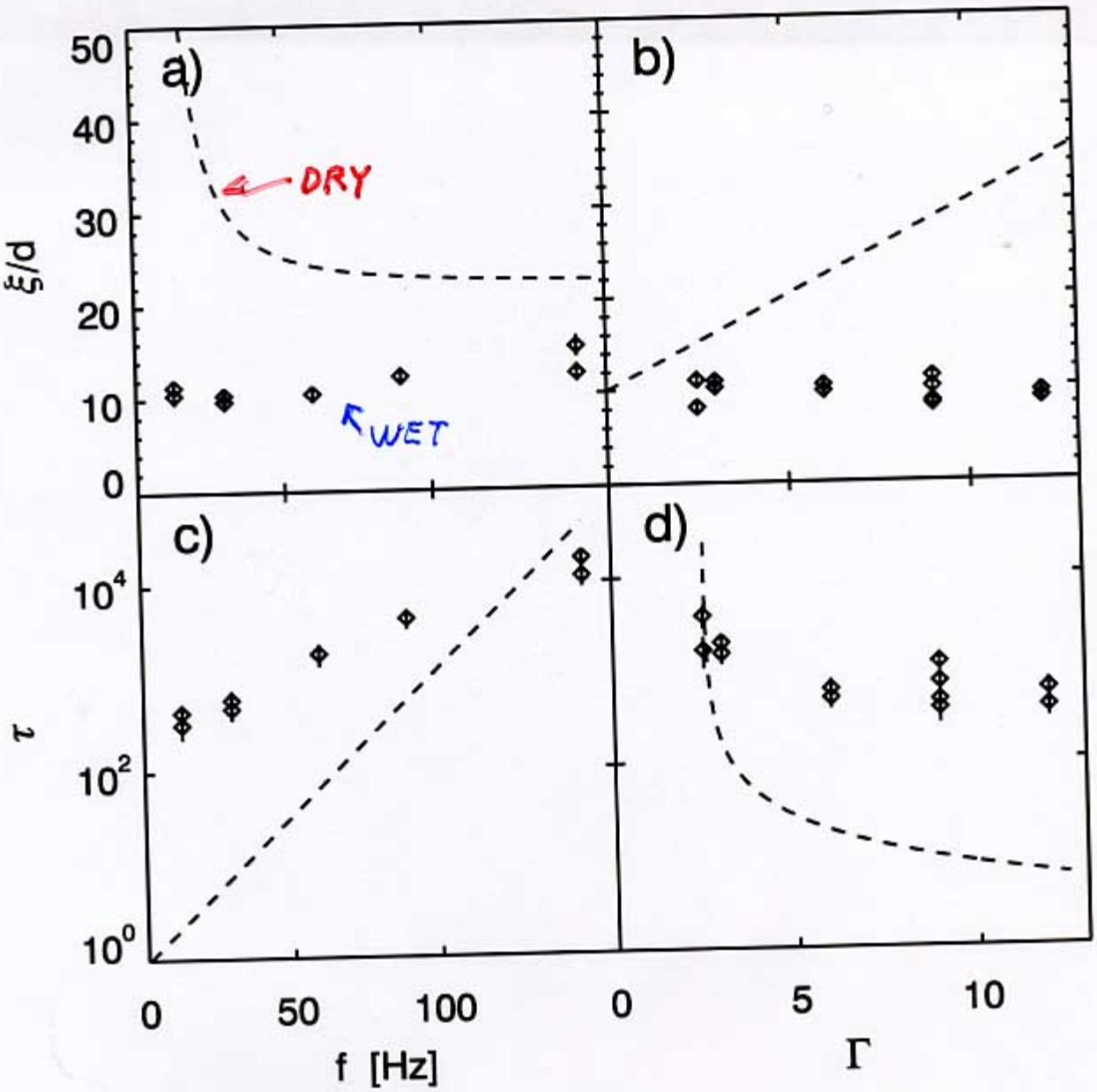

Parameters in Power-law fit: $z = A\, t^{p}$

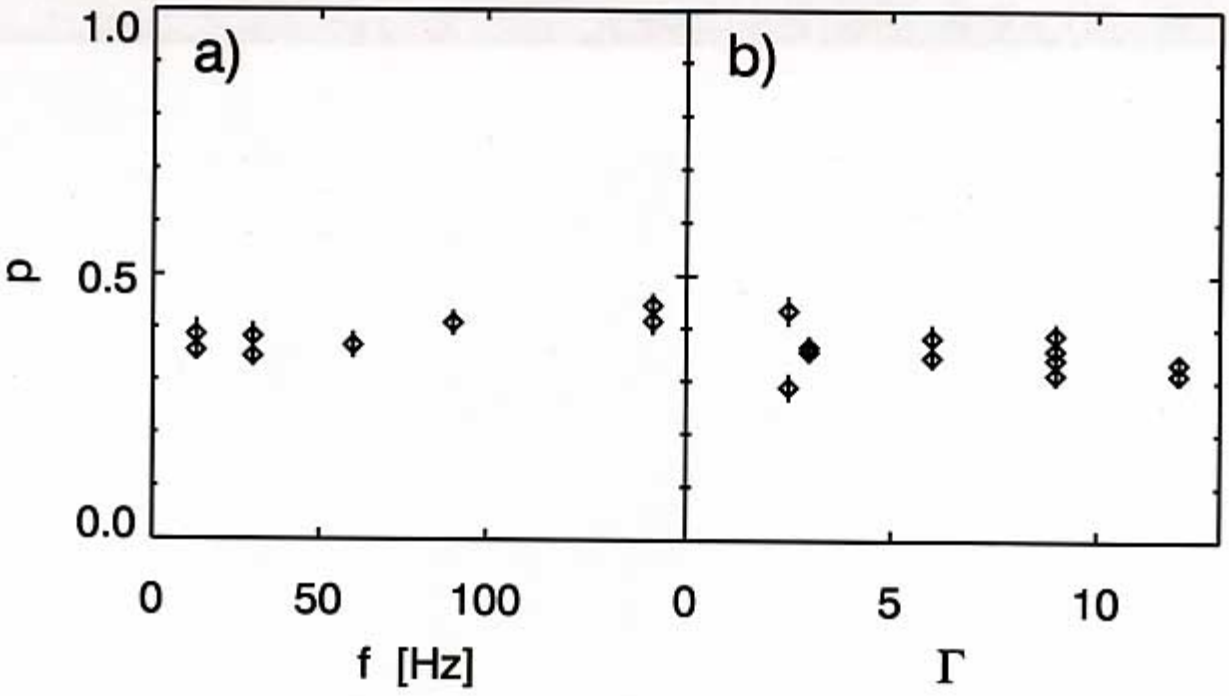

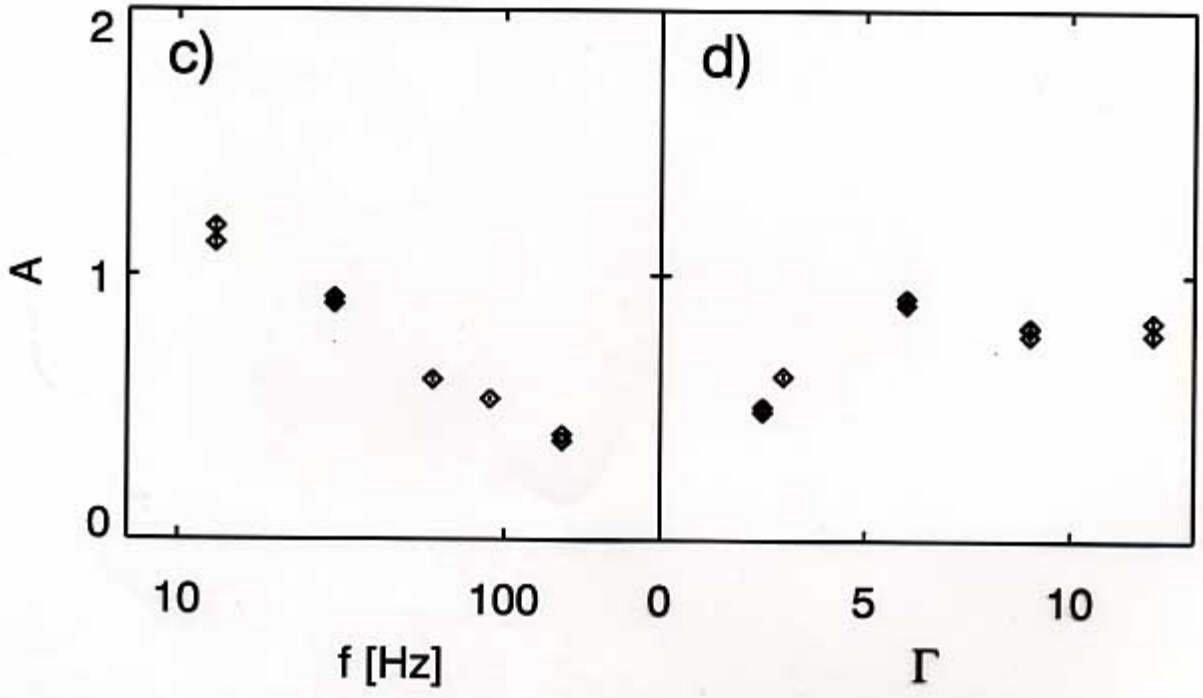

Granular flow: lessons Learned

Perched precariously between solid and fluid
⇒ sensitive to changes in many parameters

Density must decrease for flow:
vibrations
shear stress
⇒ Feedback between shear and density

MRI and X-ray micro-tomography:
High-resolution, non invasive
Velocity and density in shear band

Microstructure important for shear band profile

Convection in slurry has different form than in dry material
⇒ Different Mechanism (fluid entrainment)

Intruder is in 2 fluids:
Background particles
Interstitial air

In granular materials, something unexpected is always going to happen!

Particle Motions in a Gas-Fluidized Bed of Sand

Narayanan Menon and Douglas J. Durian

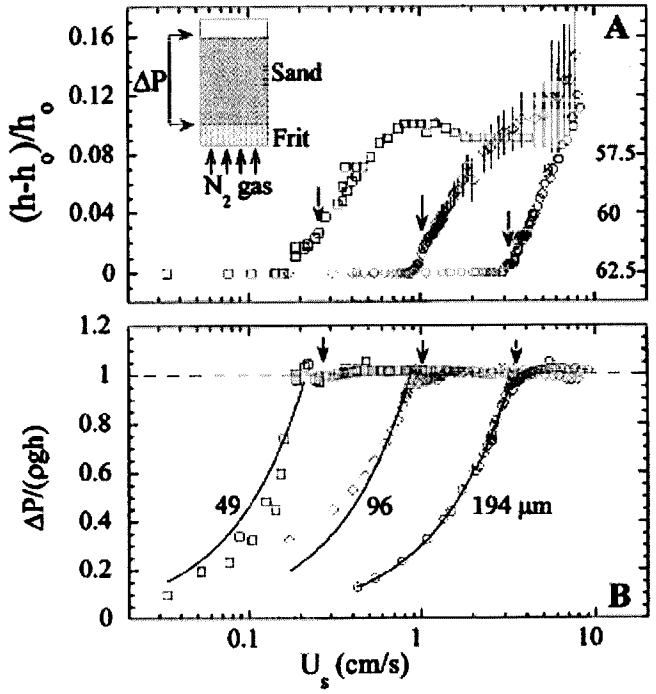

FIG. 1. Macroscopic probes of fluidized beds with particles of diameter $D = 49$, 96, or 194 μm (□, ◇, ○, respectively). (A) The fractional change in height (h) of the bed relative to its height at zero gas flow ($h_0 \approx 15$ cm) vs superficial gas velocity, U_s in cm/s. The bars show typical fluctuations of the height of the bubbling bed. On the right axis are equivalent packing percentages (the random loose and close packing limits are 56% and 63.5%). (B) The gas pressure drop across the bed, ΔP, normalized by ρgh (where ρ is the average density). The curves are linear fits in the unfluidized regime. The arrows indicate the onset of bubbling.

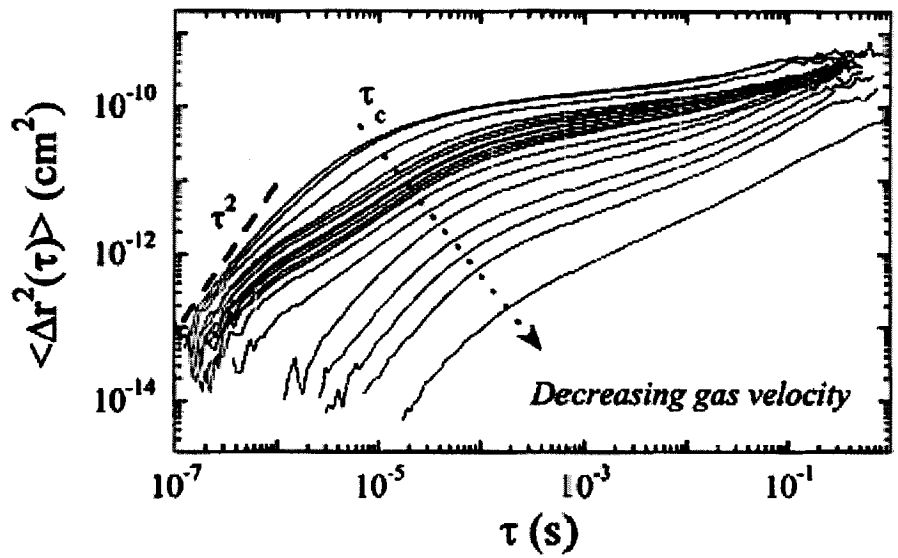

FIG. 2. DWS results for mean square displacement of beads, $\langle \Delta r^2(\tau) \rangle$ (in cm^2), as a function of time, τ (in sec) in a bed of **96** μ**m** beads. The short time dynamics are collisional with $\langle \Delta r^2(\tau) \rangle = \delta V^2 \tau^2$ for $\tau < \tau_c$, the collision time. As U_s is increased, the collisional regime shifts to shorter times and higher velocities. For $\tau > \tau_c$, $\langle \Delta r^2(\tau) \rangle$ changes very slowly with τ for several decades in time.

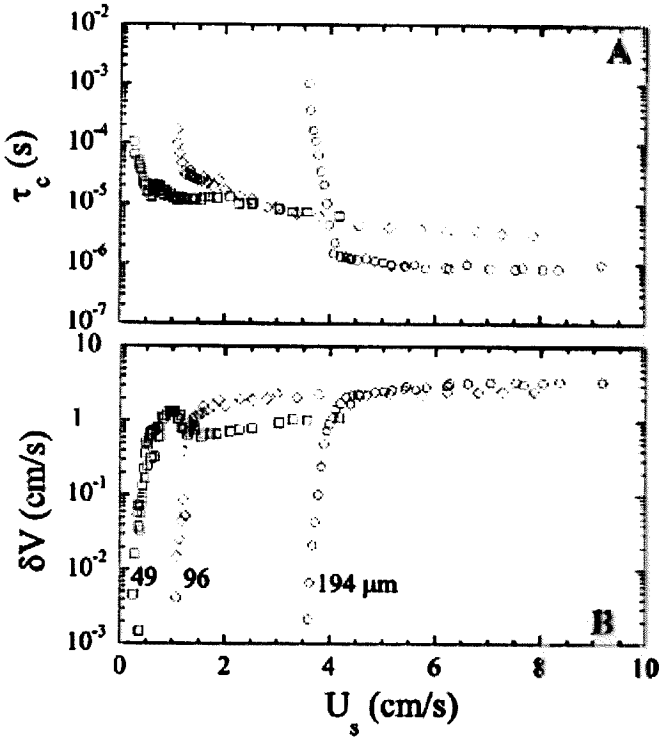

FIG. 3. Dependence on gas velocity, U_s, of parameters of the collisional regime: (A) Velocity fluctuations, δV, and (B) collision time, τ_c. Both sets of parameters change rapidly beyond the onset of bubbling [12] and thereafter turn over to a slower variation with U_s. (□, ◇, ○ are D = 49, 96, or 194 μm, respectively).

Hysteresis and packing in gas-fluidized beds

R. Ojha, N. Menon,* and D. J. Durian

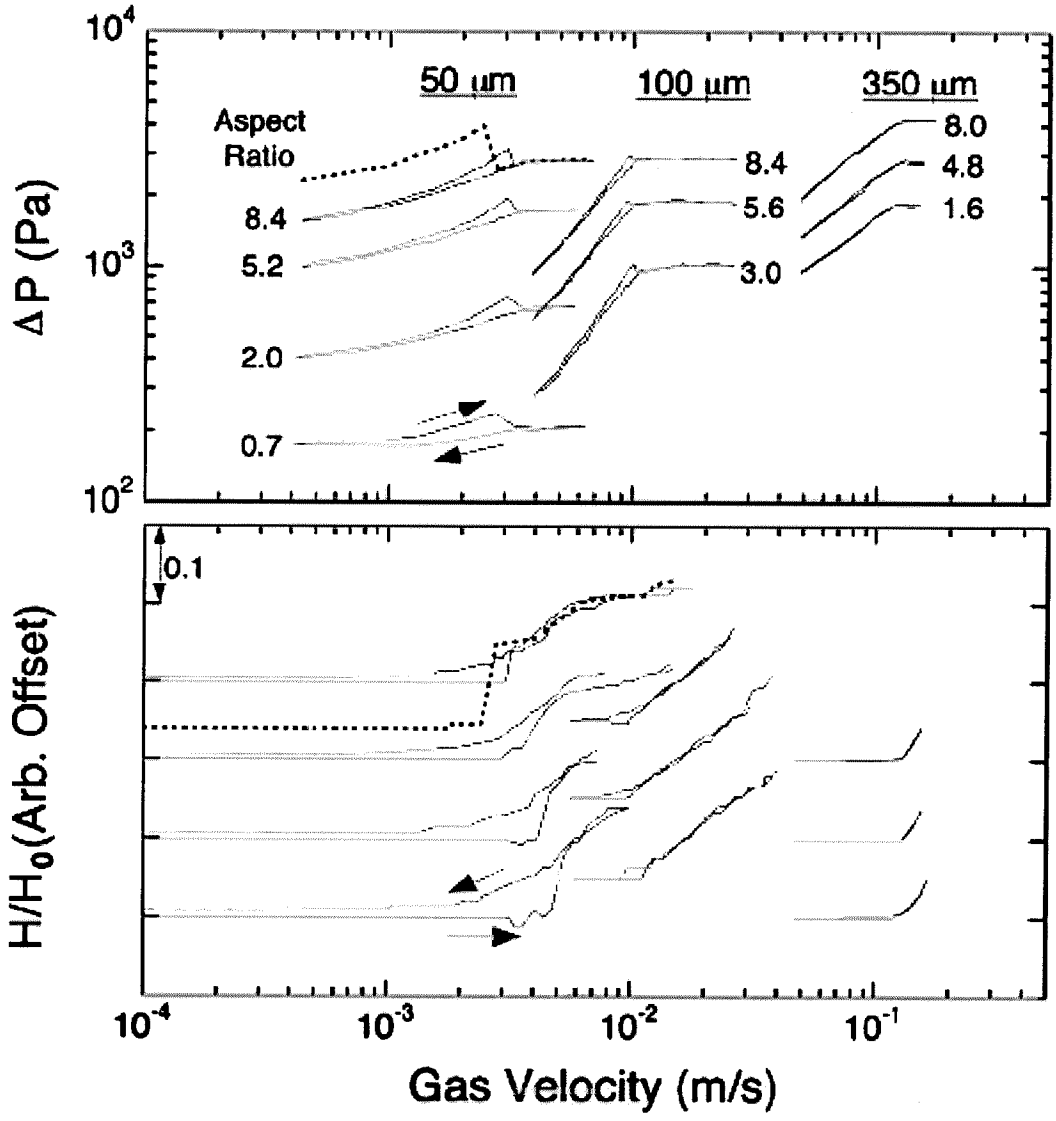

FIG. 1. Typical data for gas-pressure drop and bed height vs superficial gas velocity. Solid curves represent retraceable hysteresis loops, in the direction indicated. The dashed curve represents initial behavior, as the flow rate is ramped up for the first time for beads freshly poured into the tube. Results are for the 1-in.-diam bed, with bead sizes and aspect ratios (height to diameter) as labeled.